The Dissertation Committee for
Urairisa Birdy Phathanapirom Certifies that this is the approved version of the following dissertation:

Autonomous Dynamic Decision Making in Fuel Cycle Simulators using a Game Theoretic Approach

Committee:

Derek Haas, Supervisor

Benjamin Leibowicz, Co-Supervisor

Sheldon Landsberger

Paul Wilson

Autonomous Dynamic Decision Making in Fuel Cycle Simulators using a Game Theoretic Approach

BY

Urairisa Birdy Phathanapirom

Dissertation

Presented to the Faculty of the Graduate School of

The University of Texas at Austin

in Partial Fulfillment

of the Requirements

for the Degree of

Doctor of Philosophy

The University of Texas at Austin

December 2018

ให้คุณมา

You said you came to the States with 20 dollars in your pocket

because no matter what, you'd have a better life. For you.

ACKNOWLEDGEMENTS

To everyone, I cannot express my gratitude.

To the faculty and students, past and present, of the Nuclear and Radiation Engineering and Operations Research Programs. To my immediate supervisors, Derek Haas and Benjamin Leibowicz, for continuous support and helping bring this project into realization; to Sheldon Landsberger for barefaced consistency; to Steven Biegalski and Nedialko Dimitrov for fresh perspectives; and to Erich Schneider for giving me every opportunity.

To Anna Francis, Mark Elliot, Shay Zimmer and all who guided me through tough times.

To Kenneth Dayman for always ranking me in the A-team; to Margaret and Andrew Byers for the cheddar bunnies; and to James Horstman for his patience and care.

To my faithful companion, Mrs. Butterscotch.

Autonomous Dynamic Decision Making in Fuel Cycle Simulators using a Game Theoretic Approach

Urairisa Birdy Phathanapirom, Ph.D.
The University of Texas at Austin, 2018

Supervisor: Derek Haas
Co-Supervisor: Benjamin Leibowicz

A novel methodology for optimizing nuclear fuel cycle transitions that captures interactions between a policy maker and electric utility company is presented. The methodology is demonstrated using a two-person general-sum sequential game with uncertainty that is implemented using a nuclear fuel cycle simulator capable of calculating a material- and technology-constrained material balance, coupled to a multi-objective optimization solver. The solver explicitly treats uncertainties using a stochastic programming approach with chance nodes depicted as a *Nature* player who moves randomly. The methodology is demonstrated through a Transition Game that features tradeoffs between investments in competing reprocessing and waste disposal technologies, dynamic reactor deployment responses to resolutions in reactor capital cost uncertainty, and the influence of capital subsidies on the future nuclear technology mix. Each player in the game uses a unique set of decision criteria to identify optimal near-term hedging strategies that consider all of *Nature*'s possible moves as well as the other player's available decisions. These hedging strategies balance the exchange between the risk of

immediate action and delay and maintain flexibility to allow for intelligent recourse decisions once uncertainties are resolved. Results from the Transition Game indicate that early transition to high-temperature gas-cooled reactors is preferred, with the option to abandon the transition following a learning period if capital costs are unfavorable. Under these conditions, transition to used fuel recycling in sodium-cooled fast reactors may be spurred by policy incentives under some certain decision criteria weightings. Otherwise, operating with a baseline set of decision criteria weightings, transition to a closed fuel is never observed when players hedge optimally against *Nature*'s moves. It is only when players have perfect information regarding *Nature*'s future moves will transition to a closed fuel be observed.

TABLE OF CONTENTS

CHAPTER 1: INTRODUCTION

The U.S. Department of Energy, Office of Nuclear Energy (DOE-NE) has been researching technology to shape the nuclear fuel cycle to better balance the need for energy, economic and proliferation security, environmental sustainability, and the risks associated with development and deployment of new fuel cycle technologies. Previous fuel cycle analysis tools have been constrained by human and computer resources. Many studies have opted for a less detailed, but more expansive view of the fuel cycle due to the tradeoff between depth and breadth of modeling. As a result, some key features in fuel cycle transition analysis have suffered, including:

1. Treatment of transients, instead examining the fuel cycle operating equilibrium where facilities are continually built, operated and decommissioned as needed.
2. Simultaneous optimization across multiple objective functions, instead focusing on specific areas of interest to the researchers conducting the study.
3. A robust treatment of uncertainties, instead examining uncertainties through sensitivity or scenarios analysis that varies parameter values within a deterministic model.

As more computing resources become available, DOE-NE fuel cycle studies have better addressed these issues. The Dynamic Systems Analysis Report for Nuclear Fuel Recycle (DSARR) examines the time-dependent exchanges between fuel cycle technologies resulting from transitioning to a closed fuel cycle where used fuel is recycled (Dixon et al., 2009). Specifically, the DSARR considers the effect of timing and constraints on fuel cycle technology on uranium resource utilization and transuranic (TRU) inventories. High-level parameters such as the installed reprocessing capacity and the TRU conversion ratio in fast reactors are identified using sensitivity analysis. The Evaluation and Screening Study (E&S Study) reviewed the largest collection of fuel cycle options,

grouping them into similar physics-based evaluation groups and assessing their performance based on nine DOE-specified evaluation criteria (Wigeland et al., 2014). The E&S Study treated uncertainties in fuel cycle performance by binning the data ranges for each evaluation metric resulting in a coarser investigation. In this way, the DSARR and the E&S Study complement one another. The DSARR examines the effects of transitioning from one fuel cycle to another, while only considering effects of the transition on economics and waste management. The E&S study looked at many fuel cycle evaluation criteria, while only considering fuel cycles operating at equilibrium. Both studies acknowledge and handle uncertainties in some way, though neither offer guidance on how to best evolve the fuel cycle in light of these uncertainties.

Recently, the DOE-NE Fuel Cycle Research & Development (FCR&D) program has identified the need for a next-generation fuel cycle simulation tool to support decision making and communication and education on the multiple attributes of potential fuel cycles. The envisioned tool, now developed as the Cyclus code, is designed to employ modularity in order for users to specify the level of detail at which to model the fuel cycle – or even part of the fuel cycle. The work presented here complements these efforts, developing a proof-of-concept preconditioner tool that employs:

1. A lightweight systems model of the nuclear fuel cycle to capture dynamic effects.
2. Multiple decision criteria and fuel cycle metrics to create a complex decision space.
3. A stochastic programming approach for explicitly handling uncertainties.

The VEGAS simulator is used as the platform for this work due to its reduced runtime. The primary advantage of the VEGAS simulator is its ability to calculate a material- and technology-constrained material balance, which has been shown to have a large effect on

the mix of reactor technology at the end of a transition. Developing algorithms capable of calculating a constrained material balance has proven a challenging task in past fuel cycle analyses. Still, the VEGAS simulator is limited in its lack of discrete facility modeling, physical fidelity at the isotopic level, and time-dependencies arising from radioactive decay. Given the material balance, multiple objective function values may be rapidly solved using a variety of fuel cycle metric calculations. When uncertainties are input prior to runtime, they may be propagated to the calculated objective function values. Lastly, an explicit treatment of uncertainties in the fuel cycle transition is achieved using a stochastic programming approach, where uncertainties are explicitly accounted for in the strategic decisions that collectively define the transition evolution. Using a stochastic programming approach, near-term hedging strategies can be identified that balance tradeoffs between the risk of immediate action and delay and allow flexibility to adapt future decisions based on new information.

Unique to this work in the realm of fuel cycle transition analysis is application of a game theoretic approach to depict interactions between key participants in a nuclear project: a government entity and a utility generating company. Previous transition optimizations have assumed a single "benevolent dictator" shaping the future of the nuclear fuel cycle, acting with a single set of decision criteria. Instead, each participant shapes the transition based on his or her unique decision criteria, and each responds uniquely to uncertainty resolutions as well as the other's previous decisions as time moves forward. Incorporating these players and a *Nature* player that moves randomly brings autonomous decision making into the fuel cycle simulator.

A game theoretic approach to energy systems modeling is not in itself new, nor is the explicit treatment of uncertainties in nuclear fuel cycle transition analysis through a stochastic programming approach. The novelty of the work presented here is their merger, coupled with a sophisticated fuel cycle simulation tool, allowing for rich transition scenarios to be analyzed using a diverse set of competing fuel cycle metrics. This work demonstrates a proof-of-concept systems analysis approach to optimization of a fuel cycle transition strategy. The methodology presented here addresses the previously identified short-comings of past fuel cycle analyses.

This document is structured into three major sections. Chapter 2 provides a survey of the existing literature in nuclear fuel cycle analysis pertaining to the treatment of uncertainty in fuel cycle transition analyses, multi-objective decision making, game theory and the primary fuel cycle simulators that have been used in DOE-NE studies. Chapters 3 through 5 detail the methodology used for this work. Chapter 3 describes the nuclear fuel cycle simulator used here, including its material balance and reactor ordering algorithms and unique features that enhance its ability to act as a qualified preconditioner tool for rapid fuel cycle transition strategy scoping. Chapter 4 gives background for the decision criteria used in this study, the chosen fuel cycle metrics that are used to score these criteria and their calculations. Chapter 5 describes a fuel cycle transition game including players and their decision criteria, available strategies and payoff calculation, as well as uncertainties incorporated into the game, with results presented in Chapter 6. Chapter 7 summarizes the most important findings of this research and identifies areas of future work.

CHAPTER 2: LITERATURE REVIEW

This chapter overviews treatment of uncertainty in past fuel cycle transition analyses and introduces the stochastic programming approach employed here for explicitly handling uncertainties. Challenges and the need for multi-objective optimization and its implementation in recent fuel cycle transition studies are discussed. By examining multiple objectives and ascribing unique decision criteria to prime participants in a nuclear project allows nuclear fuel cycle transitions to be analyzed using a game theoretic lens. Past work coupling multi-agent interactions in a fuel cycle context are described. Finally, a summary of the primary past and current fuel cycle simulators used for DOE-NE fuel cycle analysis efforts are summarized. The methodology presented in this dissertation is a merger of game theory and decision analysis and fuel cycle simulation and modeling with the primary goal of optimizing a nuclear fuel cycle transition subject to uncertainty. Through this merger, autonomous decision making is brought into the fuel cycle simulator.

2.1 UNCERTAINTY IN NUCLEAR FUEL CYCLE TRANSITION ANALYSES

More comprehensive nuclear fuel cycle transition studies have recently been made possible through use of complex fuel cycle simulations coupled with increased technological capabilities. All nuclear fuel cycle transition studies determine natural resource and technology requirements for changeover from one (typically the current) nuclear fuel cycle to another. For instance, many transition studies have examined the changeover from the current U.S. open fuel cycle consisting of a light water reactor (LWR) fleet to a closed fuel cycle comprised of fast reactors (FRs) burning recycled used fuel from LWRs (Yacout et al., 2004; Dixon et at., 2009; Djokic et al., 2015). Uncertain parameters

abound in these transitions – technology costs and availability dates, demand growth for nuclear electricity and promise of government loan guarantees and tax credits, to name a few. Previously, nuclear fuel cycle transition studies have handled these uncertainties using sensitivity and scenario analysis. Newer work has taken a stochastic programming approach in order to explicitly handle uncertainties, formulating robust transition strategies (Carlsen, 2016; Phathanapirom and Schneider, 2016; Pierpoint, 2017). Kann and Weyant (2000) offer a thorough description of these approaches to uncertainty analysis, which are summarized here.

Sensitivity analysis may help allocate uncertainty in model output to different sources of uncertainty in its input. Sensitivity analysis is performed by recalculating outcomes of the model while varying uncertain input parameters over their possible ranges. When variation of an input parameter produces relatively small alteration in model output, that output is considered *robust*, while if a large variation is observed, it is considered *sensitive*. Given its straightforward nature requiring zero modifications of the model, this type of analysis is commonly used. While simple, sensitivity analysis is useful in that it allows increased understanding of relationships between model inputs and outputs that may aid in future investigations by reducing computational burden by identifying inputs that cause rise to larger uncertainty in model outputs that should be the focus of future investigations (Bistline, 2013; Wian, 2013).

Scenario analysis is roughly similar to sensitivity analysis – no model modifications are required, and input parameters are varied across their possible ranges. The crucial distinction of scenario analysis is its construction of different states of the world through some combination of uncertain parameter values, which represent a plausible

description of how the system and its driving forces may develop in the future (Walker et al., 2003; Gabbert et al., 2010). Solutions of a deterministic optimization model are unique to each individual scenario and offer a set of coherent, internally consistent futures.

Sensitivity and scenario analysis treat uncertainties as exogenous to a deterministic model. The central issue of these approaches is the assumption that decision makers have perfect information about the state of the world that will prevail. In reality, decision makers must act before uncertainties are resolved, and in many situations *to* resolve those uncertainties.

Stochastic programming explicitly handles uncertainties by simultaneously considering all possible states of the world, offering a systematic approach to decision making under uncertainty. Stochastic programming requires a decision maker to make some decision now that minimizes the (usually) expected cost or consequence of that decision. Considering stochastic programs in this way gives rise to a *recourse* model, where information available to the decision maker is updated in each sequential stage (Golub et al., 2014; Leibowicz, 2018). The simplest form of a stochastic program is the two-stage linear program with recourse, however, due to the complex, dynamic nature of the nuclear fuel cycle, linear programming is insufficient. Instead, the nuclear fuel cycle simulator is treated as a black-box that a solution algorithm can invoke to obtain an objective function value.

Fig. 2.1 below depicts a two-stage stochastic program. The cost (or objective function value) $F(d_1, \omega, d_2)$ is dependent on the first stage decision d_1, the outcome of the stochastic variable ω, and the second stage decision d_2. d_2 is termed a *recourse* decision,

as it is taken after obtaining information on the value of ω. The first stage decision (d_1) represents a near-term hedging strategy that is chosen by minimizing the expected cost of that decision through a probability weighted sum of $F(d_1, \omega, d_2^*)$, where $d_2^*(d_1, \omega)$ is the optimal recourse decision that minimizes the costs given d_1 and ω initial conditions.

Fig. 2.1 depicts two decision makers acting at d_1 and d_2, represented by the differently colored decision nodes. Binsbergen and Marx (2007) examined the relationship between decision analysis and game theory and concluded that some sequential games can be analyzed using a decision analysis approach. The sequential game considered in this dissertation is solved through the method of backward induction, where the behavior of multiple players is handled by considering multiple decision trees. The notion of payoffs in game theory is equivalent to gains in decision theory.

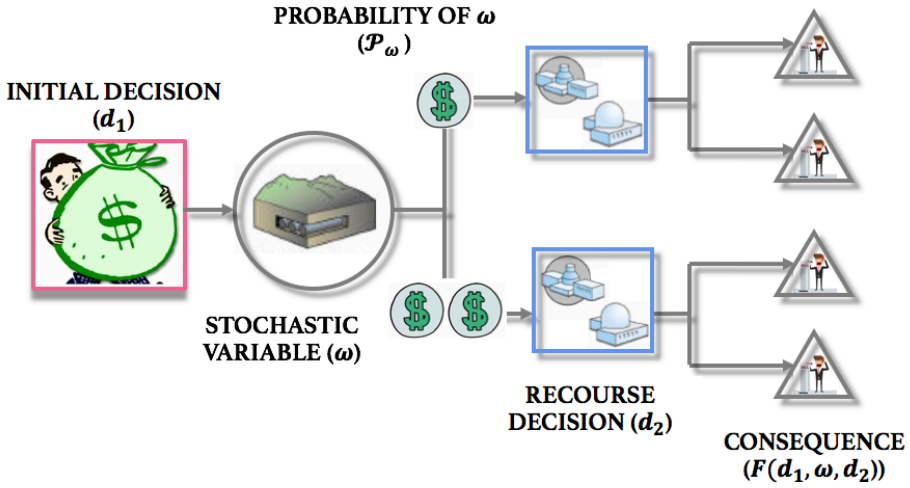

Figure 2.1: Two-stage stochastic program.

Consider the *Centipede Game*, depicted in Fig. 2.2: a pile of silver dollars is on a table, and two players (I and II) alternate turns taking either one or two coins from the pile,

keeping the coins they take (Ferguson, 2014). As soon as either player takes two coins, the game stops, and the rest of the coins are cleared away. As long as both players take only one coin at each of their turns, the game continues until the pile is exhausted. The game has a finite number of moves, which is known in advance to both players. In Fig. 2.2, I (II) at the first black circle (decision node) indicates that it is Player I's (II's) turn. The ordered pair from following a decision node "down" represents (Player I's payoff, Player II's payoff). Player I plays first: if she chooses "down", both players get 1, and if she chooses "across", II gets an opportunity to make a decision. On II's move, if he chooses "down", I gets payoff of 0 and he gets 3, but if he chooses "across", the turn passes to I, and so on. If both players always choose "across", they both receive payoff of 100 at the end of the game.

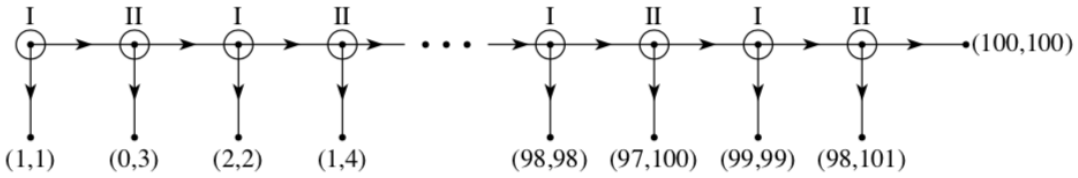

Figure 2.2: The Centipede Game. Figure source: (Ferguson, 2014).

Solution by the method of backward induction is as follows: At the last move, Player II will go down instead of across since that gives him 101 instead of 100. Therefore, at the next to last move, Player I will go down since that gives her 99 instead of 98. This continues until reaching the initial position, where I will go down rather than across because she receives 1 instead of 0. While the backward induction seems to give rise to "irrational" behavior in the Centipede Game, it is used here for illustrative purposes.

Pierpoint (2017) constructs an optimization "wrapper" that invokes the FANTSY fuel cycle simulator to examine how uncertainties in the nuclear power demand growth rate and reactor capital costs affect the decision to close the fuel cycle. The wrapper enumerates each branch of the decision tree and obtains objective function values for each branch. Once each branch is scored, the method of backward induction is used to find optimal hedging strategies. Similarly, Carlsen (2016) examines time-wise uncertainties such as disruption in fuel supply to devise optimal hedging strategies in reactor deployment strategies. Due to the fidelity of the Cyclus simulator, coupled with the fine decision space examined, Carlsen relied on a custom PSwarm optimizer to obtain an approximate solution.

2.2 Multi-Objective Decision Making

Selection of an "optimal" nuclear fuel cycle transition is complicated by external costs – those costs that are paid by society as a whole rather than exclusively by consumers of nuclear power. The terms "full cost" and (less frequently) "real cost" of electricity generation have been borne from consideration of these externalities (Hubbard, 1991; UTEI, 2018; OECD, 2018). The challenge in examining these externalities arises when deriving a mechanism for estimating the costs of the impacts and identifying appropriate importance weightings.

Several aspects of nuclear energy often identified as external costs (both positive and negative) include liabilities from decommissioning nuclear facilities, security of supply, health and environmental impacts and radioactive waste disposal. Multi-objective optimization allows for trade-offs between these objectives, offering robust decisions. Flicker et al. (2014) reviewed 20 published fuel cycle systems analyses to determine the

most widely used quantitative metrics for comparing fuel cycle options. These metrics were grouped into 5 evaluation criteria: (1) economics, (2) safety, (3) waste management, (4) proliferation and (5) sustainability.

One challenge of multi-objective optimization is combining quantitative and qualitative metrics through utility function mapping for comparison of competing metrics. This translation requires expert knowledge, and often multiorganizational working groups. Another complication arises when considering the appropriate importance weightings of the different decision criteria, and even the traditional choice to simply linearly combine utility values from the different decision criteria (Marler and Aurora, 2004). Charlton et al. (2017) demonstrate this complexity in their development of a multiattribute utility analysis for the assessment of proliferation resistance in the nuclear fuel cycle. When an expert panel has been unavailable, utility functions are often taken as the min-max normalization of a quantitative objective function, with sensitivity of the criteria weightings considered by varying these parameters over their appropriate space (Pierpoint, 2011; Carlsen, 2013).

2.3 Extension to Game Theory

The *no-data* problem arising from decision making under uncertainty may be viewed as a special variety of two-person games, in which *Nature* moves ("chooses" a strategy) without considering payoffs, or whose payoff is zero, and so plays randomly. The second rational player chooses strategies that maximize his or her expected payoff using information available about *Nature*'s strategies. This class of games is termed *Games against Nature* (Milnor, 1951), though *Nature* is not *against* the rational player. In general, games against nature may have any number of stages and players.

Binsbergen and Marx (2007) examine the relationship between decision analysis and game theory, identifying the key features of both analysis approaches (Table 2.1). Binsbergen and Marx conclude that some sequential games can be analyzed by considering multiple decision trees, with each tree corresponding to an individual player. These trees must also account for the dependence of the payoffs on the actions of the other players. A key difference in a game theoretic approach is the allowance of mixed strategies – optimal strategies as long as the decision maker randomizes over actions that each maximize his or her expected payoff. When this situation arises in a pure decision analysis framework, the decision maker is instead indifferent between the two strategies. For this situation, Binsbergen and Marx developed extended decision analysis. While the two may be mathematically equivalent in some cases, insights into the strategic interaction between decision makers can be gained by examining nuclear fuel cycle transition using a game theoretic lens.

Table 2.1: Key features of decision analysis and corresponding counterparts in game theory.

Decision Analysis	Game Theory
Set of alternatives	Strategy set
Chance and unknown events	Moves of *Nature*
Results	Payoff mapping
Solution concept	Equilibrium concept

Pierpoint (2011) proposed and briefly examined a Government-Industry interaction model. Pierpoint examined industry response to an increase in the 1 mill per kWh nuclear waste fee under the Nuclear Waste Policy Act of 1982. In her work, Pierpoint assumes that

the government absolutely benefits from the transition to fast reactors as the obligation of the government stops at waste management. The variable waste fee is exogenously applied in the simulation. Under a different guise, the variable waste fee could be viewed as a first stage strategy.

Resource allocation in safeguards and security applications to nuclear facilities have been examined using a game theoretic approach. Avenhaus (2013), Butler et al. (2013), and Ward and Schneider (2016) each examine a facility operating with static material flows, independent of the dynamics of material flow resulting from the nuclear fuel cycle system in which the facilities are emplaced. However, in addition to individually examining an enrichment and reprocessing facility, Ward explores a systems approach to optimization across the two facilities. Ward considers a Cournot game, aimed at optimal safeguards such as random inspections against a proliferation scenario. An "efficient frontier" is identified that depicts payoff as a function of budget. Butler et al. incorporate uncertainties in a sequential decision making model, though do not examine recourse decisions following uncertainty resolutions, which is equivalent to solving for the expected value solution.

2.4 Fuel Cycle Simulation

Nuclear fuel cycle simulators are systems dynamics models, consisting of a network of levels and flows. Generally, the flows between levels are static properties of the system. The key utility of fuel cycle simulators is achieved when dynamic flows or connections between levels are incorporated, allowing for analysis of transient periods during technology changes (Piet et al., 2009). Such analyses help develop a comprehensive

understanding of the fuel cycle. Many fuel cycle simulators are currently in existence (Juchau et al., 2010; Huff and Dixon, 2010; Feng et al., 2016). While all are developed for similar purposes, large variations are seen in physical fidelity and processing time. In general, lower fidelity simulators achieve a reduction in required processing power while losing physical distinction between fuel cycle scenarios. Conversely, higher fidelity simulators sacrifice processing time in order to track constituent components of material flows.

According to Jacobson et al. (2010), "the real value of a model is how many 'Aha!' moments it gives you". Fuel cycle simulators model the dynamic transition from an initial state to an end state, providing natural resource needs and technology requirements, material flows and their compositions, and other time-dependent fuel cycle data. The minimum requirements to define the initial state of the nuclear fuel cycle are the nuclear electricity generating capacity, including reactor types and their fuel requirements. Then, users define a transition scenario that typically includes reactor deployment and reprocessing capacity deployment schedules to meet a set nuclear electricity demand by the end of the simulation (end state).

DYMOND was first developed at Argonne National Laboratory for the Gen IV Fuel Cycle Crosscut Group and is the predecessor for many systems dynamics codes in use today (Yacout et al., 2004). Materials are lumped into fission products, minor actinides and several types of U and Pu, and radioactive decay is not implemented. Typical run times are less than a minute for scenarios lasting over a century with month-long time steps, which users may vary. Easy interpretation of results from the DYMOND code are prioritized over model sophistication and complex algorithms, leading to allowance of scenario failure. For

instance, a scenario failure may occur when there is insufficient feed material to fulfill reactor demand, resulting in unmet user-defined energy demand.

VISION was developed at Idaho National Laboratory for the U.S. DOE Advanced Fuel Cycle Initiative as an evolution of the DYMOND code (Yacout et al., 2005; Jacobson et al., 2010). VISION has been used as the campaign's primary analysis tool for several years. Similarly, VISION simulates a nuclear fleet, though the fleet may be composed of multiple reactor types, each with a user-specified fuel cycle and reprocessing strategy. VISION allows a fair amount of flexibility for the user to define material routing between fuel cycle facilities and material transformations occurring when material passes through facilities. 81 individual isotopes are tracked and radioactive decay is modeled along with up to 5 different fuel compositions for a single type of fuel to more accurately reflect the isotopic evolution of fuel through multiple passes through a reactor. Typical run times for VISION are less than 5 minutes.

Most recently, the Cyclus fuel cycle simulator was developed as a next-generation fuel cycle simulation tool as part of the DOE FCR&D program (Huff et al., 2016). Of the simulators developed for DOE initiatives, the Cyclus code offers the highest physical fidelity in representing the nuclear fuel cycle, with the ability for users to select an acceptable tradeoff between physical fidelity and computation time for their needs. This ability is due to Cyclus's modular ecosystem of loadable, interchangeable, plug-in libraries of fuel cycle component process physics. For instance, users interested in waste impacts may select detailed modules for separations facilities and track material at the isotopic level. Typical run times for transition scenarios such as those examined by Djokic et al. (2015) are 2-3 minutes.

METHODS

The methods used in this dissertation are presented in the following three chapters: Nuclear Fuel Cycle Simulation, Multi-Objective Decision Criteria, and the Nuclear Fuel Cycle Transition Scenario. The VEGAS nuclear fuel cycle simulator is described in Chapter 3. Its performance is compared to the Verifiable Fuel Cycle Simulation Model (VISION) code, originally developed as part of the U.S. Department of Energy Advanced Fuel Cycle Initiative studies. Documented are enhancements to the original VEGAS code that allow for added realism and distinction between fuel cycle transition strategies. The preconditioner capability of the VEGAS code is discussed. Chapter 4 introduces the decision (fuel cycle evaluation) criteria and associated fuel cycle metrics with which each player in the nuclear fuel cycle transition game chooses his or her strategies. Each player chooses his or her strategy based on a unique set of decision criteria, introducing complex interactions between the two. The calculation of each fuel cycle metric considered here is documented. Finally, Chapter 5 describes the nuclear fuel cycle transition scenario (the Transition Game) examined in this dissertation. VEGAS simulation inputs, including high-level scenario parameters and fuel cycle metric coefficients, are documented in this chapter. The Transition Game's players, their available strategies and corresponding payoffs, and the solution concept are also documented.

CHAPTER 3: VEGAS NUCLEAR FUEL CYCLE SIMULATOR

VEGAS is a dynamic nuclear fuel cycle simulation tool. The alpha version was originally developed as a lightweight, fast-executing platform for scoping and selection of certain nuclear fuel cycle transition scenarios for more detailed analysis using a higher-fidelity simulator such as NFCSim (Schneider et al., 2005). The VEGAS code is chosen here as the analysis platform as it provides a physical material- and technology-constrained model of the nuclear fuel cycle while offering a reduced runtime over more detailed fuel cycle systems tools. Performance of a nuclear fuel cycle transition strategy is calculated using the general methodology depicted in Fig. 3.1. Fuel cycle transition paths are input to the VEGAS simulator, that then computes a material balance for each path. Objective function values (which measure the performance of a nuclear fuel cycle transition path) are then obtained using objective function calculators that require the material balance. These calculators are described in Chapter 4.

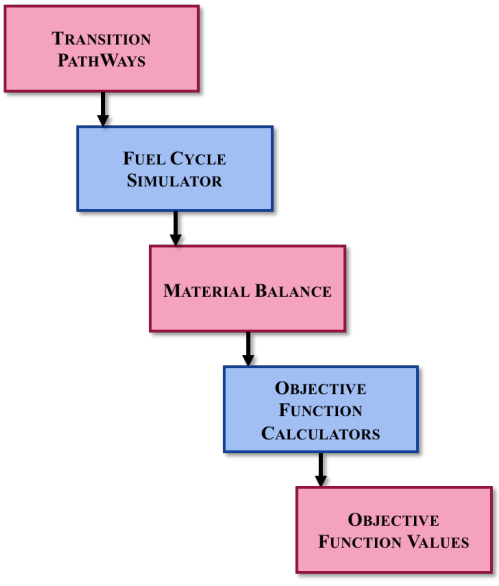

Figure 3.1: Basic objective function value calculation method. Input and output data in pink; calculation processes in blue.

Benchmark comparisons of the VEGAS code against the Verifiable Fuel Cycle Simulation Model (VISION) code, developed at Idaho National Laboratory (Jacobson et al., 2010), are documented and presented in Section 3.1. The material balance and reactor deployment algorithms utilized by VEGAS are summarized from Schneider and Phathanapirom (2016) in Section 3.2. Unique to the VEGAS simulator is a roll-back feature that undoes reactor build decisions if material- or technology-constraints are violated. Section 3.3 catalogs several enhancements to the VEGAS code that have been added to further distinguish and add richness to fuel cycle transition strategies. These enhancements include modifications to VEGAS's original material balance and reactor deployment algorithms.

3.1 VALIDATION

To test the performance of the VEGAS simulator, reactor deployment and used fuel inventories calculated from VEGAS are compared to those published in the Dynamic Systems Analysis Report for Nuclear Fuel Recycle (DSARR) by the Idaho National Laboratory (Dixon et al., 2009). Analyses in the DSARR were performed using the VISION code, originally developed as part of the U.S. Department of Energy Advanced Fuel Cycle Initiative studies. VISION is a systems tool of the nuclear fuel cycle programmed in the commercial system dynamics tool PowerSim Studio. The VISION model tracks 81 isotopes and chemical elements. A key difference between the two simulators is its use of reprocessing capacity – VISION always utilizes installed capacity to its fullest extent and inventories of separated used fuel are allowed to accumulate, whereas in the original version of VEGAS, used fuel is reprocessed annually only as reactor fuel is demanded, discussed further in Section 3.2.1.

Presented in the DSARR are three scenarios: once-through, nominal 1-tier, and nominal 2-tier. Complete description of the scenarios reviewed in the DSARR can be found in its Appendix C and validation of the VEGAS simulator is further illustrated by Schneider and Phathanapirom (2016). In the 1-tier scenario, reprocessed light water reactor (LWR) used fuel supports commercial fast reactors (FR), while in the 2-tier scenario, reprocessed LWR fuel is burned in mixed U/Pu oxide (MOX)-fueled LWRs, with FRs following as fuel residency and cooling times allow. Each scenario tracks the nuclear fuel cycle beginning in 2000 with 86 GW_e-year of nuclear electricity generation, ending in 2100. No nuclear electricity demand growth is observed until 2015, when demand growth is assumed to resume at a rate of 1.75 percent per year.

3.1.1 ONCE-THROUGH SCENARIO

All nuclear electricity generated in the once-through scenario is assumed to come from LWRs using standard uranium oxide (UOX) fuel. Fig. 3.2 shows the annual electricity generated during the simulation time period, with cumulative used fuel quantities in Fig. 3.3. Dashed and solid lines represent results from the VISION and VEGAS fuel cycle simulators, respectively. In the DSARR scenario, a geologic repository is assumed to begin accepting commercial used fuel beginning in 2017, with the repository filled to 63,000 tIHM with legacy UOX used fuel by 2038. At the beginning of the VEGAS simulation, a lump sum of ~45,000 tIHM legacy UOX used fuel is placed in dry storage to replicate the DSARR conditions. Fuel in reactors at start-up have a residency time of 5 years, after which used fuel enters wet storage.

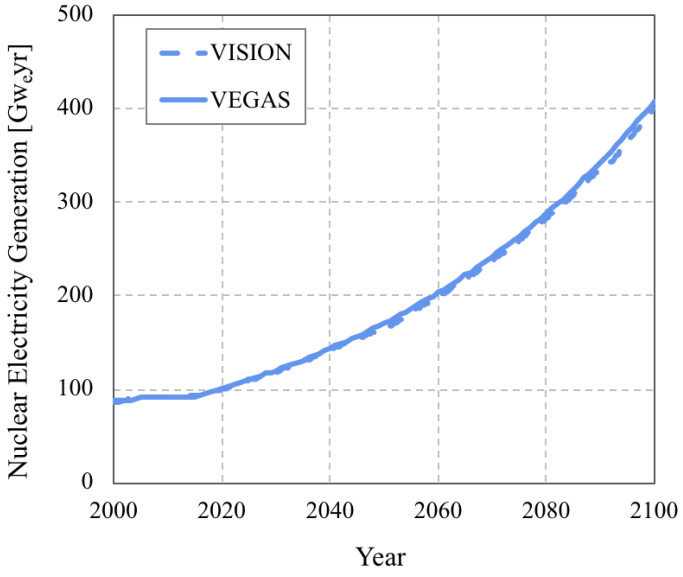

Figure 3.2: Nuclear electricity generation for once-through scenario.

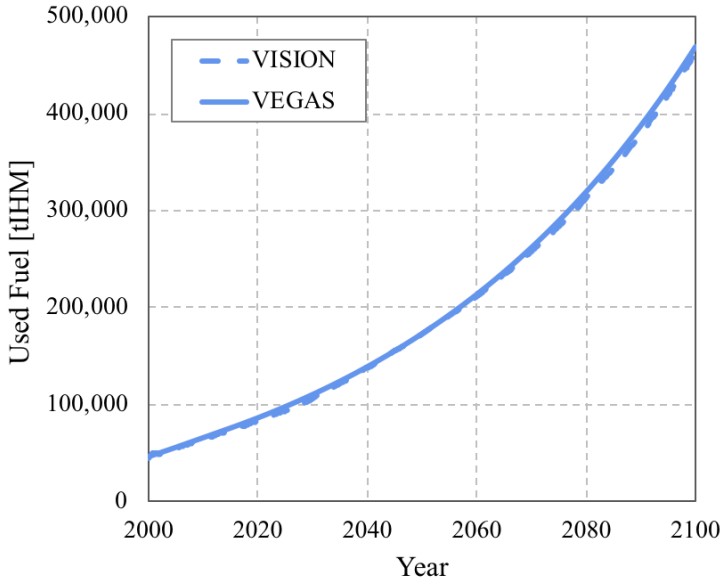

Figure 3.3: Used fuel quantities for the once-through scenario.

3.1.2 ONE-TIER AND TWO-TIER CLOSED FUEL CYCLE SCENARIOS

Total nuclear electricity demand growth for the 1-tier and 2-tier scenarios follow the same growth curve shown in Fig. 3.2. FR deployment is limited to less than 1 GW_e installed capacity per year for the first 5 years of commercial availability (2032 to 2036 for the 1-tier scenario, 2047 to 2051 for the 2-tier scenario) and again limited to less than 2 GW_e installed capacity per year for the next 5 years.

In the DSARR scenarios, LWR used fuel reprocessing begins in 2020 with a small pilot plant (800 tIHM per year capacity) with additional plants added (1600 tIHM per year capacity) as needed in order to ensure excess stores of used fuel are eliminated by 2100. Deployment of commercial LWR reprocessing is limited to less than 3,000 tIHM per year in a given year, and total capacity deployed by 2060 is less than 6,000 tIHM per year. In the 2-tier scenario, where LWR used fuel makes a pass in MOX-fueled LWRs before being used as FR fuel, a pilot MOX reprocessing facility has a capacity of 89 tIHM per year, with follow-on commercial plants at 178 tIHM per year. Since fuel is only reprocessed when reactors demand fuel in a VEGAS simulation, capacity added before 2031 goes entirely unutilized as FRs are only built in 2032. As a result, capacity added before 2031 in the DSARR scenarios is delayed for the VEGAS simulations such that the total amount of used fuel reprocessing capacity, integrated over time, is equivalent in both cases.

Fig. 3.4 shows the FR electricity generation in both scenarios in absolute and percentage terms. In the DSARR scenarios, FR deployment is restricted to less than 1 GW_e capacity per year (i.e., 2 reactors at 380 MW_e) for the first 5 years (2032 to 2036), and less than 2 GW_e capacity per year (i.e., 5 reactors at 380 MW_e) for the next 5 years (2037 to 2041) after commercial availability. FR deployment constraints are employed similarly for the VEGAS case. For both the 1-tier and 2-tier cases, general agreement is seen from both simulators. A lesser number of FRs are built in the nominal 1-tier VEGAS

simulation due to differences in installed reprocessing capacity utilization between the two simulators. A large amount of installed capacity goes underutilized until 2041 when the FR build constraint is lifted, since VEGAS reprocesses fuel on demand.

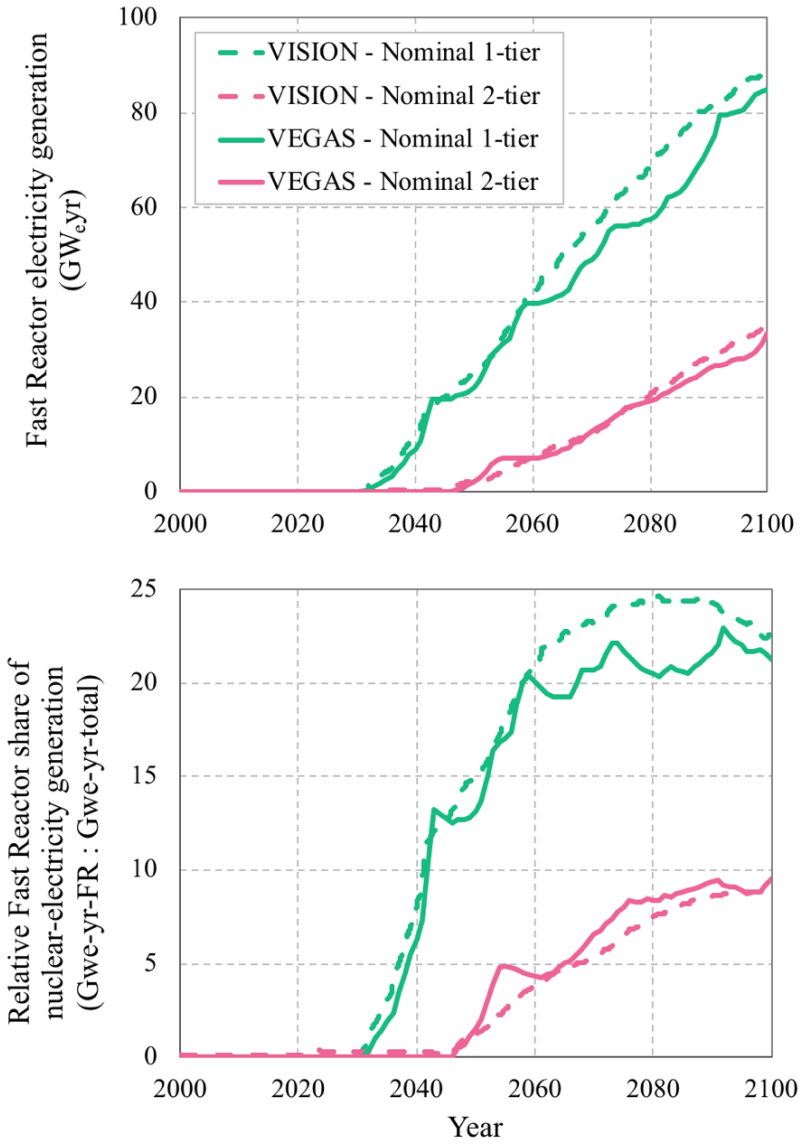

Figure 3.4: Fast reactor electricity generation in absolute and percentage terms for 1-tier and 2-tier scenarios (shared legend).

Used fuel quantities for the 1-tier scenario are shown in Fig. 3.5. The used fuel quantities for the 2-tier scenario are very similar, and so are not depicted. The total amount of used fuel generated using the VISION and VEGAS fuel cycle simulators follow the same trend, though the VEGAS simulator shows more used fuel generated through the lifetime of the simulation. The discrepancy in total used fuel generated between the two simulations is again due to their differences in handling reprocessing capacity. The VISION simulator always reprocesses fuel at the maximum capacity of the reprocessing plants, storing any excess actinides which are not used to fuel other reactors, while the VEGAS simulator only reprocesses fuel on demand. For this reason, a large portion of the installed capacity from 2031 to 2041 is underutilized for the VEGAS scenario, since FRs builds are limited in this time period.

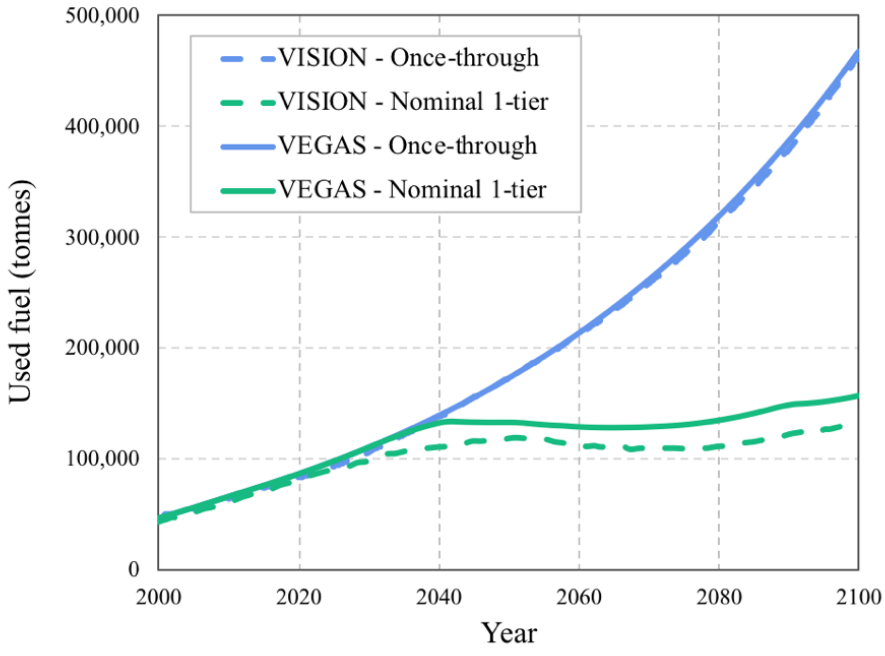

Figure 3.5: Used fuel quantities for the 1-tier scenario.

Fig. 3.6 shows the result of varying LWR reprocessing capacity on the number of FRs built in a simulation. The legend in the figure gives the total reprocessing capacity deployed in 2031 for the VEGAS cases. The precise deployment scheme for the data shown in Fig. 3.6 is not given in the DSARR report, so could not be matched exactly. Here, the limit on FR deployment is lifted for the VEGAS scenarios. When this restraint is no longer applied, the VEGAS simulator builds more FRs early in the simulation than the VISION simulator, with the difference becoming more pronounced with higher amounts of installed capacity. The number of FRs ultimately deployed by both simulators, on the other hand, is quite similar. VEGAS continues to deploy FRs even after the final increment of reprocessing capacity is built, while it appears that VISION ceases to do so. This may be related to the conservatism of the algorithm applied by VISION to determine whether a reactor which uses recycled fuel will have sufficient feed available to warrant being built. The "stair-step" pattern in the number of FRs predicted by the VEGAS simulator is likely due to the requirement for used fuel to accumulate in sufficient quantities prior to FR deployment. If sufficient quantities are unavailable, VEGAS does not build FRs due to its roll-back algorithm as material constraints occur (described in Section 3.2).

3.2 MATERIAL BALANCE AND REACTOR DEPLOYMENT CALCULATIONS

The reactor ordering algorithm creates a material- and technology-constrained electricity generation profile for each VEGAS simulation. The resultant material balance characterizes the flow of resources through the nuclear fuel cycle and its calculation includes a roll-back feature that ensures all reactor fuel requirements are met each year. The root purpose of the VEGAS simulator is this material balance calculation, which allows for quantifying the performance of fuel cycle transition strategies through the use of objective function coefficients. The material balance calculation is simplified by foregoing

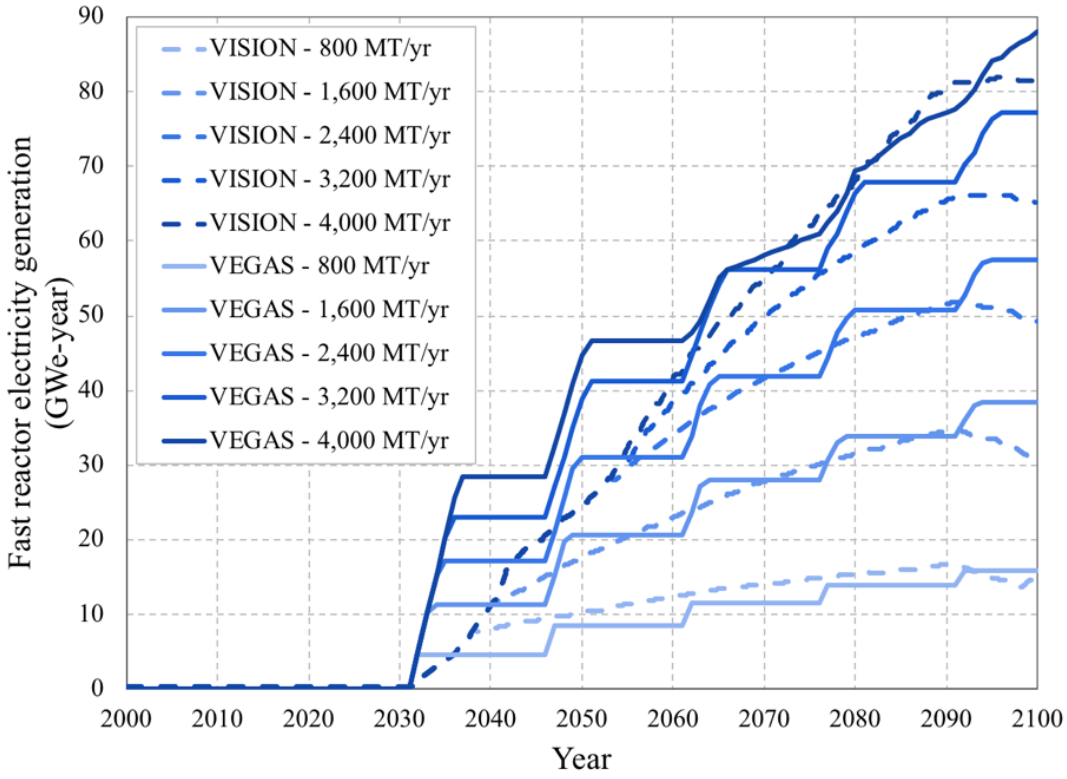

Figure 3.6: Impact of varying UOX reprocessing capacity on total fast reactor electricity generating capacity installed.

distinctions between reactors and fuel cycle facilities of the same general type, tracking material as continuously flowing streams rather than discrete batches, consolidating material flows into U, Pu, minor actinides (MA) and fission products (FP) components and omitting radioactive decay, allowing the VEGAS code to achieve a reduced runtime. Each simulation operates with a yearly time step, with seven primary processes carried out (Fig. 3.7). At the beginning of each year, old reactors are retired upon reaching their full lifetime. Then, new reactors are built to fulfill remaining electricity demands according to a user-input build strategy which may vary over time. A VEGAS simulation is defined by user-input files for reactor and nuclear fuel cycle parameters.

The number of reactor types is fully customizable. For each reactor type in a VEGAS simulation, an input fuel recipe is defined by the input U, Pu and MA mass fractions x_U, x_{Pu} and x_{MA} and the corresponding output fuel recipe is defined by the output mass fractions y_U, y_{Pu} and y_{MA}. The output FP mass fraction is obtained through Eq. 3.1:

$$y_{FP} = (x_{U_i} + x_{Pu} + x_{MA}) - (y_U + y_{Pu} + y_{MA}) \qquad \text{Eq. 3.1}$$

The annual demand for reactor fuel of each type is calculated, and using the input mass fraction for each specified fuel component $x_{U,Pu\ or\ MA}$, the demand for U, Pu, or MA fuel components is obtained (Step 3, Fig. 3.7). Likewise, multiplying the annual mass of discharged fuel from each reactor type by the output mass fraction for the specified fuel component, $y_{U,Pu\ or\ MA}$, gives the amount of U, Pu, or MA contained in the used fuel for a given reactor type in that year.

Reactor types are subcategorized by their recycling tier: tier 0 reactors use virgin feed only, tier 1 reactors operate on a thermal neutron spectrum and at least some feed comes from tier 0 or 1 fuel discharges, and tier 2 reactors operate on a fast neutron spectrum with at least some feed coming from tier 0, 1 and/or 2 fuel discharges. Generally, recycled material flows upwards through tiers (e.g. recycled material from tier 1 reactors are burned in tier 2 reactors, but material from tier 2 reactors is assumed to be unsuitable for recycle into tier 1). Fig. 3.8 shows an example of the preferred methods for obtaining fuel for a tier 2 reactor. If a reactor is capable of using separated actinides, it first attempts to pull from existing stockpiles of Pu and MA (Circle 1). Then, if demand remains, it reprocesses used fuel, typically starting from the highest tiered reactors' used fuel, denoted "T2" for used fuel discharged from tier 2 reactors, to the lowest (Circles 2-4, typically in that order, although the user can specify any priority order).

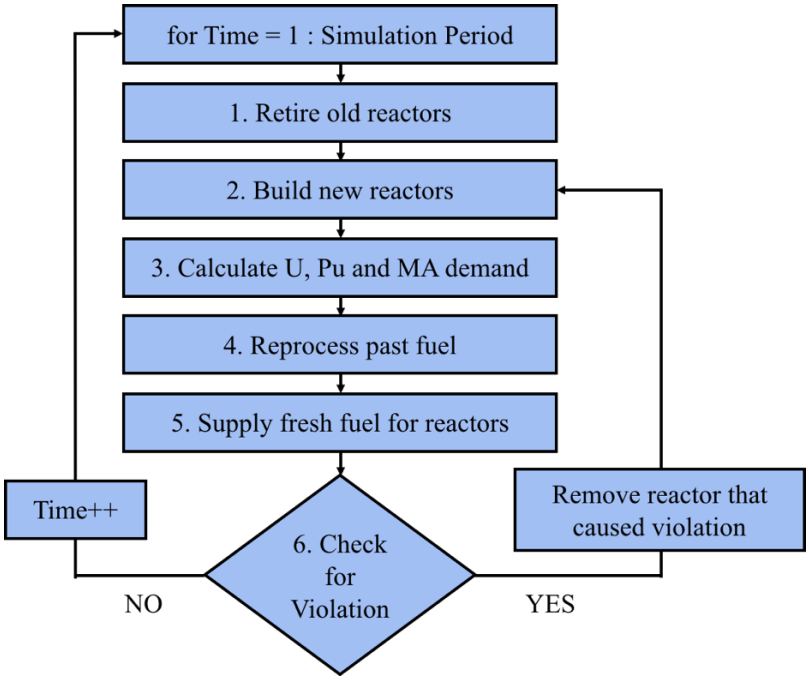

Figure 3.7: Primary processes comprising a VEGAS simulation.

The order in which a reactor type obtains feed from reprocessed used fuel is a user-defined reprocessing preference 'hierarchy'. This hierarchy is a list that determines the order in which a reactor type tries to issue reprocessing commands. The list may have any number of members (up to the number of reactor types in the simulation), and a reactor type is allowed to reprocess its own spent fuel. The "Check for Violation" step in Fig. 3.7 evaluates whether or not the demand for Pu or MA for each reactor type can be fulfilled through these means. If it cannot, then the simulation clock is rolled back to the year that the most recently added offending reactor type was built and removes it from the simulation. The simulation resumes from that point in time, with a reactor of another type (specified by user input) ordered to fill the demand gap. Otherwise, the simulation progresses to the next year.

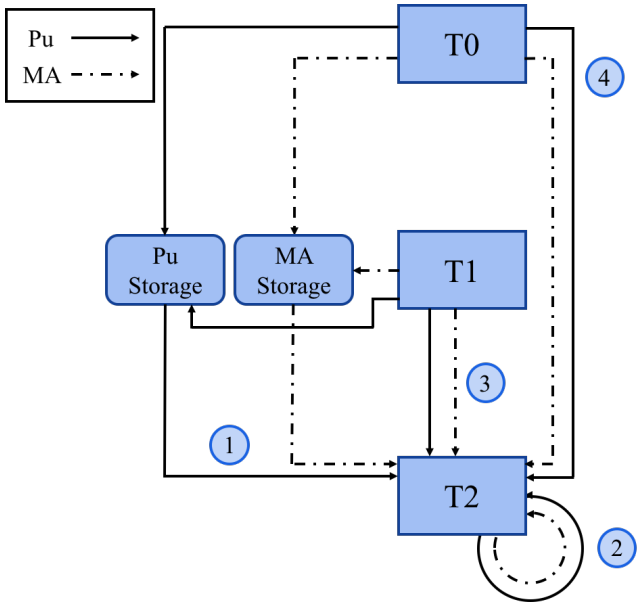

Figure 3.8: Typical tier 2 reactor used fuel reprocessing hierarchy. To fulfill their fresh fuel demand, Tier 2 reactors ('T2') pull from Pu and MA stores, followed by reprocessed T2, T1 and T0 used fuel, in that order.

3.2.1 Material Balance

The primary output from a VEGAS simulation is the material balance. By default, the VEGAS simulation has five front end (U mining and milling, conversion to UF_6, enrichment, fuel fabrication, and transportation to reactor site) and seven back end (SNF storage, transportation, and disposal; used fuel reprocessing; and high-level waste (HLW) vitrification, storage, and disposal) fuel cycle technologies. A user-defined mass flow in kg of throughput for the technology per kgIHM of reactor fuel for each reactor type must be specified. In this way, the number and type of front and back end fuel cycle technologies available to a VEGAS simulation are fully customizable.

The demand for reactor fuel of each type in kgIHM is calculated each year from user-input reactor power parameters and the total installed generating capacity of each reactor type that year. Input mass flows in kg of throughput for each front and back end technology per kgIHM of reactor fuel is then applied to the demand for reactor fuel to

obtain the total mass flow between each technology in kg of throughput per year in order to fulfill the total reactor fuel demand during the VEGAS simulation.

Each year, reactor fuel demand is processed starting from the highest tiered reactors to the lowest. If a reactor is capable of using separated actinides, it pulls from existing stockpiles of Pu and MA, respectively, to fulfill its Pu and MA demand. The amount of Pu and MA required to fulfill the demand for the reactor is decremented from stores; these stores are taken from the oldest first. If all stores are depleted and demand remains, used fuel is reprocessed according a reactor's reprocessing hierarchy. The hierarchy lists reactors in the order in which each type attempts to issue reprocessing commands to fulfill the remaining demand for Pu and MA. The amount of separated actinides required to fulfill the remaining reactor fuel demand through reprocessing of the available used fuel inventory of a reactor type in the hierarchy is obtained by applying output mass fractions for the specified fuel component. The oldest stores of used fuel are reprocessed first. Then, if the used fuel inventory of the first reactor in the hierarchy is depleted, the used fuel inventory of the next reactor type in the hierarchy is reprocessed.

Upon reaching the last reactor type in the hierarchy, two types of material balance violations may occur when attempting to satisfy fuel demand: (1) all used fuel stores for each reactor type in the hierarchy are depleted or (2) the reprocessing capacity is insufficient to reprocess the requisite used fuel. If a reactor type causes either of these material balance violations to occur, the VEGAS roll back feature is employed in order to conserve the material balance. Using the roll back feature, the VEGAS simulation reverts back to the year in which the last instance of the offending reactor type was built. Then, that reactor type is replaced with equivalent[1] generating capacity from a different

[1] If the generation gap between installed capacity and capacity demand is less than half the plant size of reactor type, then no reactor is built.

user-specified type of reactor and the simulation continues from that point on. Typically, the replacement reactor type is of a lower tier than the offending type but is not restricted to be so. Each reactor type should ultimately be replaced by a tier 0 reactor if necessary. Tier 0 reactors use U fuel, of which there is an unlimited supply.

Using the roll back feature, the VEGAS simulator is capable of maximizing the material and technology resources available. A user is able to input a build strategy that is 100 percent[2] of the highest tier reactor in the simulation, which would likely cause many material balance violations to occur, but the roll back feature replaces these reactors with lower tier reactors that will ultimately satisfy electricity demand. However, since only the last reactor added that causes the material balance violation to occur is removed, the maximum amount of reprocessing capacity or used fuel (and subsequently Pu and/or MA content) that remains within material- and technology-constraints is utilized, whichever is limiting. Currently, technology constraints are limited to a user-defined deployment schedule for used fuel reprocessing capacity, which is customizable for each reactor tier.

3.2.2 REACTOR DEPLOYMENT

The number and type of reactors in a VEGAS simulation are fully customizable. The primary inputs needed to specify a unique reactor type include an input/output fuel recipe as well reactor power parameters. Coupled with these inputs, an electricity generation profile of initial reactor types and a demand growth profile define a VEGAS simulation. The way in which VEGAS orders reactors for handling electricity demand, as well as the method for calculating demand, is described in Schneider and Phathanapirom (2016) and summarized here.

[2] A typical support ratio might be 4 tier 0: 1 tier 2 MW at equilibrium, depending on the material balance, which VEGAS will reach by replacing tier 2 reactors with tier 0 until the material balance violations cease.

New reactors are deployed in a VEGAS simulation to handle retirement of old reactors and demand changes. Demand changes are generally defined by specifying an annual demand growth rate in percentage increase per year, but an option also allows for a specific target generating capacity to be met by a certain year. The number of demand growth scenarios specified for the VEGAS simulation is only limited by the number of years in the simulation.

The type of new reactors built is determined by the demand growth, parameters affecting the initial generation fleet, and a reactor 'Try to Build' strategy. A unique 'Try to Build' strategy is comprised of two components: (1) the year in which the strategy is initialized, and (2) the desired build percentage of generating capacity from different reactor types in the simulation. For example, the deployment strategy beginning in 2040 may be 25 percent capacity from FRs and the remaining capacity from LWRs. The number of build strategies is again limited by the number of years in the simulation. When there is a shortfall between the currently-installed and target generating capacity levels, a reactor type specified by the build strategy is deployed only if its size is greater than one-half of the shortfall.

3.3 SUPPLEMENTAL VEGAS CAPABILITIES

Several enhancements to the VEGAS code have been made and are documented in the following subsections. These enhancements allow for added distinction and richness between fuel cycle transition strategies, incorporation of realistic uncertainty evolutions as well as realistic technology deployment schedules, and closer benchmarking against existing, verified simulators. In turn, these enhancements allow for endogenous decision making within the simulator itself. Not all of these capabilities are utilized in the analysis described in Chapter 6 but are documented here for completeness.

3.3.1 REPROCESSING CAPACITY UTILIZATION

The original VEGAS code determined the amount of used fuel to be reprocessed each year solely based upon the Pu and MA requirements of reactors demanding fuel in a given simulation year (Section 3.2). Excess annual reprocessing capacity was not utilized in order to minimize the amount of separated Pu and MA present in the system. While the original reprocessing *on-demand* feature is a key functionality of the VEGAS code, it is at odds with the reprocessing algorithms used in other existing fuel cycle simulators that utilize reprocessing capacity to the fullest extent, with inventories of separated actinides allowed to accumulate (Schneider et al., 2005; Jacobson et al., 2010; Feng et al., 2016).

An option to utilize all reprocessing capacity (as used fuel quantities will allow) has been added to the VEGAS code, and is implemented with a user-input switch. The *full-capacity* feature may be specified for each year in the simulation and may be switched on or off contingent on conditions during a simulation. For instance, during a learning period when the 10 first mover FRs are deployed, the reprocess *on-demand* feature could be employed to avoid excess stockpiles of separated Pu and MA. During this period, information gained about FRs will drive future decisions based on technology costs and performance. If the transition calls to continue FRs builds, then the reprocess at *full-capacity* feature may be selected, allowing for the highest rate of FR deployment based on material- and technology-constraints.

The added feature allows for improved benchmarking against existing simulators. Fig. 3.9 shows the installed FR electricity generation when the LWR used fuel reprocessing capacity is limited to 800 tIHM per year, as calculated by the VISION simulator and as calculated using the reprocessing *on-demand* and *full-capacity* features from the VEGAS simulator. While both reprocessing options of the VEGAS simulator follow the same trend as the VISION simulator, the number of FRs installed with the *on-demand* feature is

consistently less than predicted results from either the VISION simulator or, as expected, the *full-capacity* feature. Using VEGAS's *full-capacity* feature, excess capacity (installed capacity less the requirement to fuel separated actinide demand) is utilized and stockpiles of Pu and MA are allowed to accumulate. Later in the simulation, if a reactor demands Pu and MA at a rate slightly more than the annual installed capacity, it can pull Pu and MA from stockpiles rather than being removed from the simulation.

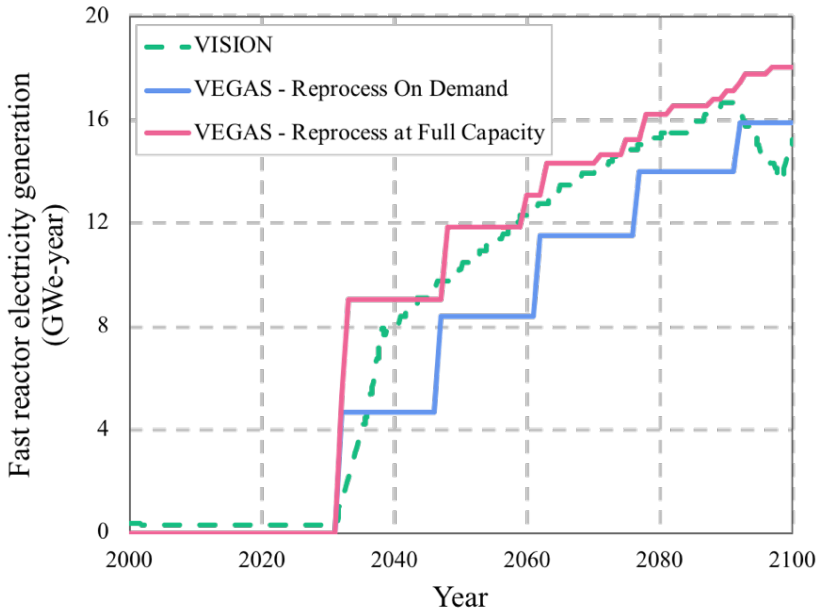

Figure 3.9: Comparison of fast reactor electricity generation as calculated using VISION and VEGAS's *on-demand* and *full-capacity* features for DSARR 1-tier scenario when reprocessing capacity is constrained to 800 tIHM per year.

3.3.2 UNIT-BASED LEARNING

The "learning by doing" phenomenon, was originally observed by Wright (1936) in the manufacturing sector. The concept reflects the increase (decrease) in productivity as experience is gained, leading to decreasing (increasing) costs for a good over time. One-factor learning curves (or "experience curves") are incorporated using Eq. 3.2 for used

fuel and HLW waste disposal technologies as well as reactor capital costs in the VEGAS simulator. In Eq. 3.2, C_0 is the unit cost of the first unit and C is the unit cost of the technology after G cumulative experience.

$$C = C_0 \cdot G^{\alpha} \qquad \text{Eq. 3.2}$$

Here, α is related to the learning rate by Eq. 3.3, where the term 2^{α} is the "progress ratio" which indicates the fractional reduction in cost after a doubling of cumulative capacity (or production).

$$L = 1 - 2^{\alpha} \qquad \text{Eq. 3.3}$$

For reactor capital costs, G represents the cumulative installed capacity (MW_e) and C represents the total overnight capital cost of the n^{th} reactor of a given type. The relationship between the n^{th}-of-a-kind (NOAK) total overnight capital cost (TOC) for a reactor of type r and the first-of-a-kind (FOAK) reactor of type r is shown in Fig. 3.10, along with the calculated learning exponent for a range of relative NOAK TOCs; since reactors in VEGAS are deployed in increments of the plant size (MW_e), the relative TOC is given in relation to the number of reactors of type r deployed. It is assumed that the NOAK TOC is the lowest realized cost of reactor construction and is reached once 9 units of reactor type r are deployed; the TOC for subsequent units is equal to the cost of the 9^{th} unit (EMWG, 2007). VEGAS takes the input FOAK and NOAK reactor TOC and computes the learning rate using Eq. 3.2 and 3.3.

Learning effects in SNF and HLW disposal were examined by Schneider and Phathanapirom (2015). For SNF and HLW disposal, learning is meant to capture aspects of waste disposal such as endogenous and regulatory learning which could cause the decline or rise as more waste is disposed. Such behavior has been seen in solid waste disposal in the U.S., where landfills charge a "tipping fee" per ton of garbage that has

increased over time (Braathen, 2004). Users input the unit cost of the first unit of SNF or HLW disposal C_0 (in $ per kg IHM or $ per kg IHM in HLW, respectively) as well as the progress ratio α.

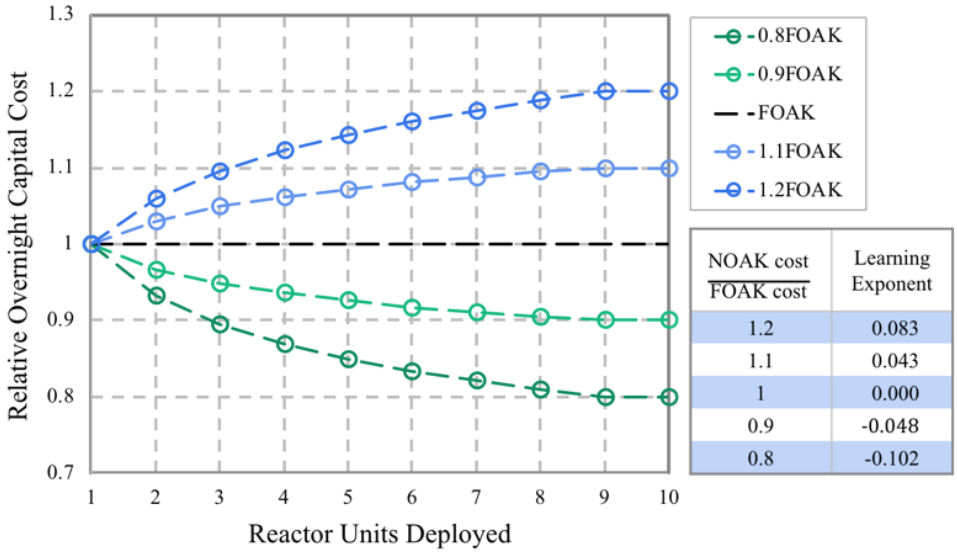

Figure 3.10: Learning effects on reactor costs as generating capacity is installed.

3.3.3 PRECONDITIONER PROOF OF CONCEPT

A key application of VEGAS is its ability to act as a preconditioner, offering an iterative method for accelerating the convergence of fuel cycle optimization problems. Operating as a preconditioner, VEGAS uses the results of a parameter sweep over a domain of interest to generate a fully-determined input to a more sophisticated fuel cycle simulator. The fuel cycle input information describes a reactor fleet that satisfies material balance and reprocessing capacity constraints while also maximizing a user-defined objective function.

The preconditioner application of VEGAS has been demonstrated by Schneider and Phathanapirom (2016). Two optimized UOX reprocessing capacity deployment schemes were selected from a suite of 16,384 VEGAS simulations, each with a

different UOX reprocessing capacity deployment scheme. Each of these deployment schemes is unique in its penetration of FR generating capacity due to VEGAS's material balance calculation. The two deployment strategies that were selected represent (1) the lowest time-integrated installed reprocessing capacity and (2) the latest possible start date for reprocessing capacity deployment, both while achieving the same target system TRU level at the end of the simulation, see Fig. 3.11. Using this preconditioner application of VEGAS removes the requirement of the user to define a reprocessing deployment scheme that obeys material and technology constraints, including the (in)ability of users to optimize such a deployment scheme. Jacobson et al. (2010) state that "balancing the amount of (used) fuel available from LWR reactors as a feed fuel to FRs with an aggressive growth rate is very difficult".

The enhancements to the VEGAS simulator described in this section allow for further distinction between fuel cycle transition strategies, adding richness and realism, furthering VEGAS's value and versatility as a preconditioner tool. Most notably, the reprocess used fuel at *full-capacity* feature, supplemental to the reprocess *on-demand* feature, and its allowed adjustments during a simulation allow realism during an initial learning period when building advanced reactor technology. Above all, VEGAS offers a reduced runtime (less than 5 s for simulations involving recycle in FRs) opposed to Cyclus's 2-3 min runtime for simulations such as those examined by Djokic et. al. (2015) or VISION's 5 min runtime for simulations such as those examined by Jacobson et. al. (2010). The comparison to Cyclus and VISION is chosen as they are the currently chosen DOE investigative fuel cycle simulators. In particular, Cyclus is under continuous development from users freely contributing modules that fit their fuel cycle analysis needs. This VEGAS preconditioner tool could be inserted as a module in Cyclus,

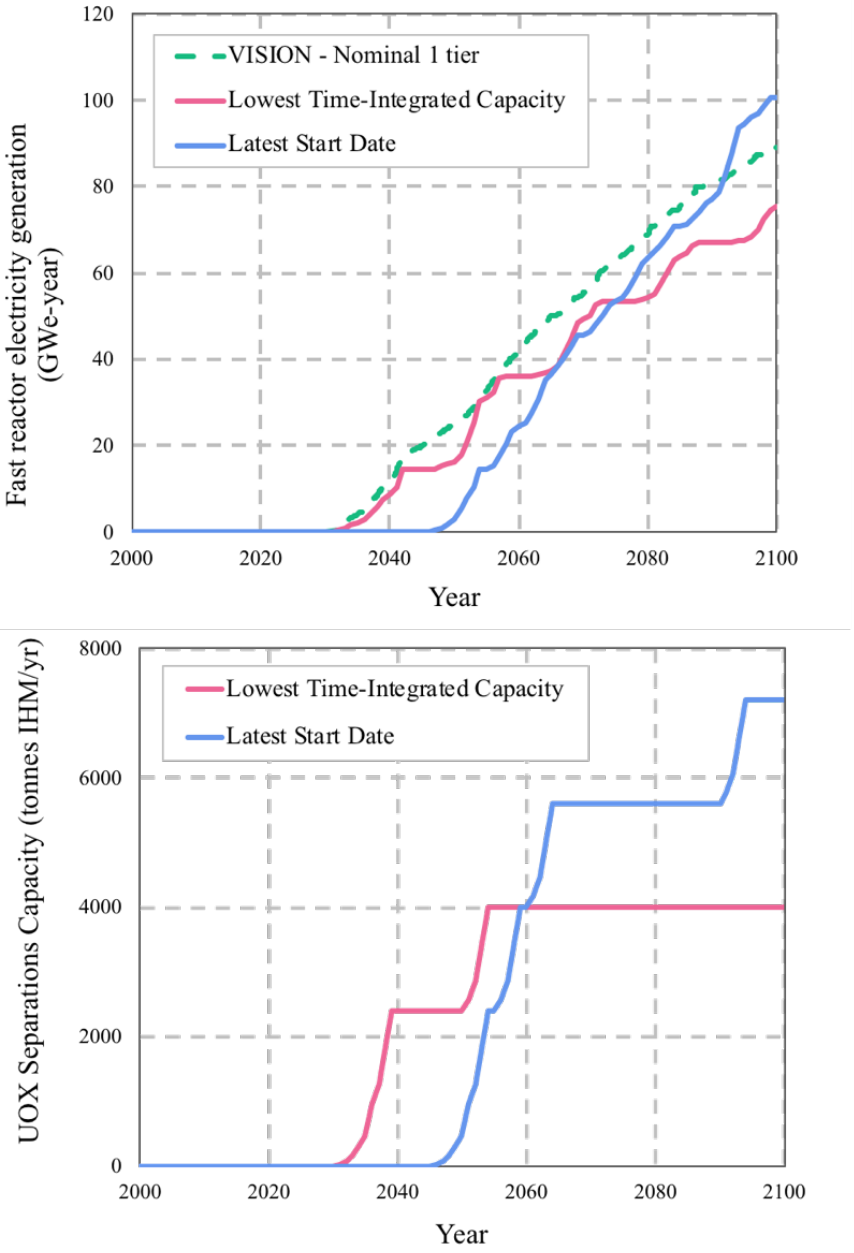

Figure 3.11: Optimized UOX reprocessing capacity deployment schemes.

allowing a larger solution space to be analyzed rapidly, and then input to the higher fidelity simulator for further realistic analyses. The potential coupling targets several shortcomings of the VEGAS simulator, such as its lack of discrete facility modeling, physical

fidelity through tracking materials at the isotopic level and time-dependencies arising from radioactive decay.

CHAPTER 4: MULTI-OBJECTIVE DECISION CRITERIA

The fuel cycle evaluation criteria and associated metrics that are used to measure the performance of a fuel cycle transition path are documented in the following chapter. Fig. 4.1 summarizes the calculation of a transition path performance. ORIGEN is invoked for each reactor type prior to the VEGAS simulations to perform burn-up and decay calculations for reactor fuel. Isotopics from ORIGEN are rolled up into U, Pu and MA fuel components for VEGAS's input and output fuel recipes. Detailed isotopics from ORIGEN are used to calculate objective function coefficients when necessary. Then, fuel cycle transition paths are input to the VEGAS simulator to calculate a material balance. This material balance is fed to metric calculators that ultimately score the performance of the transition path. Reactor modeling using ORIGEN is discussed in Section 4.1. In Section 4.2, the fuel cycle evaluation criteria are described, and the calculation of the metrics used to quantify these criteria is documented. The evaluation criteria chosen here are economics, waste management and proliferation resistance.

4.1 REACTOR MODELING

Reactor fuel burnup calculations were performed using the Oak Ridge Isotope Generation (ORIGEN) code included in the SCALE 6.2 package (Rearden and Jessee, 2016). ORIGEN tracks 2,237 isotopes and allows for the explicit simulation of all pathways of transmutation from neutron interactions, fission and decay. Spent nuclear fuel (SNF) is then characterized by (1) nuclide concentrations, (2) activities, (3) radiotoxicity, (4) decay heat, and (5) gamma-ray emission rates.

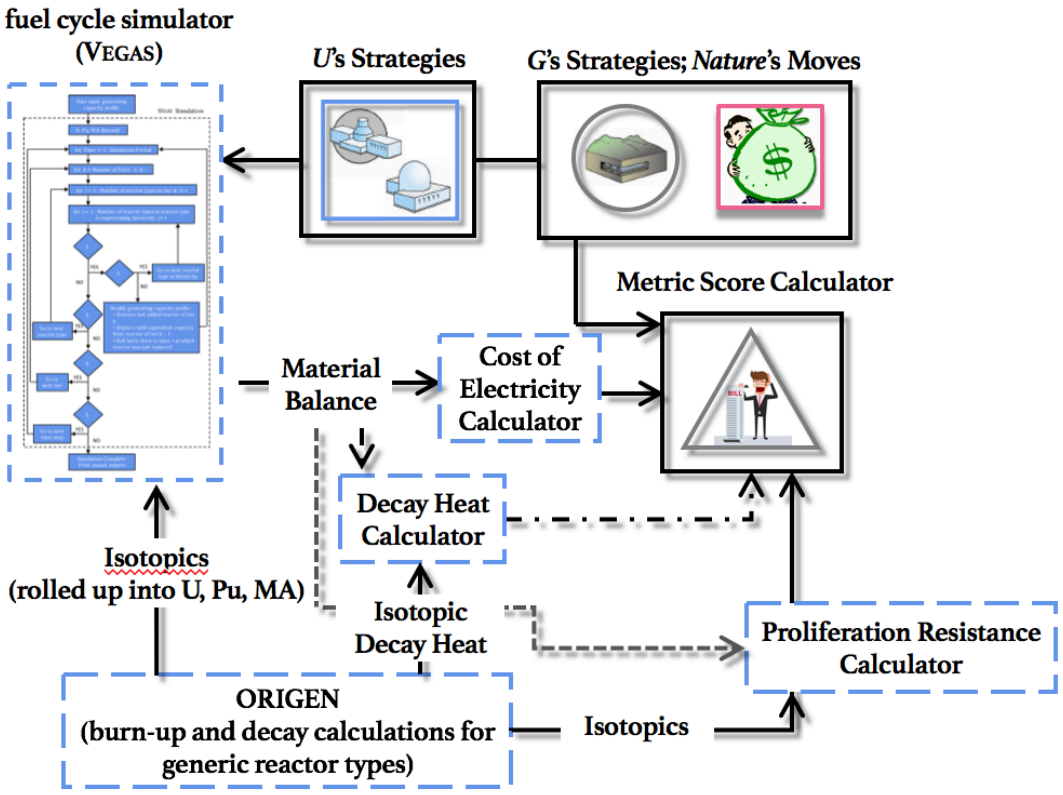

Figure 4.1: Overview for calculation of transition path performance using ORIGEN, VEGAS fuel cycle simulator and metric calculators.

Fuel depletion calculations in ORIGEN solve the Bateman equations (Eq. 4.1) that describe nuclide concentrations for the radioactive decay case of an n-nuclide series in linear chain (Gauld et al., 2011; Cetnar, 2006). In a transmutation system (reactor core during operation) nuclides are constantly transmuted due to interaction with a particle flux, consisting mainly of neutrons. The decay constants that govern the Bateman equations for a decay case are then substituted by transmutation constants, calculated using Eq. 4.2. The transmutation constant $\lambda_{i,j}$ is interpreted as the probability of the i^{th} nuclide production

per unit time from the destruction of the j^{th} nuclide as a result of nuclear interaction with the particle flux or through nuclear decay.

$$\frac{\mathrm{d}N_1}{\mathrm{d}t} = -\lambda_1 \cdot N_1$$
$$\frac{\mathrm{d}N_i}{\mathrm{d}t} = -\lambda_{i-1} \cdot N_{i-1} - \lambda_i \cdot N_i \tag{4.1}$$

- N_i is the concentration of the i^{th} nuclide
- λ_i is the decay constant of the i^{th} nuclide and $I = 2, \ldots, n$

$$\lambda_{i,j} = b_{i,j}^{\mathrm{d}} \cdot \lambda_j^{\mathrm{d}} + \int \Phi \cdot \sigma_{i,j}(E) \cdot \mathrm{d}E \tag{4.2}$$

- λ_j^{d} is the decay constant of the i^{th} nuclide
- $b_{i,j}^{\mathrm{d}}$ is the branching ratio of the j^{th} nuclide decay into the i^{th} nuclide
- Φ^x is the neutron flux
- $\sigma_{i,j}$ is the cross-section for production of nuclide i during interaction with nuclide j

Fuel depletion calculations are dependent on nuclear decay data and neutron cross sections[3], as well as user input initial nuclide concentrations and an input power that defines the neutron flux and irradiation time. One-group cross section data is obtained from reactor libraries that contain burnup-dependent cross sections. A coupled transport and depletion calculation is used to generate one-group cross sections that remove energy and spatial dependencies of the cross section. The interpolated one-group cross section is then obtained through flux-weighting of neutron energies and averaging of geometry and

[3] While decay data are well known, cross section data have larger uncertainties and are problem dependent for a system, which is (not limited to being) characterized by fuel type, enrichment, burnup, assembly design, fuel temperatures, moderator properties, etc. Then, accuracy of ORIGEN is determined by the accuracy of the nuclear data.

material masses. As operation continues, these one-group cross sections must be recalculated due to material transmutations; therefore, a library of 1-group cross sections are constructed and interpolated using ORIGEN's Automated Rapid Processing (ARP) module (Bowman and Gault, 2010).

A number of pre-generated reactor libraries are available in SCALE 6.2. For instance, a reactor library is available for a Westinghouse PWR 17x17 fuel assembly, with enrichments from 0.5 to 6.0 weight percent ^{235}U, and burnups up to 70.5 GWd per MTU. The ARP utility code then interpolates between pre-generated cross-sections to obtain appropriate cross sections based on user-defined parameters, such as burnup, enrichment and ^{239}Pu, depending on reactor type. When a pre-generated reactor library is unavailable for a given reactor type and burnup, a custom library is obtained by executing a coupled multigroup transport and depletion calculation using SCALE's TRITON code, a modular, general-geometry, reactor physics sequence (DeHart and Bowman, 2017). Decay calculations are performed using the Bateman equations to obtain the fuel compositions following a specified cooling (decay) time.

Relevant reactor modeling parameters for each reactor type are given in Table 4.1. Selection of these reactor types is based on the 2014 DOE-NE Evaluation and Screening Study (Wigeland et al., 2014). Calculated reactor fuel recipes are given in Table 4.2. ORIGEN simulations as well as guidance on reactor modeling methodology were performed and provided by staff research scientist Kenneth Dayman at Oak Ridge National Laboratory.

4.1.1 Reprocessing Methodology

Used fuel from each reactor type may be reprocessed. For simplicity, the methodology for obtaining the isotopic composition of recycled U and TRU elements and

Table 4.1: Primary reactor modeling parameters from Appendix B of DOE's Evaluation and Screening Study (Wigeland et al., 2014).

A. EG01 – LWR			
Nuclear Power Plant	Core Thermal Power (MWth)		3000
	Core Power Density (MWth/tIHM)[a]		30.84
	Net Thermal Efficiency (%)		33
Nuclear Fuel Composition	Average Discharge Burn-up (GWd/tIHM)		50
	Fuel Composition	Initial Nuclear Material	LEU
		235U/Total U (%)	4.21
B. EG02 – HTGR			
Nuclear Power Plant	Core Thermal Power (MWth)		350
	Core Power Density (MWth/tIHM)[a]		74.07
	Net Thermal Efficiency (%)		50
Nuclear Fuel Composition	Average Discharge Burn-up (GWd/tIHM)		120
	Fuel Composition	Initial Nuclear Material	LEU
		235U/Total U (%)	15.5
C. EG24 – SFR			
Nuclear Power Plant	Core Thermal Power (MWth)		1000
	Core Power Density (MWth/tIHM)[a]		55.55
	Net Thermal Efficiency (%)		40
Nuclear Fuel Composition	Average Discharge Burn-up (GWd/tIHM)		73
	Fuel Composition	Initial Nuclear Material	U-TRU-Zr
[a] Core power density is calculated using 3 power cycles at 540 days each, with a 30 day refueling time: $\text{core power density}\left[\frac{\text{MW}_\text{d}}{\text{tIHM}}\right] = \beta\left[\frac{\text{GW}_\text{d}}{\text{tIHM}}\right] \cdot \frac{1}{\text{Total days in operation [d]}} \cdot \frac{1000\ \text{MW}}{\text{GW}}$			

separated fission products is given here in generic form. The method is referred to as `reprocessUF()`. The isotopic composition (isotopics) for fresh reactor fuel is input to

ORIGEN and a depletion calculation with the appropriate reactor library is performed using the (1) core power density, (2) fuel discharge burnup and (3) reactor operating time (online and offline time periods). The depletion calculation outputs the isotopic composition of irradiated, used fuel at discharge and performs a decay calculation to a user-specified cooling time. The decay calculations yield the isotopic composition at the specified cooling time(s), decay heat and gamma emission spectra of the used fuel.

Table 4.2: Reactor fuel recipes from ORIGEN fuel depletion and decay calculations.

Reactor Type	LWR	HTGR	SFR
Mass Fraction	Fuel Input Recipe (g per gIHM)		
x_U	1.00000	1.00000	0.66610
x_{Pu}	0.00000	0.00000	0.29571
x_{MA}	0.00000	0.00000	0.03819
	Fuel Output Recipe (g per gIHM)		
y_U	0.93439	0.92446	0.58709
y_{Pu}	0.01198	0.01242	0.23899
y_{MA}	0.05168	0.00278	0.02516

After a specified cooling time, used fuel is reprocessed and separated into two streams: (1) U, Pu[4] and TRU (product) and (2) FPs and MAs (waste). While ORIGEN gives the decay heat and gamma emission rate for each isotope contained in the used fuel, its constituents are not readily separable. The isotopic composition of the used fuel product

[4] For this work, reactor input and output recipes in VEGAS consist of only U, TRU and waste streams. U consists of NU for fabrication of fresh fuel for LWR or HTGR reactors, or for top off following FP and MA removal in SFRs. For higher fidelity reactor modeling, some optimization of input isotopics may be performed in which case disaggregating fuel components may be desired. Here, since no optimization is performed and all product streams of U and TRU are assumed to be input into FRs, Pu is not carried forward as its own material flow.

stream at discharge is then manually separated, on which a decay calculation is performed. The decay heat and gamma emission rate for the used fuel product stream are then obtained. The decay heat and gamma emission rate for the used fuel waste stream can then be taken as the remainder of the total used quantity and the product stream (Eq. 4.3).

$$W = F - P \tag{4.3}$$

- F is the decay heat or gamma emission rate of the feed fuel per kg IHM
- P is the decay heat or gamma emission rate of the fuel product stream per kg IHM
- W is the decay heat or gamma emission rate of the fuel waste stream per kg IHM

In summary, `reprocessUF()` comprises the following steps:

1. Obtain used fuel isotopic composition by performing a depletion calculation on fresh reactor fuel in ORIGEN
    a. Run decay calculations for used fuel isotopics to 10 years[5]
        i. Store decay heat and gamma emission rates
2. Separate U, Pu and TRU elements (product) from MA and FPs (waste)
    a. Run decay calculations for product and waste streams to 10 years
        i. Store decay heat and gamma emission rates
3. U, Pu and TRU elements are refabricated into reactor fuel on demand
    a. If excess U, Pu or TRU is produced from reprocessing, then store until demanded for fresh fuel
    b. Perform `reprocessUF()` again as needed

[5] The E&S Study assumes a 5-year cooling time, after which reprocessing is promptly completed and time required from fuel fabrication to fuel charging is 2 years. Dixon et al. (2009) assume a 10-year cooling time based on the decay heat wattage limits of current shipping cask designs, which can accept full loads of used fuel at current burnup levels approximately 6 or more years after discharge. Here, a "10-year cooling time" refers to time from discharge in LWR and HTGR reactors, reprocessing of used fuel, and fuel fabrication to fuel charge. Dixon et al. (2009) do propose a "efficiently functioning" system with variable cooling times. More TRU may be tied up in used fuel not yet available for reprocessing, but fuel handling costs could be minimized, with a tradeoff on fuel quality.

Fig. 4.2 depicts the sequence in which `reprocessUF()` is used for the tier 1 recycling scenario. ORIGEN input files used for reactor modeling in this dissertation are available from the author upon request.

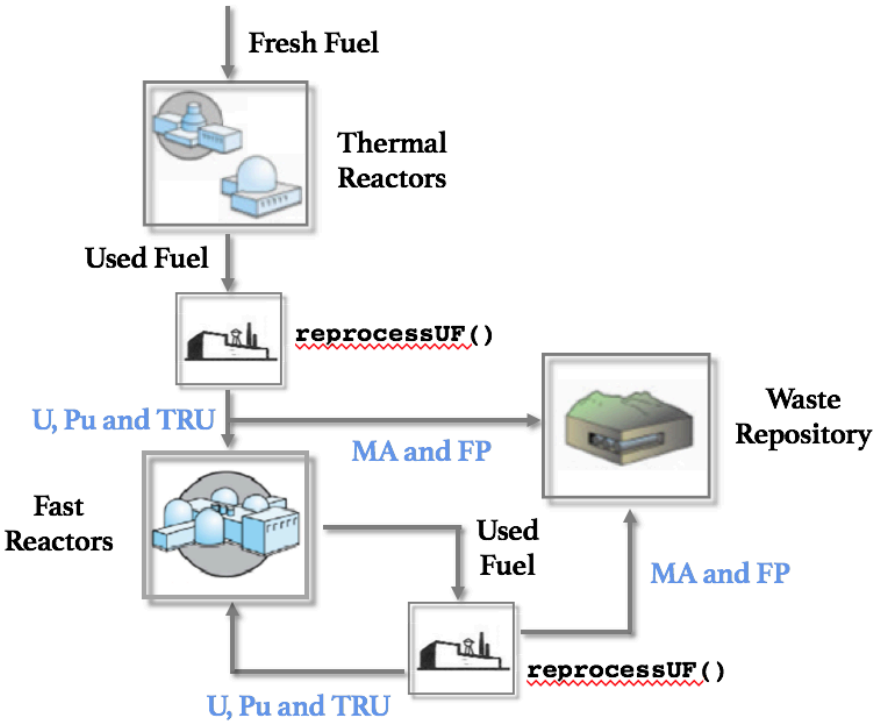

Figure 4.2: Iterative `reprocessUF()` method as applied to tier 1 recycling scenario, where ORIGEN is invoked for fuel depletion calculation (fresh fuel to used fuel); decay calculated performed for used fuel separated into product (U, Pu and TRU) and waste (FPs and MA) streams; product stream refabricated and fuel depletion calculation performed.

4.1.2 LWR AND HTGR MODELING

LWRs are modeled using ORIGEN's built in generic Westinghouse 17x17 PWR reactor library. HTGRs are modeled using a custom reactor library for uranium-oxycarbide (UCO) fuel, with a burnup to 120 GW_d per tIHM. The fuel residency

time for both reactor types is approximated at 5 years, with 3 batches per core. The ratio between reactor up and down times is taken to yield a capacity factor 90 percent. Decay calculations to 10 years are then performed. The reactor fuel schedule from initial charge to recycle and disposal is summarized in Table 4.3A.

4.1.3 SFR MODELING

For simplicity, the following methodology for reactor fuel recipes for SFRs is given only for utilizing discharged used fuel from LWRs. The methodology for obtaining reactor fuel recipes from recycled used fuel from HTGRs is identical. All calculations are performed assuming a base unit of 1 tIHM fuel.

Discharged used fuel from LWRs is recycled into SFRs, assuming a cooling time of 10 years[6]. Gram quantities of Pu and TRU isotopes, m_i, from discharged LWR fuel are obtained via the `reprocessUF()` method. Wigeland et al., (2014) give the weight percentage of TRU in SFRs as 13.9 percent. Then, the input of isotope *i* in g per tIHM of SFR fuel is given as follows:

$$\frac{m_{i,out}}{\sum_i^I m_{i,out}} \cdot \frac{10^6 \text{ g}}{\text{tonne}} \cdot \frac{13.9}{100} = m_{i,in} \tag{4.3}$$

- $m_{i,out}$ is the mass of isotope *i* per tIHM of discharged used fuel from LWR fuel (g)
- $m_{i,in}$ is the mass of isotope *i* input to SFR per tIHM (g per tIHM)

Zr cladding is assumed at 10 weight percent per tIHM (Lee et al., 2016). NU is assumed to comprise the remaining mass of input fuel to SFRs. Fuel residency time as given in

[6] Decay calculations of TRU isotopes include ^{17,18}O (LWR used fuel) and ^{13}C (HTGR used fuel) isotopes. During decay, these isotopes are pathways for (α,*n*) reactions. This calculation must be performed when disaggregating the neutron dose rates of actinides and fission products.

Wigeland et al. (2014) is 3.6 years. Assuming a capacity factor of 90 percent, fuel irradiation times are given in Table 4.3B.

Table 4.3: Reactor fuel residency and decay time periods.

		Duration	Unit
A. LWR and HTGR			
Up Time (Cycle 1)	Subcycle 1:2	270	days
	Subcycle 2:2	270	days
Down Time		54	days
Up Time (Cycle 2)	Subcycle 1:2	270	days
	Subcycle 2:2	270	days
Down Time		54	days
Up Time (Cycle 3)	Subcycle 1:2	270	days
	Subcycle 2:2	270	days
Fuel Discharge		Immediate	
Decay Time		10	years
B. SFR			
Up Time (Cycle 1)		395	days
Down Time		65	days
Up Time (Cycle 2)		395	days
Down Time		65	days
Up Time (Cycle 3)		395	days
Fuel Discharge		Immediate	
Decay Time		10	years

To approximate continuous recycle in SFRs, the method `reprocessUF()` is performed following fuel irradiation at each reactor cycle's up time. The total FP and MA masses and their isotopics are collected and aggregated following each call of `reprocessUF()`. These mass flows are averaged over the three irradiation cycles (and between LWR- and HTGR-seeded SFRs) to obtain an average reactor output recipe for

SFRs. SFR used fuel and vitrified high-level waste (HLW) enter wet storage for 10 years prior to disposal.

4.2 Evaluation Criteria and Metrics

A group of Massachusetts Institute of Technology (MIT) faculty issued the study on The Future of Nuclear Power in 2003 (with a 2009 update) that identified four important challenges to ensuring that nuclear power remains a viable marketplace option at a time and at a scale that could materially mitigate climate change risks (Deutch et al., 2003; Deutch, 2009). The challenges examined were (1) cost, (2) safety, (3) waste management, and (4) proliferation risk. Flicker et al. (2014) reviewed twenty published fuel cycle systems analyses to determine the most widely used quantitative metrics for comparing fuel cycle options. Flicker et al. group the metrics into 5 evaluation criteria: (1) economics, (2) safety, (3) waste management, (4) proliferation and (5) sustainability. The first four evaluation criteria are analogous to those identified in the 2003 and 2009 MIT study. The metrics identified by Flicker et al. for the overlapping four challenging evaluation criteria are listed in Table 4.4. When possible, the evaluation criteria chosen here are guided by the Evaluation and Screening Study. Their importance is highlighted in their prevalence in past fuel cycle analyses.

The safety evaluation criterion is not examined in this work. As stated in the Evaluation and Screening Study, "promising fuel cycles are capable of safe deployment, with many having safety challenges comparable to the current U.S. fuel cycle. Enhanced safety is not provided by choice of fuel cycle but may be provided by the choice of fuel cycle but may be provided by the choice of implementing technologies and facility design."

Table 4.4: Summary of overlapping evaluation criteria identified by MIT (2003) and Flicker et al. (2014) with common quantitative metrics as identified by Flicker et al.

Metric		Units per MWh_e (unless specified)	
Economics			
Cost of Electricity		$	
Fuel Cycle Costs		Transportation Cost; Fuel Cycle Cost	
Difficulty of Fuel Handling		$\frac{\text{Mass consumed by fission}}{\text{Mass mined}}$	
Back End Costs		Marginal Cost of Avoiding TRU Disposal	
Safety			
Public or Occupational Dose		mSv	
Fission Product Mass Flow		tonnes	
Risk of Severe Core Damage		Risk for Reactor per year	
Waste Management			
Quantity	Mass of Waste	tonnes	
	Volume of Waste	m^3	
Quality	Radiotoxicity	Bq or Sv	
	Decay Heat	watts	
	TRU Mass Flow	tonnes	
	HM Mass Flow	tonnes	
	FP Mass Flow	tonnes	
Proliferation			
Enrichment Required		Fuel Loads Requiring Enrichment	
Material Attractiveness		Bathke FOM	FOM1
			FOM2
Stored or Disposed Weapons Useable Material		tonnes per year	
Weapons Useable Material Throughout Fuel Cycle		tonnes	
Transport Required		Distance Traveled by Fuel	

The cost of electricity is impacted by these choices in technology and facility design, and so influence the decision in fuel cycle option through the economics criteria. For example, ensuring adequate safety for nuclear reactors is folded into the design of the reactor, which is accounted for in its capital costs. Further, the sustainability evaluation criterion is not examined here. Carbon emissions of nuclear and renewables is favorable to that of traditional fossil fuel generators (Sathaye et al., 2011), making the argument between nuclear and fossil fuel generators evident from a sustainability standpoint.

4.2.1 ECONOMICS

The Evaluation and Screening Study evaluated relative differences in financial risk and economics among nuclear fuel cycle options, not the economic viability of nuclear power in the U.S. Likewise, a fixed demand for nuclear energy production is assumed, independent of the technology's economic viability in comparison with other energy generation technologies.

The economics evaluation criterion is evaluated by examining the levelized cost of electricity[7] (LCOE), which is the constant dollar ("real") price of electricity that would be necessary over the life of the plant to cover all operating expenses, interest and principal repayment obligations on project debt, and taxes and provide an acceptable return to equity investors over the economic life of the project. The VEGAS nuclear fuel cycle simulator outputs the annual LCOE; a summary of the calculation follows.

The LCOE consists of three components: front end fuel cycle charges, back end fuel cycle charges, and reactor charges. Default unit costs are assigned to each fuel cycle

[7] The E&S Study evaluated the levelized cost of electricity at equilibrium (LCAE), which is the cost of electricity which renders the net present value of the project cash flow equal to zero.

process in VEGAS, which are provided in Chapter 5. Reactor cost inputs are broken into capital costs (dollars) and annual operations and maintenance costs (dollars per year).

Front-end and back-end mass flows are used to calculate the total fuel cycle cost (C_{FC}) using Eq. 4.4. The present value function discounts the charge to the year the technology was employed through lead and lag times input to the VEGAS simulation. Back end costs are ascribed to the year that fuel was discharged and are calculated using a zero percent discount rate. These costs are assumed to be covered by a sinking fund from revenues generated while the fuel is in reactors producing electricity.

$$\mathrm{C}_{FC} = \sum_{i=1}^{I} M_i \cdot UC_i \cdot \mathrm{PVF}_i \tag{4.4}$$

- i indexes over all I fuel cycle technologies
- M_i is the mass throughput of the i^{th} technology
- UC_i is the unit cost of the i^{th} technology
- PVF_i is the present value function of the i^{th} technology

Reactor costs ($C_{reactor}$) are calculated using Eq. 4.5 and are the sum of the annual capital cost and fixed operations and maintenance (FOM) charges.

$$\mathrm{C}_{reactor} = \left(\mathrm{TOC} + \sum_{i=0}^{T_c-1} \mathrm{TOC} \times f_i[(1+r)^{T_c-i} - 1] \right) \times \frac{r}{1-(1+r)^{-T_o}} + \mathrm{FOM} \tag{4.5}$$

- TOC is the total overnight cost ($ per kW_e)
- FOM is the fixed operations and maintenance cost ($ per year)
- T_c is the duration (years) of construction
- T_o is the duration (years) of operation
- f_i is the fraction of TOC expended in year i of construction (summing f_i over T_c equals 1.0)
- r is the real discount rate (percent per year)

Given C_{FC} and $C_{reactor}$, the annual LCOE is then given by Eq. 4.6 where E is the total amount of electricity produced in that year in kWh.

$$\mathrm{LCOE} = \frac{\mathrm{C}_{FC} + \mathrm{C}_{reactor}}{E} \tag{4.6}$$

Here, the total cost of electricity is the chosen metric for the economics decision criterion (and the decision criterion will be referred to as the Cost of Electricity criterion from this point forward). The total cost of electricity is calculated using Eq. 4.7 and is then the total cost of producing nuclear electricity to meet demand requirements during the simulation.

$$\mathrm{COE} = \sum_{t=t_0}^{T} E_t \cdot \mathrm{LCOE}_t \tag{4.7}$$

- E_t is the total amount of electricity produced in year t in kWh
- LCOE_t is the levelized cost of electricity in year t in cents per kWh

4.2.2 WASTE MANAGEMENT

The radioactive waste repository size is controlled by radioactive decay heat (Hardin et al., 2011; Wigeland et al., 2006). Waste packages must be spread out underground in tunnels to keep repository temperatures within allowable limits. Further, the amount of SNF per waste package is limited by individual heating limits. The decay heat of SNF is dominated by fission products for approximately 50 years after discharge (for LWRs with burnups to 50 GW_d per tIHM). Major contributions during this period are from ^{137}Cs and ^{90}Sr, which reduce in decay power by 40 percent from 10 years to 30 years. More advanced reprocessing technologies may reduce short-term heat load to the repository (Shropshire et al., 2009). Later times see decay heat dominated by ^{241}Am, with

its 430-year half-life (Forsberg, 2015). Given the importance of the decay heat on the repository size, the waste management criterion is evaluated using the decay heat metric (and the waste management decision criterion will be referred to as the Decay Heat criterion from this point forward). The decay heat *H* in watts, of SNF and HLW is given as a weighted sum of its heat generating isotopes, given as:

$$H = \sum_{i=1}^{I} m_i \cdot h_i \tag{4.8}$$

- h_i is the decay heat of isotope *i* in watts per gram
- m_i is the mass of isotope *i* in grams

The isotopic composition of SNF and HLW to be disposed is obtained from ORIGEN reactor models (Section 4.1). The decay heat intensities per tIHM of reactor fuel (post burnup according to parameters in Table 4.1) are calculated using Eq. 4.9. In Eq. 4.9, $M_{r,t} \cdot \left(1 - r_{r,t}\right)$ and $M_{r,t} \cdot r_{r,t}$ are the mass of fuel (kgIHM) from reactor type r in year t ultimately disposed and reprocessed, respectively. y_{FP_r} is the mass fraction of FPs from reactor type r, which when multiplied by $M_{r,t} \cdot r_{r,t}$ gives the mass of FPs – the mass ultimately vitrified in HLW – in SNF from reactor type r in year t. Multiplying both the disposed and recycled fuel constituents by their respective decay heat constants and summing over every year in the simulation yields the total decay heat load to the repository. The decay heat constant of reactor fuel constituents (d_r^{SNF} and d_r^{FP} in watts per tIHM) is obtained using the `reprocessUF()` method described in Section 4.1. These decay heat constants are taken as the static decay heat rate at 10 years for both SNF and HLW, assuming a 10-year cooling time. Dynamic calculation of decay heat to the repository is

limited by VEGAS's omission of decay calculations. Then, the decay heat load to the repository is taken as the static decay following the 10-year cooling time.

$$D = \sum_{t=t_0}^{T} \sum_{r} M_{r,t} \cdot \left\{ \left(1 - r_{r,t}\right) \cdot d_r^{SNF} + y_{FP_r} \cdot r_{r,t} \cdot d_r^{FP} \right\} \tag{4.9}$$

- $M_{r,t}$ is the mass throughput of reactor type r in year t
- $r_{r,t}$ is the fraction of fuel discharged from reactor type r in year t ultimately reprocessed
- y_{FP_r} is the output FP mass fraction from reactor type r
- d_r^{SNF} is the decay heat constant of reactor type r from SNF
- d_r^{FP} is the decay heat constant of reactor type r from FPs

Calculated decay heat intensities are given in Table 4.5. These values are approximately consistent with values calculated by Burgelson et al. (2005), which calculated the decay heat for FPs and TRU for the time period between fuel discharge and 300,000 years for LWR SNF fuel with burnup of 40 MWd per tIHM. On a per kgIHM basis, SNF generated from LWRs contains less than half the decay heat power of HTGRs and SFRs. However, the fuel efficiency (burnup) of LWRs is less than half HTGRs. Further, used fuel from SFRs is continuously recycled, with a relatively low amount of HLW generated per kg IHM. Due to these factors, of the three technologies, LWRs perform the least well in terms of decay heat on a per MWd_e produced. This can later be seen in Chapter 6.

Table 4.5: Calculated decay heat intensities for used fuel and vitrified high-level waste.

	LWR	HTGR	SFR
SNF Disposal (watts per tIHM)	1.849E+03	4.145E+03	8.929E+03
HLW Disposal (watts per tFP in HLW)	1.322E+03	3.396E+03	2.738E+03
SNF Disposal (watts per GWd_t produced)	1.109E+02	6.908+01	3.058E+02

4.2.3 PROLIFERATION RESISTANCE

The Evaluation and Screening Study defines Proliferation Risk as:

> ***Proliferation Risk*** *– A broad definition of proliferation risk includes the risk of a nation ("host-state") obtaining nuclear weapons where that nation currently does not possess nuclear weapons. Proliferation risk involves a number of factors, both technical and non-technical, including considerations such as facility location and host state intent.*

Two technical considerations in the assessment of proliferation risk from the civilian nuclear fuel cycle are:

1. ***Material Attractiveness*** *– the usefulness of a material for proliferant activities*
2. ***IAEA Safeguards*** *– a series of technical measures designed to provide credible assurances to the international community that nuclear material remains in peaceful use*

Then, the proliferation resistance as defined by Charlton et al. (2017) is:

> ***Proliferation Resistance*** *– a measure of the relative increase in barriers [both intrinsic to the material or process and extrinsic (or engineered)] to impede the proliferation of nuclear weapons either by diversion of material by a state in possession of a system or theft of material by a terrorist or sub-national group.*

Charlton gives commonly agreed upon attributes that increase these barriers and as a consequence, the proliferation resistance:

1. *Extraordinary reduction in the quantity of special nuclear material (SNM), which includes plutonium and high enriched uranium*
2. *Avoidance of separated SNM streams (e.g., maintaining the plutonium physically mixed with minor actinides and/or fission products)*
3. *Designing the material or process such that it can be more readily safeguarded (in terms of both material accountancy and containment/surveillance)*

The Evaluation and Screening Study does not assess the proliferation risk, stating that most factors were beyond the scope of the study such as the facility location, facility

design and socio-political considerations. Further, the Evaluation and Screening Study reviewed evaluation groups and their corresponding fuel cycles when attractive materials (for proliferant activities) were used and determined that in principle these fuel cycles could be developed and implemented using unattractive materials by making different choices for fuel cycle operating parameters (e.g., reactor refueling interval and fuel burnup at discharge). While the E&S Study did not ultimately include a quantified proliferation resistance metric, it is included here to ensure a rigorous evaluation method and avoid a posteriori interpretation of the data.

Evaluation of the proliferation resistance of a given fuel cycle transition follows the methodology developed by Charlton et al. (2017)[8]. The key advance of Charlton's methodology is focus on the proliferation resistance on the material moving through the fuel cycle, allowing for assessment of the fuel cycle as a dynamic process, with material constantly in a state of change (either chemically, physically or radiologically). A series of attributes are used to determine a proliferation resistance value, and each attribute has some importance weighting and associated utility function that relates the changes in the value of the attribute to its effect on the proliferation resistance value. The static proliferation resistance value of process i is given by Eq. 4.10. The time- and mass-weighted average of the static proliferation resistance values for a fuel cycle comprising of $i = 1, 2, \ldots, I$ processes is termed the *total nuclear security measure* for a single fuel cycle, given by Eq. 4.10.

[8] The methodology was developed based on work performed in collaboration with Sandia and Los Alamos National Laboratories, and the Amarillo National Resource Center as part of an Accelerator Transmutation of Waste, Advanced Accelerator Applications, and the Advanced Fuel Cycle Initiative. The attributes and weights were developed through that effort were modified as part of collaboration with Oak Ridge National Laboratory in order to include a greater degree of safeguards-related metrics.

$$NS = \frac{\sum_{i=1}^{I} m_i \cdot \Delta t_i \cdot PR_i}{\sum_{i=1}^{I} m_i \cdot \Delta t_i} \tag{4.10}$$

- m_i is the amount of material in process i in significant quantities
- Δt_i is the time the material is in process i at the static proliferation resistance value for process i
- PR_i is the static proliferation resistance value for process i

$$PR_i = \sum_{j=1}^{J} w_j \cdot u_j(x_{ij}) \tag{4.11}$$

- w_j is the weight for attribute j
- u_j is the utility function for attribute j
- x_{ij} is the input value for the utility function for attribute j in process i

The average nuclear security measure during the decision making time period (calculated using Eq. 4.12) is the chosen metric for the Proliferation Resistance decision criterion.

$$\mathcal{NS} = \frac{1}{T} \cdot \sum_{t=t_0}^{T} NS_t \tag{4.12}$$

- NS_t is nuclear security measure in year t
- $\mathcal{NS}$ is the average nuclear security measure for a given fuel cycle transition path during the decision making time period

Each attribute with corresponding measures and weighting factors as given in Charlton et al. (2017) are given in Table 4.6. Significant quantities (SQs) of special nuclear material as defined by the International Atomic Energy Agency (2001) are 8 kg for Pu, 25 kg for HEU, 75 kg for LEU, 25 kg for ^{237}Np, 25 kg for elemental Am, and 20,000 kg

for elemental Th. Use of SQs allows for normalization of a variety of possible weapons material.

Table 4.6: Nuclear security attributes and weighting factors from Charlton et al. (2017). Weighting (Left w_j column) in Charlton et al. (2017) and (Right w_j column) re-normalized weighting used due to omitted attributes.

j	Attribute	w_j		Included
A. Material Attractiveness Level				
1	DOE attractiveness level (IB through IVE)	0.10		✓
2	Heating rate from Pu in material (W)	0.05		✓
3	Weight fraction of even Pu isotopes	0.06		✓
B. Concentration				
4	Concentration (SQs per tonne)	0.10		✓
C. Handling Requirements				
5	Radiation dose rates (rem per hr at distance of 1 m)	0.08		✓
6	Size/weight	0.06	×	×
D. Type of Accounting System				
7	Frequency of measurement	0.09	×	×
8	Measurement uncertainty (SQs/yr)	0.10	×	×
9	Separability	0.03		✓
10	Percentage of processing steps that use item accounting	0.05	×	×
E. Accessibility				
11	Probability of unidentified movement	0.07	×	×
12	Physical barriers	0.10	×	×
13	Inventory (SQs)	0.05	×	×
14	Fuel load type (batch or continuous reload)	0.06	×	×

This work only considers intrinsic barriers to proliferation (inherent to the material itself); correspondingly, eight attributes are not examined here, for reasons as follows. When an

attribute relies on assumptions on eventual safeguards[9] and their performance, it is not included here. These attributes include: (1) the frequency of measurement, (2) measurement uncertainty, (3) percentage of processing steps that use item accountability, (4) probability of unidentified movement and (5) physical barriers; (7, 8, 10, 11 and 12 respectively in Table 4.6). When an attribute relies on specific design parameters, especially those pertaining to advanced reactor types, it is not included here. These attributes include: (6) size or weight, (7) inventory and (8) fuel load type; (6, 13 and 14 respectively in Table 4.6). In the case of size or weight, the proliferation resistance is a binary function with the threshold being a single unit being greater than 2 ft^3 or 200 lbs. Specifically for advanced reactor types (FRs), the design of fuel loading is unsure. Recently, much work has investigated the performance of molten salt reactors, with aqueous fuel; the decision between molten salt or more traditional fuel assemblies is not presumed here. Lastly, VEGAS is incapable of tracking SQs of fissile materials at individual facilities. VEGAS aggregates facilities of the same general type, and tracks materials as continuously flowing streams rather than discrete batches. Especially in the case of co-located reprocessing and fuel fabrication facilities, SQs of material would be confined to the reactor facility in which they were produced. Instead, VEGAS aggregates this material as one stockpile, from which each reactor's fuel demand is fulfilled. Further, this issue may be complicated by decisions for reprocessing capacity deployment. Reprocessing facilities may be operated at full capacity, allowing for stockpiles of fissile material to accumulate to a greater degree than if facilities are operated on an on-demand basis, where only

[9] If the proliferation resistance of a given fuel cycle underperforms compared to another fuel cycle, the difference in metrics may give an indication of how heavily safeguards must be implemented in order to account for the inequality, see (Ward, 2012).

sufficient fuel to fulfill demand for Pu and MA is reprocessed. In the latter case, less reactors that operate on separated fuel are brought online (see Chapter 3). The tradeoff between the two operating procedures for reprocessing facilities may be the subject of future work. The calculation of static proliferation resistance values for all fuel cycle processes is given in Appendix A.

CHAPTER 5: NUCLEAR FUEL CYCLE TRANSITION SCENARIO

Results from the VEGAS nuclear fuel cycle simulator are used to inform a two-person general-sum multi-stage sequential game (Transition Game) where the two players represent two of the prime participants in a nuclear project: a government entity (Player *G*) and a utility generating company (Player *U)*. These players and their interactions create complexity, posing a major challenge in the development of nuclear infrastructure, specifically in a de-regulated electricity market. In the Transition Game, both players choose their strategies with complete information, that is, each knows the other's available strategies and corresponding payoffs. Players act sequentially, with *G* acting first with the option to offer incentives to alter *U*'s actions in a way that benefits *G*. Due to the sequential property of the game, each player makes their decision anticipating the influence of that decision on all subsequent decisions, both his or her own and the other player's. In this sense, the outer optimization problem of the first player is constrained by the inner optimization problem of the second player (and for each sequential sub-game). A key characteristic of the Transition Game is that one player's wins do not equal another's losses; this type of game is termed a general-sum game. Further, *Nature* is present as a player that moves randomly, representing uncertain parameters in the fuel cycle evolution. *G* and *U* are assumed to know the true probability of *Nature*'s moves.

The fuel cycle Transition Game is documented here. Section 5.1 gives the simulation parameters and available reactor technologies for the Transition Game. Section 5.2 describes the players (as well as *Nature*) in the Transition Game and their available strategies, including their interactions. The calculation of payoffs and the weighting between different decision criteria for the individual players is also documented.

Section 5.3 gives the scenario tree-based approach to stochastic programming solution concept to the Transition Game.

5.1 TRANSITION GAME

A VEGAS simulation is defined by user-input files for nuclear fuel cycle and reactor parameters. An ordering algorithm deploys reactor to fulfill an electricity generation profile for each simulation. These inputs are described in this subsection and text input files are available upon request from the author.

5.1.1 VEGAS SIMULATION PARAMETERS

A summary table of the Transition Game input parameters for the VEGAS simulator is given in Table 5.1. The WNA (2017a) projects an aggressive 2.3 percent[10] annual demand growth rate for nuclear electricity due to overall increasing electricity demands and the desire to reduce greenhouse gas emissions. The legacy used fuel stockpile is set to 0 tIHM for simulation purposes only. The transition assumes the current stockpile of SNF is sent directly to disposal, only considering the plan for future used fuel produced from the operation of nuclear reactors. The scenario begins in 2018 with an initial nuclear electricity generating fleet of 100 GW_e of LWRs, and VEGAS simulations are carried out through 2160, an additional lifetime of the longest operating facility, to ensure liability costs are accounted for. Objective function values are only computed through 2100, the end of the decision making period.

[10] The WNA estimates this demand growth rate until 2040.

Table 5.1: Summary of Transition Game electricity generation profile input parameters.

Year	Item	Value	Unit	Reactor Type
A. Simulation Parameters				
2018	Start Year	2018	yr	-
2018	Decision Making Start Year	2018	yr	-
2100	Decision Making End Year	2100	yr	-
2160	Simulation End Year	2160	yr	-
2018	Legacy Used Fuel Stockpile	0	tIHM	-
2018	Electricity Demand Growth Rate	2.3	%/yr	-
B. Reactor fleet data				
2018	Initial Generation Capacity	100	GWe	-
2018	Initial Capacity Data	100	%	LWR
2018	Year Initial Fleet Begins Retiring	2018	yr	-
2040	Year Initial Fleet Finishes Retiring	2040	yr	-
-	New Reactor Lifetime	60	yr	-
-	Reactor Construction Time	4	yr	-
C. Reactor "Try to Build" Strategies				
	Reactor Type (Primary | Replace With)	Value	Unit	
2035, 2045, 2055	LWR	100	%	
	HTGR	100	%	
	SFR | LWR	100 | 0	%	
	SFR | HTGR	100 | 0	%	

Fuel cycle unit cost data was primarily obtained from Shropshire et al. (2009)[11], with costs adjusted to current 2018-dollar amounts using the Bureau of Labor Statistics CPI Inflation Calculator. The value of unit costs for fuel cycle processes and their sources

[11] While dated, the 2009 Advanced Fuel Cycle Cost Basis represents the largest collection of fuel cycle cost estimates from a single economic working group.

are provided in Table 5.2. If a parameter is uncertain, the nominal value appears in Table 5.2, and its range of values and probability distribution is given in Section 5.2.

Table 5.2: Fuel cycle unit cost input data.

Technology	Value	Unit	Source
Uranium Mining & Milling	89	\$/kg U as U_3O_8	[1]
Conversion to UF_6	12	\$/kg U as U_3O_8	[1]
Enrichment	131	\$/SWU	[1]
Fuel Fabrication (LWR)	298	\$/kg IHM	[1]
Fuel Fabrication (HTGR)	3335	\$/kg IHM	[2]
Fuel Fabrication (SFR)	2668	\$/kg IHM	[2]
SNF Storage	358	\$/kg IHM	[1]
Reprocessing[a] (LWR and HTGR)	1850	\$/kg IHM	[1]
Reprocessing (SFR)	4002	\$/kg IHM	[2]
SNF Disposal	650	\$/kg IHM	[1]
HLW Disposal	6500	\$/kg IHM in HLW	[1]
Separated Actinide Storage	1050	\$/kg/yr	[1]
Separated Actinide Vitrification & Disposal	5967	\$/kg FP	[1]

[a] Includes HLW storage and vitrification
Sources: [1] (Shropshire et al., 2009), [2] private correspondence, Erich Schneider, former member of the AFCI Economic Working Group

5.1.2 Reactor Technologies

During the Transition Game, *U* may choose to adopt one of two advanced reactor technologies during the simulation: sodium-cooled fast reactors (SFR) or high-temperature, helium-cooled, graphite-moderated thermal reactors (HTGR). Transition to SFR technology closes the fuel cycle, while transition to HTGR technology continues operation of an open fuel cycle. These technologies are based on the

identification by the Evaluation and Screening Study (the Study) of promising fuel cycles with the potential for achieving substantial improvements compared to the current U.S. nuclear fuel cycle (DOE, 2014). If *U* determines the transition to either advanced technology is expected to be unfavorable, he may instead choose to continue building LWRs. Reactor modeling parameters are provided in Chapter 4, Table 4.1. In all cases *U* builds reactors to meet a user-specified nuclear electricity demand.

The Study groups fuel cycles into evaluation groups (EG) that represent groupings of fuel cycle options with similar physics-based performance. While the Study identified several promising EGs of nuclear fuel cycles, two are chosen for examination here, both of which rely on less proven, advanced reactor technology: EG02 (once-through HTGRs) and EG24 (recycle in SFRs). These technologies have been identified among six advanced reactor concepts by the Generation IV International Forum believed to represent the future shape of nuclear energy. About $6 billion over 15 years has been expended for further development of these technologies (WNA, 2017b).

The currently existing U.S. nuclear fuel cycle is represented by EG01, the once-through commercial LWR fuel cycle with direct disposal of spent nuclear fuel (SNF) in a geologic repository. EG01 is modeled under the assumption that existing LWRs are able to receive power upgrades through use of higher enrichment UOX fuel. Correspondingly, VEGAS's initial nuclear capacity is taken to be A(dvanced)LWRs with higher enrichment and burnup than their Gen II/III counterparts.

At equilibrium, EG02 is comprised of an HTGR fleet, requiring enriched NU to fabricate uranium oxy-carbide (UCO) fuel. The discharge burnup of HTGR fuel is assumed at 120 GWd per tIHM and is a significant improvement on even advanced LWRs. Fuel is

irradiated in fuel particles containing enriched U in a graphite matrix[12]. After irradiation, SNF is sent to disposal in a geologic repository.

EG24 considers recycle of metallic fuel consisting of transuranic elements (TRU) in SFRs. A U-TRU-Zr driver fuel is used in SFRs to achieve a break-even TRU conversion ratio in the equilibrium state. Following irradiation, discharged used fuel is reprocessed to recover TRU and recovered uranium that are recycled into the same SFR. FPs (as HLW) are sent to disposal. Fuel electrochemical[13] reprocessing and fuel fabrication facilities are co-located in a Consolidated Fuel Treatment Center[14]; interim storage and waste stabilization facilities may also occur in the same plant. During fuel reprocessing, fuel is separated electrochemically into waste and product streams via a molten salt electrolyte, and the fuel fabrication step is likely to be totally integral to the reprocessing technology. Fuel reprocessing employs the Multistep UREX+[15] separations process, involving molten salt chemistry at elevated temperatures, releasing many of the FPs, with the remaining material undergoing a final reduction step to create the necessary composition for use in

---

[12] General Atomics has the Modular High-Temperature Gas-cooled Reactor design with prismatic blocks with smaller graphite cylinders or "compacts" imbedded in vertical holes in the block, which contain the fuel particles. Another HTGR concept relies on UCO fuel in the form of billiard-ball sized graphite spheres or "pebbles" with the fuel particles imbedded within. The latter design is used in the HTR under construction in Shidaowan.

[13] Electrochemical reprocessing is used here as a blanket term for those reprocessing technologies that employ the "dry" process (e.g., pyrochemimcal, pyroprocessing and molten salt methods); that is, processes that do not employ aqueous solution chemistry.

[14] Co-located facilities are the preference for nonproliferation, radiation safety, and cost minimization purposes (Shropshire et al., 2009).

[15] The Plutonium-Uranium Extraction (PUREX) aqueous reprocessing technology produces two primary streams: U and Pu, and fission products and minor actinides (the primary HLW stream). The UREX+ process is a modified version of the PUREX process which has more product or by-product streams tailored to meet specific fuel cycle by-product objectives, such as a U/TRU product that can be used ins actinide burning fuel in FRs (Shropshire et al., 2009).

recycled fuel. The Multistep UREX+ separations process produces a U/TRU product that can be used as actinide burning fuel in fast reactors. In the Transition Game scenario, the SFR reprocessing hierarchy is set to prioritize HTGR fuel, as HTGR fuel has a higher Pu concentration at discharge. As a result, greater penetration of the SFR technology is expected.

5.2 Player Descriptions and Interactions

Each decision node is characterized by (1) the player acting and (2) that player's available decisions (strategies). For each player's decision node (and *Nature*'s chance nodes) depicted in Fig. 5.1, the available strategies are listed in Table 5.3. These decisions are made sequentially, allowing each player to observe the other's previous decisions and *Nature* moves, anticipate the other's future moves, and account for his or her own recourse opportunities. Descriptions of Players *G* and *U*, who represent a government entity and a utility generating company, follow, which include their available decisions at each stage and the decision criteria upon which these decisions are made.

At each decision node, the acting player aims to maximize his or her expected payoff. The expected payoff must be computed due to uncertainty in *Nature*'s moves, though other decision criteria exist that do not require a probability distribution on *Nature*'s moves. The expected payoff is calculated using Eq. 5.1. Each player's payoff is a function of their unique decision criteria and corresponding weights. This distinctive feature is responsible for introducing the complexity of interaction between the two players.

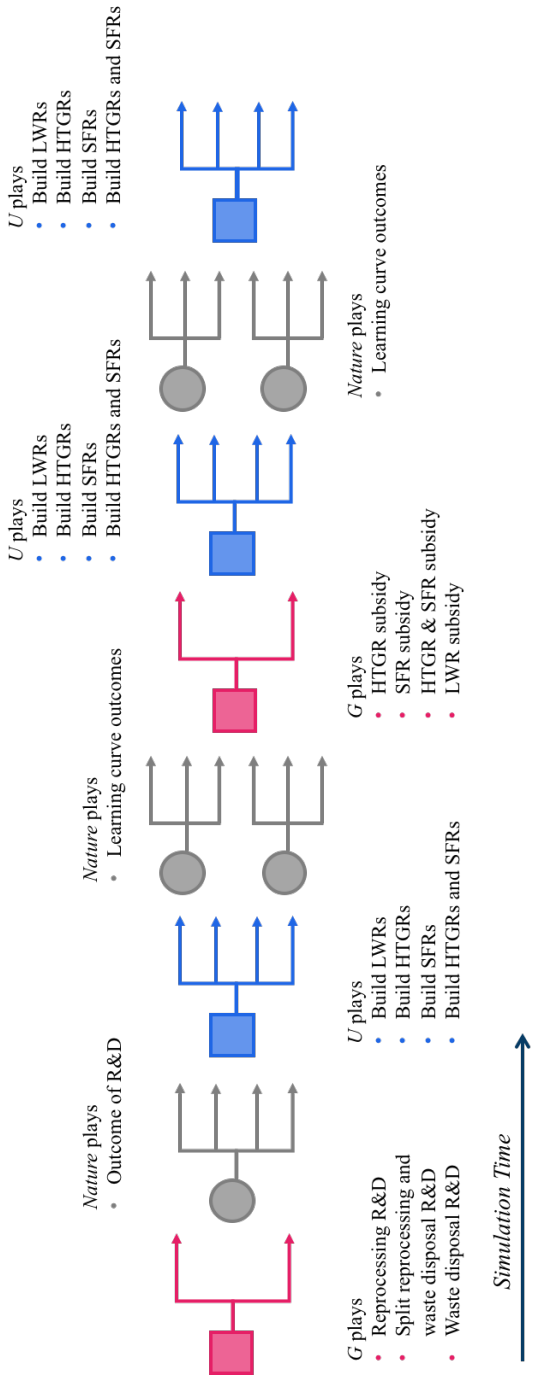

Figure 5.1: Transition Game decision tree with *G*'s decision nodes (pink), *U*'s decision nodes (blue) and *Nature*'s chance nodes (grey). See Table 5.3 for text.

Table 5.3: Ordering of sequential player decisions (and available strategies at appropriate decision node) and *Nature*'s moves (and possible outcomes at appropriate chance node) during Transition Game. Supplement to Fig. 5.1.

Stage No.	Player	Available Strategies
1	*G*	• Process R&D (reprocessing technology) level ○ Outcome of reprocessing cost • Product R&D (waste disposal technology) level
Chance	*Nature*	• Outcome of waste disposal cost ○ Probability affected by product R&D
2	*U*	• Build LWRs • Build HTGRs • Build SFRs • Build HTGRs and SFRs
Chance	*Nature*	• Learning curve outcomes for HTGRs and SFRs ○ n^{th} of a kind cost realized if advanced technology built
3	*G*	• Capital Subsidy for HTGR • Capital Subsidy for SFR • Capital Subsidy for LWR
4	*U*	• Build LWRs • Build HTGRs • Build SFRs • Build HTGRs and SFRs
Chance	*Nature*	• Learning curve outcomes for HTGRs and SFRs ○ n^{th} of a kind cost realized if advanced technology built
5	*U*	(Filtered by *U*'s upstream strategies) • Build LWRs • Build HTGRs • Build SFRs • Build HTGRs and SFRs

$$\mathrm{P}^{P} = \sum_{c} \mathrm{S}_{c}^{\vartheta} \cdot w_{c}^{P} \tag{5.1}$$

$\mathrm{S}_{c}^{\vartheta}$ is the score of (fuel cycle transition) path ϑ for criterion c, where c indexes over the criteria listed in Table 5.4 and w_{c}^{P} is the weight of criterion c for Player *P*. Fig. 5.2A depicts a single path ϑ, defined by *G*'s and *U*'s chosen strategies at their respective decision nodes (pink and blue squares, respectively, in Fig. 5.1) and all of *Nature*'s moves at his chance nodes (grey circles in Fig. 5.1). Then, ϑ is one path from root to leaf of the Transition Game decision tree, see Fig. 5.2A, and the set $\vartheta \in \Theta$ produces the entire tree depicted in Fig. 5.1.

The criterion score $\mathrm{S}_{c}^{\vartheta}$ for criterion c and path ϑ is calculated using Eq. 5.2 if seeking to maximize the objective function (Proliferation Resistance) or using Eq. 5.3 if seeking to minimize the objective function (Cost of Electricity or Decay Heat). f_{c}^{ϑ} is the objective function value for criterion c and path ϑ. The objective function value for each criterion is computed identically for both players (Chapter 4, Section 4.2), though this is not always the case. Then the score (and subsequent payoff constituent) for criterion c and path ϑ is the min-max normalization of f_{c}^{ϑ} over all objective function values. Using the min-max normalization avoids a posteriori interpretation of the data.

$$\mathrm{S}_{c}^{\vartheta} = \frac{f_{c}^{\vartheta} - \min\limits_{\Theta} f_{c}^{\vartheta}}{\max\limits_{\Theta} f_{c}^{\vartheta} - \min\limits_{\Theta} f_{c}^{\vartheta}} \tag{5.2}$$

$$\mathrm{S}_{c}^{\vartheta} = 1 - \frac{f_{c}^{\vartheta} - \min\limits_{\Theta} f_{c}^{\vartheta}}{\max\limits_{\Theta} f_{c}^{\vartheta} - \min\limits_{\Theta} f_{c}^{\vartheta}} \tag{5.3}$$

Table 5.4: Evaluation criteria and reference case baseline weighting factors.

	Criterion Weighting	
Evaluation Criterion (c)	Player G	Player U
Cost of Electricity	$0.\overline{3}$	1.0
Decay Heat	$0.\overline{3}$	0.0
Proliferation Resistance	$0.\overline{3}$	0.0

The Transition Game is a special case where only U's strategies affect the material balance since only U decides which reactors to build[16]. This feature allows for a significant reduction in the amount of VEGAS simulations required to analyze a large number of uncertainties. The VEGAS simulator is called for all U-paths ϑ^U, where ϑ^U are all combinations of U's strategies at each of his decision nodes (Fig. 5.2B depicts a single ϑ^U). In the Transition Game, G's strategies and *Nature*'s moves determine fuel cycle technology unit costs and reactor capital costs, and their associated probabilities.

Fig. 5.3 depicts the method for calculating payoffs. First, ORIGEN (described in Chapter 4) is used to simulate generic reactor types identified in the Study to obtain isotopic vectors for discharged reactor fuel. These isotopics are summed over U, Pu and MA constituents to obtain reactor input and output recipes for VEGAS. The VEGAS simulator is called for all $\vartheta^U \in \Theta$ with the simulation parameters listed in Table 5.1, resulting in a unique material balance. The material balance characterizes the flow of materials through the nuclear fuel cycle, in units of kg U, SWU or IHM. After VEGAS calculates the material

[16] In other transition games, G might be responsible for the deployment of reprocessing facilities, or *Nature* might determine losses in reprocessing, in which case this condition would not apply due to VEGAS's technology and material constraints. Even if G's strategies or *Nature*'s moves alter the material balance, only the subset of paths $\vartheta \in \Theta$ that result in a unique material balance must be simulated.

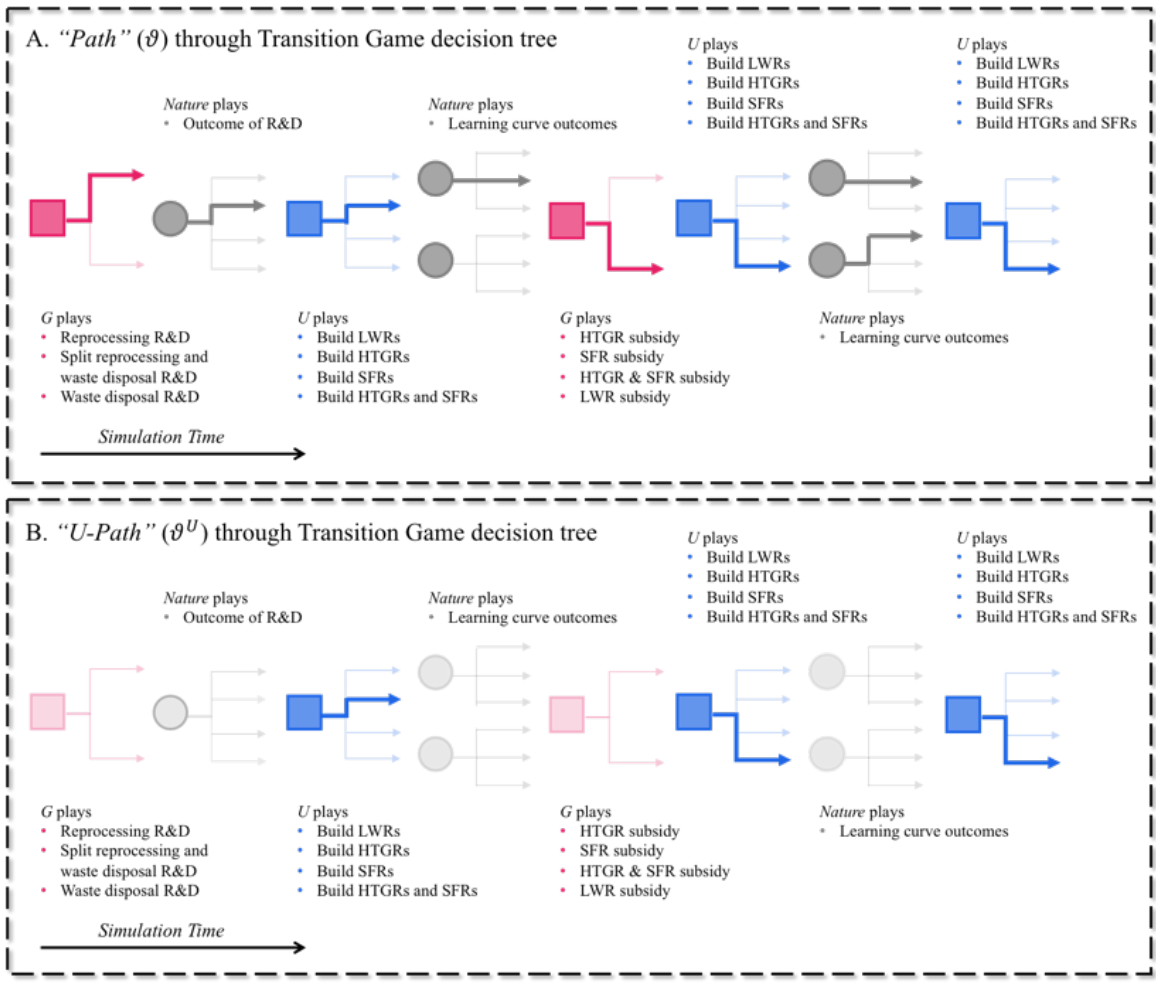

Figure 5.2: (Top) Depiction of single path ϑ through Transition Game decision tree consisting of all of *G*'s and *U*'s selected strategies at their respective decision nodes and *Nature*'s moves at his chance nodes. (Bottom) Depicted of a single *U*-path ϑ^U through Transition Game decision tree consisting only of *U*'s selected strategies at his decision nodes.

balance, the Cost of Electricity, Decay Heat and Proliferation Resistance calculators are invoked. These calculators take the material balance, *G*'s strategies and *Nature*'s moves as inputs and determine metric scores for each criterion and paths in Θ. In addition, the Decay

Heat and Proliferation Resistance calculators require the isotopic breakdown of SNF and HLW from burnup of reactor fuel.

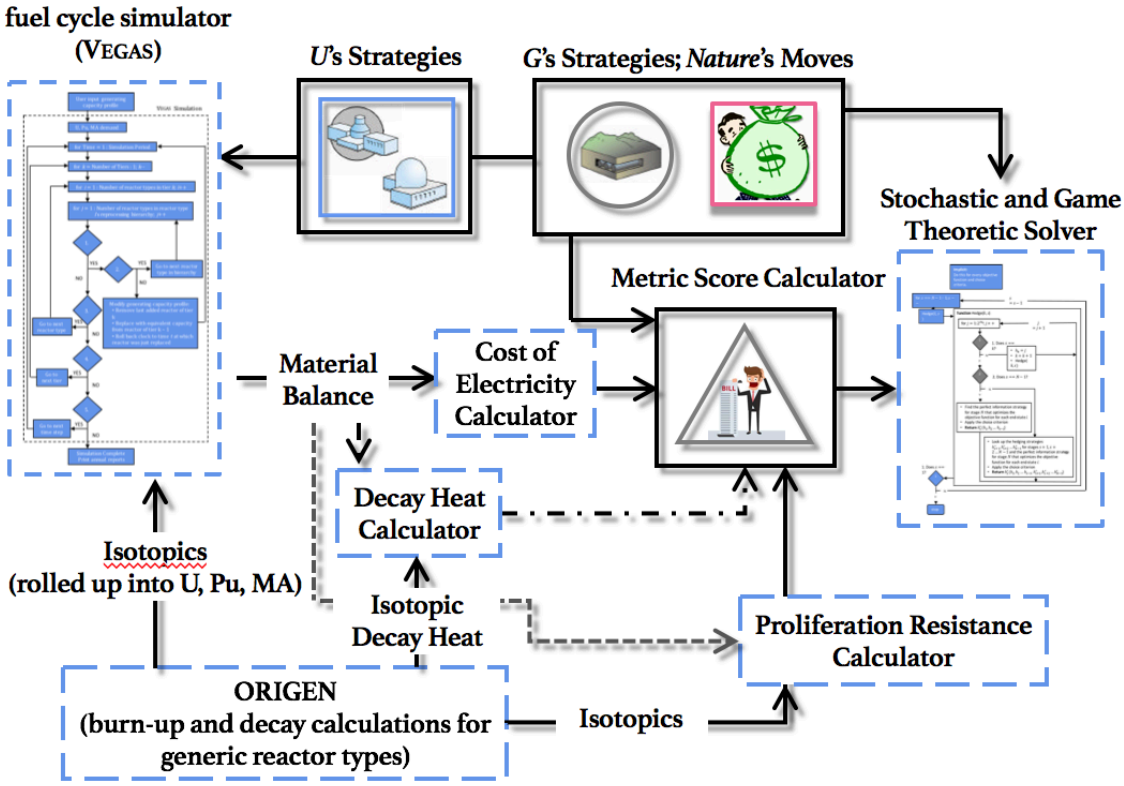

Figure 5.3: Overview of payoff calculation method and selection of optimal transition and hedging strategies.

5.2.1 PLAYER G

G's payoff is comprised of the Cost of Electricity, Decay Heat and Proliferation Resistance criteria scores. In the reference case, *G*'s three criteria are assumed of equal importance. Ensuring that nuclear power remains a viable marketplace option with other electricity generation technologies is advantageous if climate change policy is enacted. The

international consensus is that geologic repositories represent the best-known method for permanently disposing of SNF and HLW generated from nuclear power production. Siting, construction and licensing of a geologic repository is assumed federal responsibility (DOE, 2013). Since the decay heat from SNF and HLW ultimately determine the size of the repository needed, minimizing the heat load is favorable. Lastly, from a national security standpoint, the need for developing a proliferation resistant fuel cycle is apparent.

G's Decisions (Available Strategies)

G's intent is to influence *U* to adopt reactor technologies that benefit her. The available strategies to influence the transition are process research and development (R&D), product R&D and capital subsidies.

Strategy 1: Process R&D

The initial unit cost for a technology is c_0. *G* may choose an investment level, $b_{process}$, into process R&D which reduces the unit cost of a technology through improvements in efficiency. The technology examined here is the UREX+ aqueous reprocessing technology that separates U, Pu and MA for recycle in higher tiered reactor types. Due to difficulties in correctly parameterizing the result of process R&D, the result is assumed known in the Transition Game for demonstration purposes only (Balachandra and Friar, 1997).

Used fuel separation proceeds using aqueous reprocessing that isolates used fuel into its elemental components. The traditional Plutonium-Uranium Extraction (PUREX) process has been utilized for commercial Mixed-Oxide (MOX) thermal reactors, however the UREX+ process may be tailored to meet specific fuel cycle by-product objectives, such

as a U/TRU product that can be used as actinide burning fuel in FRs (such as those in EG24). Several aqueous reprocessing facilities connected with military programs have been built though little cost information available for them. Cost data from the two commercial reprocessing sites are limited as the information is proprietary. Cost estimates from Shropshire et al. (2009) of the UREX+ reprocessing technology are given in Table 5.5; the triangular distribution between low, nominal and high estimates was used to determine estimates at the quartiles. It is assumed that, given past experience, R&D efforts aimed at reprocessing technologies would successfully yield a target cost.

Table 5.5: Reprocessing process R&D outcomes for all $b_{process}$ investment levels.

	Cost ($ per kg IHM)		
Investment Level ($b_{process}$)	0	1	2
(Shropshire et al., 2009)	2,387	2,171	1,964

Strategy 2: Product R&D

G may also choose an investment level, $b_{product}$, into product R&D which allows new technologies to be developed which may significantly reduce costs. The result of product R&D is to alter the probability distributions on which the waste disposal technology unit costs are defined. Product R&D allows the initially non-zero probabilities of certain waste disposal unit costs to become positive. New products offering great cost savings may include improved waste canisters allowing the fuel load density to increase in the repository, or entirely new waste disposal technologies to be successfully developed such as deep borehole disposal. Costs estimates are summarized in Table 5.6 and are obtained from Shropshire et al. (2009) for conventional geologic disposal and from

Driscoll et al. (2015) for deep borehole disposal. The probability distribution associated with each product R&D investment level is highly uncertain and difficult to define and is chosen here only for demonstration purposes. This issue of partial perfect information may be the subject of future work. All costs are normalized to 2018-dollar amounts.

Table 5.6: SNF and HLW disposal cost estimates and probability distributions associated with all $b_{product}$ levels of product R&D.

	Cost			
SNF Disposal ($/kg IHM)	144	602	801	987
HLW Disposal ($/kg FP in IHM)	933	4,133	6,359	8795
Investment Level ($s_{product}$)	Probability			
0	0.00	0.25	0.50	0.25
1	0.05	0.30	0.45	0.20
2	0.10	0.35	0.40	0.15

The investment level (B) across process and product R&D is fixed at 2, see Eq. 5.4:

$$B = b_{process} + b_{product} == 2 \tag{5.4}$$

Here, B is the total units of "budget" allotted for investment. Again, B is a quantity that is extremely difficult to determine; its fixed quantity and constraint across R&D investment in the two competing technologies is for demonstration purposes only.

Strategy 3: *Capital Subsidy*

If policies are implemented that are meant to incorporate the external costs of electricity production, such as production of CO2 emissions, the economic benefit of nuclear power would become more visible to potential investors. The MIT Future of Nuclear Power study issued by Deutch et al. (2003; 2009) recommend three actions to

increase the economic viability of nuclear power. The preferred incentive is the production tax credit of up to \$200 per kW_e of the construction of up to 10 "first mover" plants which bear the burden of one-time risks and provide followers with valuable information and experience. The production tax credit offers the greatest incentive for projects to be completed, and further, may be extended to other carbon-reducing technologies. Here, the production tax credit is implemented as a capital subsidy[17]. While the capital subsidy is meant to encourage the move to advanced reactor technologies by subsidizing first mover plants, *U* may still choose not to adopt these technologies. In this case, following the allotted 10-year timeframe in which the capital subsidy is reserved for advanced technologies, the equivalent subsidy is instead provided to future LWRs.

5.2.2 PLAYER U

Player *U*'s payoff is simply the Cost of Electricity score. Utilities are typically businesses in many respects, and increased electricity sales result in increased revenues and therefore profits, specifically in an unregulated electricity market.

Historically, under the Nuclear Waste Policy Act of 1982, utilities were charged 1 mill per kWh of nuclear electricity paid to a Nuclear Waste Fund, which was to fund development of repositories for the disposal of used fuel high-level waste disposal (DOE, 2004). Yucca Mountain was designated as the first site for a geologic repository for nuclear waste in 1987 and was originally approved in 2002. However, the federal

[17] The production tax credit to be paid out at 1.7 cents per kWe-hr- over a year and a half of full-power plant operation. Based on operation of a 1000 MWe plant with capacity factor of 90 percent, the production tax credit is equivalent to a \$200 per kWe government subsidy. The dollar amount is adjusted to 2018-dollar values for consistency. The production tax credit is implemented as a capital subsidy in this work, due to its lessened modeling complexity in the VEGAS framework. In addition, new nuclear plants are assumed to be successfully built and operated in VEGAS, voiding the incentive for completing a nuclear project.

government has failed to meet its obligation to dispose of nuclear waste, due to DOE shut down of the Yucca Mountain project in 2010, leaving 39 states to store radioactive waste on-site (NEI, 2018). Due to the issues surrounding licensing, constructing and operating a nuclear waste repository, utilities may be responsible for long-term storage of their nuclear waste. In Chapter 6, the effects of introducing this obligation for *U* are examined through alternative weighting of *U*'s decision criteria to include the Decay Heat decision criterion.

U's Decisions (Available Strategies)

U builds reactors to meet an exogenously specified power demand. Currently existing LWR technology is available to *U*, as well as advanced SFR and HTGR technology. *U*'s strategies are then his decisions on which reactor technology to employ to meet power demand and are referred to as:

- *LWR strategy* — build only LWRs
- *HTGR strategy* — build only HTGRs
- *SFR strategy* — build SFRs at material-constrained maximum limit, relying on reprocessed used fuel from LWRs – if electricity demands unmet by SFRs, build LWRs
- *HTGR-SFR strategy* — build SFRs at material-constrained maximum limit, relying on reprocessed used fuel from HTGRs, then LWRs – if electricity demands unmet by SFRs, build HTGRs

U's upstream strategies act to filter his future available strategies (recourse decisions); Fig. 5.4 gives an example of this filtration. Advanced HTGR and SFR technologies are only available at *U*'s final decision node *if* these technologies were chosen at either the first or second decision node. This can be seen by following the lowermost branch in *U*'s decision tree, depicted in Fig. 5.4. Fig. 5.4 shows only a portion of *U*'s decision tree, where

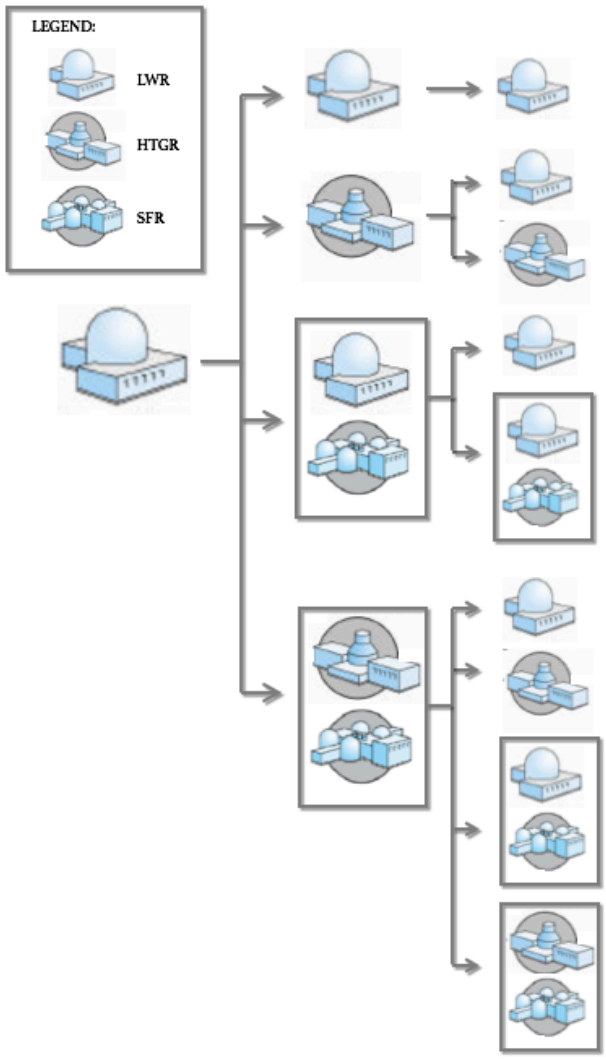

Figure 5.4: Filtration examples for *U*'s sequential reactor technology choices.

U has chosen the *LWR* strategy at his first decision node. At the second decision node, following the lower branch indicates that HTGR and SFR technologies are chosen. Then, at the final decision node, only that branch allows for these two technologies to be chosen. Note that this does not preclude delaying and then later resuming the transition. The first

and second decision nodes occur in years 2035 and 2045, respectively, with the final decision node occurring in 2055, with that decision propagated until the end of the simulation. *U*-Paths ϑ^U where *U* chooses the same strategy at each of his decision nodes are termed *Absolute U-Paths* whereas a *Partial U-Path* is one where *U* chooses different strategies at minimum two of his decision nodes (*absolute* and *partial paths*, for simplicity). If d^i is *U*'s strategy at each stage i, then the *absolute HTGR path* is denoted $\vartheta^U_{HTGR} \in \vartheta^U_{d^1,d^2,HTGR}$ for simplicity. *U*'s absolute paths are a special case of his partial paths. A *partial path* could be $\vartheta^U_{SFR,HTGR\text{-}SFR,SFR}$.

HTGR and SFR prototype reactors are built with first-of-a-kind (FOAK) construction costs. As the next units are built, the final n^{th}-of-a-kind (NOAK) cost is realized. See Chapter 3, Section 3.3 for implementation of learning curves for reactor capital costs within the VEGAS simulator. Table 5.7 gives the FOAK and possible NOAK reactor capital costs, converted to 2018-dollar amounts and their sources. FOAK HTGR capital costs are obtained from Shropshire et al. (2009) for the Fort St. Vrain reactor, while NOAK capital costs are obtained from estimates of China's HTR-PM unit, currently under construction in Shandong province (WNA, 2018). The FOAK SFR cost is taken as France's Superphenix reactor capital cost. Given past issues with the facility leading to inflated costs compared to original engineering estimates, the FOAK estimate may be overly pessimistic. NOAK SFR capital costs were collected from fuel cycle experts of the Advanced Fuel Cycle Initiative Economic Working Group, who also informed updated LWR capital costs.

If *U* chooses either advanced reactor technology, then prototype reactors are deployed and limited to 1 per year for the first 10 years. If *U* chooses to recycle used fuel (chooses SFR technology), an 800 tIHM per yr pilot reprocessing facility is built that

supports SFR reactors deployed during the 10-year learning period. During this period, while the available reprocessing capacity follows the ramp-up schedule in Table 5.8, only the capacity needed to support the new SFR reactors is used (reprocessing is used on demand, see Chapter 3, Section 3.3). After the first 10 years, if *U* chooses SFR technology, reprocessing capacity is utilized at full capacity, and separated actinides are allowed to accumulate. If *U* abandons his *SFR* strategy, reprocessing capacity is only used on demand for previously deployed SFRs. *U* choosing a recycle strategy, then abandoning it, then choosing a recycling strategy again, causes reprocessing capacity to be utilized on demand for the time period between decision nodes 1 and 3, and then utilized at full capacity from the time period beginning at decision node 3 and onward.

Table 5.7: First-of-a-kind reactor capital costs and possible nth-of-a-kind capital costs.

	Cost ($/kW$_e$)			
Reactor Technology	first-of-a-kind	Source	n^{th}-of-a-kind	Source
LWR	4,177	[1]	4,177	[2]
HTGR	5,135	[1]	3,000	[3]
			4,000	
			4,500	
SFR	8,870		3,300	[2]
			4,155	
			5.900	
Sources: [1] (Shropshire et al., 2009), [2] private correspondence, AFCI Economic Working Group, [3] (WNA,2018)				

If *U* chooses a path following $\vartheta^{U}_{d^1,d^2,(SFR|HTGR\text{-}SFR)}$ where his final strategy involves recycle of used fuel, additional reprocessing capacity is deployed to bring excess inventories of used fuel near zero by the end of the VEGAS simulation. The assumption here

is that transition to a nuclear fuel cycle that incorporates recycling of used fuel is aimed at minimizing the repository burden and eliminating the need for multiple repositories. A reprocessing capacity deployment schedule is chosen that achieves this goal while simultaneously minimizing the total integrated reprocessing capacity installed during the simulation.

Each U-path ϑ^U requires identifying a unique optimal reprocessing capacity deployment schedule. For each ϑ^U where U chooses to recycle used fuel at this last decision node ($\vartheta^U_{d^1,d^2,(SFR|HTGR\text{-}SFR)}$, totaling 21 strategies), a suite of VEGAS simulations is carried out to determine the optimal deployment schedule. Beginning in 2055, and every 5 years following until the end of the simulation, reprocessing capacity may be deployed in units of 1,500 tIHM per year. In this way, 2^9 = 512 simulations are performed for all 21 $\vartheta^U_{d^1,d^2,(SFR|HTGR\text{-}SFR)}$. Reprocessing facilities follow the 4-year capacity ramp-up schedule shown in Table 5.8. Table 5.9 shows the optimized reprocessing capacity deployment schedule, where '0' indicates no reprocessing facility is built, and '1' indicates a single reprocessing facility is built.

Table 5.8: Reprocessing facility capacity ramp up schedule.

	Available Capacity (%)
Year 1	10
Year 2	30
Year 3	60
Year 4	100

The optimal reprocessing capacity deployment schedule is chosen to (1) utilize 90 percent of installed capacity at all times (except during the initial prototype phase) and

Table 5.9: Optimized reprocessing capacity deployment schedules for paths $\vartheta^{U}_{d^1,d^2,(SFR|HTGR\text{-}SFR}$. Reprocessing facilities have a 1,500 tIHM per yr capacity that follows the ramp-up schedule in Table 5.8: '0' indicates no facility is built, and '1' indicates a single facility is built.

2035 Strategy	2045 Strategy	2055 Strategy	2055	2060	2065	2070	2075	2080	2085	2090	2095
LWR	LWR and SFR	LWR and SFR	0	0	0	0	0	1	0	1	1
	HTGR and SFR	LWR and SFR	0	0	0	0	0	1	0	1	1
		HTGR and SFR	0	0	0	0	0	1	1	1	1
HTGR	LWR and SFR	LWR and SFR	0	0	0	0	0	1	0	1	1
		HTGR and SFR	0	0	0	0	0	1	1	1	1
	HTGR and SFR	LWR and SFR	0	0	0	0	0	0	1	1	1
		HTGR and SFR	0	0	0	0	1	0	0	1	1
LWR and SFR	LWR	LWR and SFR	0	0	0	0	1	0	0	1	1
	HTGR	LWR and SFR	0	0	0	0	1	0	0	1	1
		HTGR and SFR	0	0	0	0	0	1	1	1	1
	LWR and SFR	LWR and SFR	0	0	0	0	0	0	1	1	1
	HTGR and SFR	LWR and SFR	0	0	0	0	0	0	1	1	1
		HTGR and SFR	0	0	0	1	0	0	0	1	1
HTGR and SFR	LWR	LWR and SFR	0	0	0	0	1	0	0	1	1
		HTGR and SFR	0	0	0	0	0	1	1	1	1
	HTGR	LWR and SFR	0	0	0	0	0	0	1	1	1
		HTGR and SFR	0	0	0	0	1	0	0	1	1
	LWR and SFR	LWR and SFR	0	0	0	0	0	0	1	1	1
		HTGR and SFR	0	0	0	1	0	0	0	1	1
	HTGR and SFR	LWR and SFR	0	0	0	0	0	0	1	1	1
		HTGR and SFR	0	0	0	0	0	1	0	1	1

(2) ensure less than 20,000 tIHM net cumulative waste is stored at the end of the simulation.

When both conditions are met by more than one deployment schedule, the schedule with

the least time-integrated reprocessing capacity is chosen. If both conditions cannot be met simultaneously, then the schedule that utilizes 90 percent of installed capacity while reaching as close to the 20,000 tIHM goal is chosen.

5.2.3 NATURE

Nature's moves "choose" the outcome of uncertain parameters, determining the state of the world that is realized as a response to decisions made by *G* and *U*. Uncertain parameters include (1) the cost of SNF and HLW disposal, (2) the NOAK capital cost of HTGRs, and (3) the NOAK capital cost of SFRs. Possible cost outcomes for these technologies are given in Tables 5.5 and 5.6. As all cost data for these technologies are limited, the uncertain parameters are modeled as discretized values, though the method may be extended to allow for parameters with continuous probability distributions.

5.3 SOLUTION CONCEPT

A scenario tree-based approach to stochastic programming is used to analyze the sequential multi-stage Transition Game with uncertainty. Stochastic programs are mathematical programs that incorporate uncertain variables (here, *Nature*'s moves or states of the world) using their probability distributions. The goal is to identify a feasible solution that considers all possible states of the world and performs well on average. Using the scenario tree-based approach, variables are assumed to take on discrete values, each with an associated probability. The result of solving the stochastic program is identification of robust hedging (here, transition) strategies that level negative consequences associated with all realizations of the uncertain variables. In contrast, a deterministic program only minimizes the negative consequences of one outcome of the uncertain variable. Chapter 2

details the backward induction method solution concept for a multi-stage stochastic program. This solution concept is employed in this work.

Each *U*-path ϑ^U is simulated in VEGAS obtaining a unique material balance. This material balance is provided to the Cost of Electricity, Decay Heat and Proliferation Resistance calculators. Then, the payoff for both *G* and *U* can be computed for all ϑ, a single path from root to leaf of the Transition Game decision tree. Once the payoff for *G* and *U* is defined for all ϑ, the backward induction method is used to find a solution. While the method may be computationally costly for problems with many uncertainties, it was determined sufficient for the Transition Game examined. By leveraging the physics of the Transition Game and determining *G*'s and *U*'s payoffs by simulating only a subset of Θ, significantly less computational power was needed.

CHAPTER 6: TRANSITION GAME RESULTS

This chapter presents results from solving the Transition Game. Section 6.1 examines the primary data from simulating the Transition Game in the VEGAS fuel cycle simulator. These data include decision criteria metric scores and impacts of material- and technology-constraints on metric scores. Tradeoffs in fuel cycle performance due to competing decision criteria are illustrated. Electricity generation profiles with corresponding SNF generated, as well as cumulative inventories of SNF based on an optimized reprocessing technology deployment schedule are illustrated. Section 6.2 demonstrates the difference in Players *G*'s and *U*'s perfect information strategies and their optimal hedging strategies based on information available on *Nature*'s moves under their baseline criteria weighting. Finally, Section 6.3 explores the interaction between *G* and *U* as their criteria weightings are varied. Solving the Transition Game suggests that in the absence of a regulated market, or electric utilities expanding their decision criteria beyond electricity generating costs, transition to a closed fuel cycle is not observed. Conversely, advanced reactor technology that keeps the fuel cycle open is seen to be readily adopted.

6.1 TRANSITION GAME DATA OVERVIEW

The decision tree of the Transition Game examined here is described in Section 5.2 and is depicted in Fig. 6.1. A single path from root to leaf of the Transition Game decision tree is defined by *G*'s and *U*'s chosen strategies at their respective decision nodes (pink and blue squares, respectively, in Fig. 6.1) and all of *Nature*'s moves at his chance nodes (grey circles in Fig. 6.1), with each path through the tree resulting in unique metric scores. The evaluation criteria and their chosen metrics for evaluating transition paths are:

- *Cost of Electricity* – total cost of generating electricity
- *Decay Heat* – total decay heat load to the repository from SNF and HLW disposal
- *Proliferation Resistance* – average time- and mass-weighted nuclear security measure

The methodology for calculating the scores associated with each criterion is given in Section 4.1.

Recall that *U*'s upstream strategies act to filter his future available strategies (recourse decisions), see Fig. 6.2. For illustration purposes, Fig. 6.2 omits *G*'s and *Nature*'s moves and *U*'s first decision is assumed to be deployment of LWRs. Advanced HTGR and SFR technologies are only available in *U*'s final decision node *if* these technologies were chosen at either the first or second decision node, seen by following the lowermost branch in *U*'s decision tree. Only this lowermost branch allows for HTGR and SFR technologies to be chosen at *U*'s final decision node. Note that this does not preclude delaying and then later resuming the transition or abandoning a transition when more information is available. Instances where transitions are delayed or abandoned are referred to here as *partial paths*. *Absolute-paths* refer to those in which *U* chooses the same reactor technology at each of his decision nodes. Section 5.2 gives a more detailed definition of these paths and their effect on the solution of the Transition Game. *U*'s paths $\vartheta^{U}_{d^1,d^2,d^3}$ are defined by his decisions d^i at each of his decision nodes. For simplicity, *U*'s partial paths are referred to as his (for example) LWR path with $\vartheta^{U}_{d^1,d^2,LWR}$, though *U*'s absolute LWR path is defined as $\vartheta^{U}_{LWR} = \vartheta^{U}_{LWR,LWR,LWR} \in \vartheta^{U}_{d^1,d^2,LWR}$, where at each decision node, *U* chooses his *LWR* strategy.

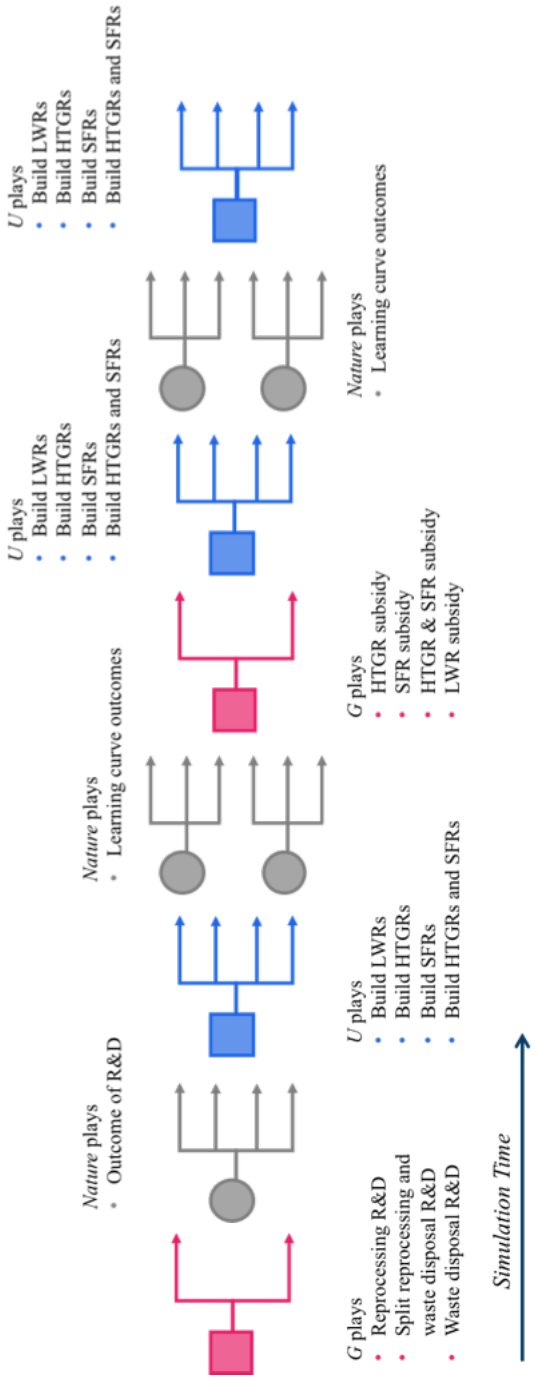

Figure 6.1: Transition Game decision tree with *G*'s decision nodes (pink), *U*'s decision nodes (blue) and *Nature*'s chance nodes (grey).

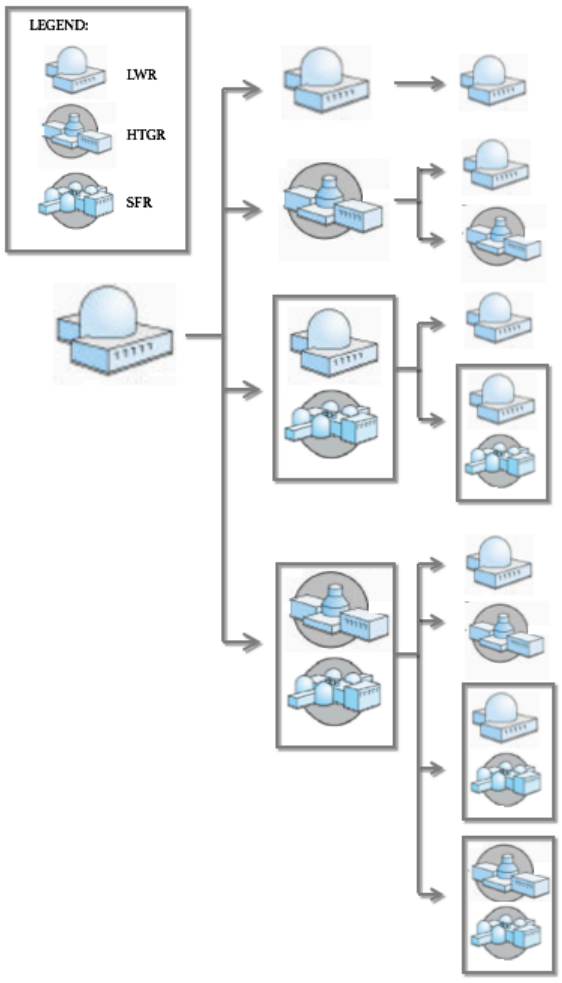

Figure 6.2: Filtration examples for *U*'s sequential reactor technology choices.

The scores for each metric for each path along the Transition Game decision tree are shown in Fig. 6.3, with constituent parts in Fig. 6.4. Symbols in Fig. 6.3 and 6.4 are defined by d^3; for instance, in Fig. 6.4, the top-right data points are all metric scores for *U*'s HTGR paths, $\vartheta^{U}_{d^1,d^2,HTGR}$. The first and second decision nodes occur in years 2035 and 2045, respectively, with the final decision node occurring in 2055, with that decision propagated until the end of the simulation in 2100. Due to the longer time horizon of *U*'s

final decision, it is chosen to depict the paths shown in Fig. 6.3 and 6.4. The longer time horizon of the final decisions allows greater penetration of the chosen technologies over the first two. This effect is further examined in the next subsection.

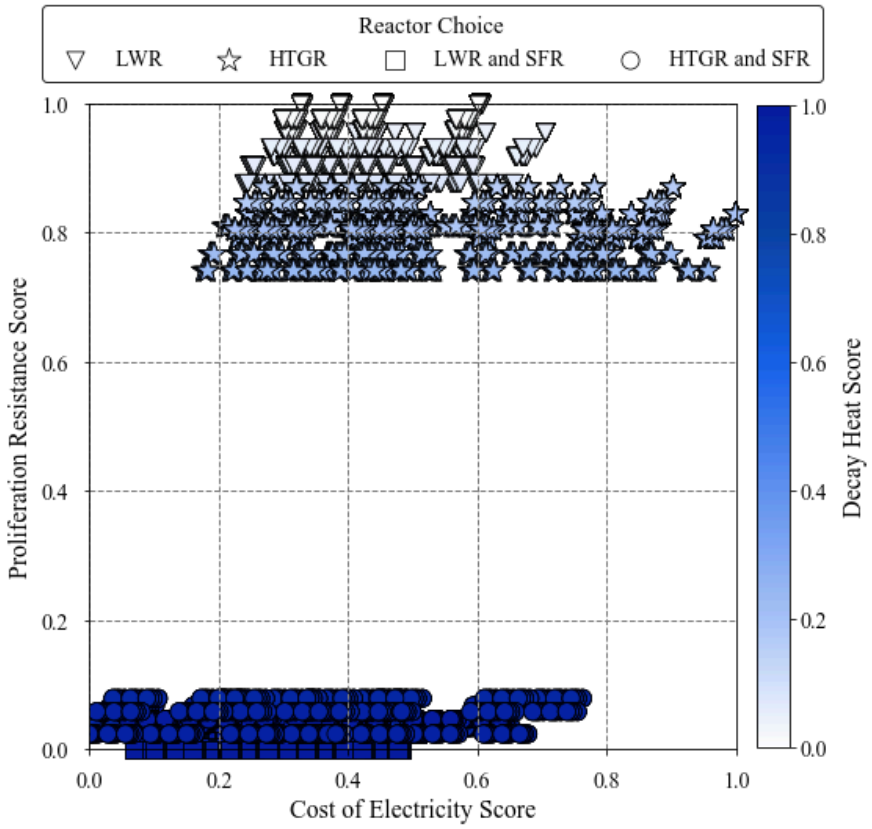

Figure 6.3: Metric scores for all paths along Transition Game decision tree.

Differentiation in the transition strategies according to the Cost of Electricity score represent different moves by *Nature* and *G*'s stage one strategy that determines the cost of reprocessing. Combinations of *Nature*'s moves (as new information is gained depending on *U*'s chosen strategies) are termed *states of the world*. It is assumed that LWR reactor

capital costs are known, while HTGR and SFR reactor capital costs are uncertain (the possible values of which are given in Chapter 5, Table 5.6). *U*'s LWR paths ($\vartheta^{U}_{d^1,d^2,LWR}$) are seen to have middle-of-the-road performance in terms of the Cost of Electricity score, though with less uncertainty. In Fig. 6.3, four LWR data points are seen with a Proliferation Resistance score of 1.0, corresponding to the absolute LWR path with different realizations of the SNF and HLW disposal cost. The absolute LWR path avoids separated actinides flowing through the fuel cycle; as well, lower ^{235}U enrichment levels are required for LWRs at the cost of lower fuel utilization. The Cost of Electricity score of 1.0 is achieved when following the absolute HTGR path, though only under favorable states of the world – successful product R&D which develops a new waste disposal technology with superior performance and cheap HTGR capital costs. Lastly, the 1.0 Decay Heat score is achieved when *U* follows path $\vartheta^{U}_{HTGR-SFR,HTGR-SFR,SFR}$. In order to reduce inventories of used fuel, *U* takes advantage of HTGR's greater fuel utilization. By 2055 (*U*'s last decision node), sufficient used fuel is available to continue top-up while achieving burn down of LWR used fuel inventories, eventually depleting those stores, so SFRs are chosen at *U*'s last decision node.

Both HTGRs and SFRs offer an opportunity to improve the Cost of Electricity score over traditional LWR technology, though with some risk. Approximately 50 percent of the data for *U*'s paths $\vartheta^{U}_{d^1,d^2,HTGR|SFR|HTGR-SFR}$ fall under the mid-point in the Cost of Electricity score. While a larger uncertainty in the cost of SFR reactor technology exists, material constraints limit the installation of new SFRs, and so the effective uncertainty with the performance of *U*'s recycling paths $\vartheta^{U}_{d^1,d^2,SFR|HTGR-SFR}$ are less than the uncertainty in the HTGR paths $\vartheta^{U}_{d^1,d^2,HTGR}$.

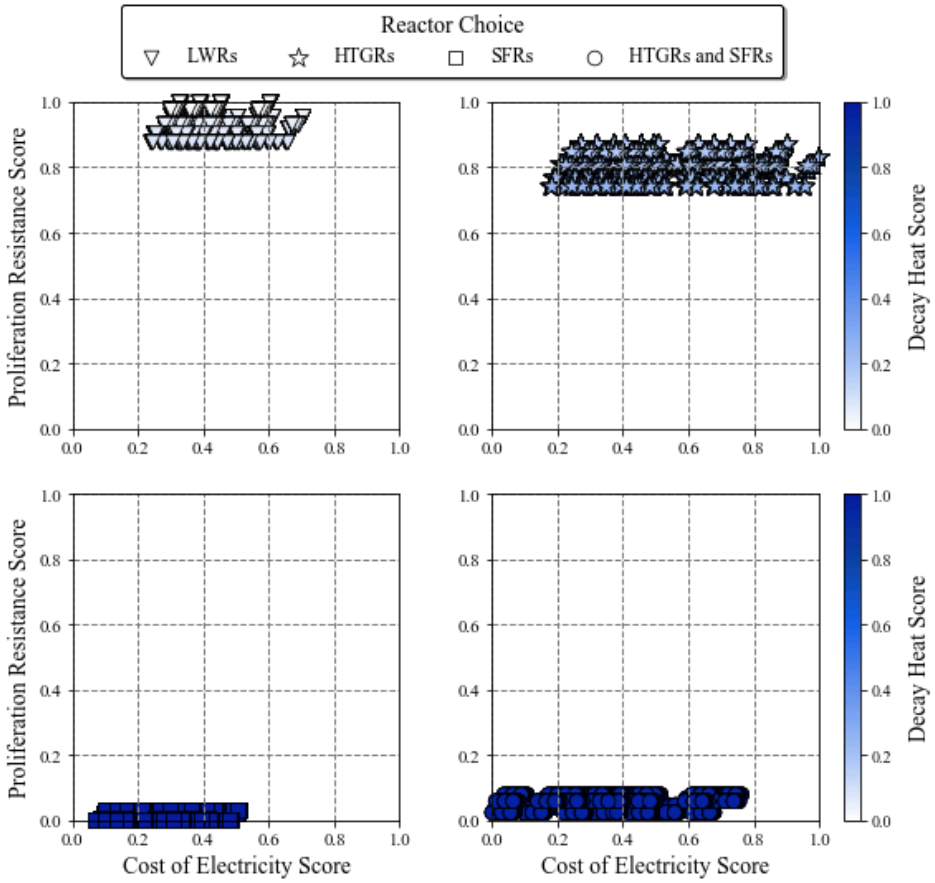

Figure 6.4: Constituent reactor technology metric scores for all paths along Transition Game decision tree.

The primary contributor to the range of Cost of Electricity scores is due to the uncertainty associated with reactor capital costs. Fig. 6.5 shows the range of possible metric scores when *U* follows his *HTGR* paths ($\vartheta^{U}_{d^1,d^2,HTGR}$) when reactor capital costs are held fixed; then, the spread in data for each subplot is due to uncertainty in SFR capital costs that affect scores for $\vartheta^{U}_{d^1,d^2,HTGR}$ with $(d^1|d^2) == (SFR|HTGR - SFR)$, as well as uncertainties in the cost of SNF and HLW disposal.

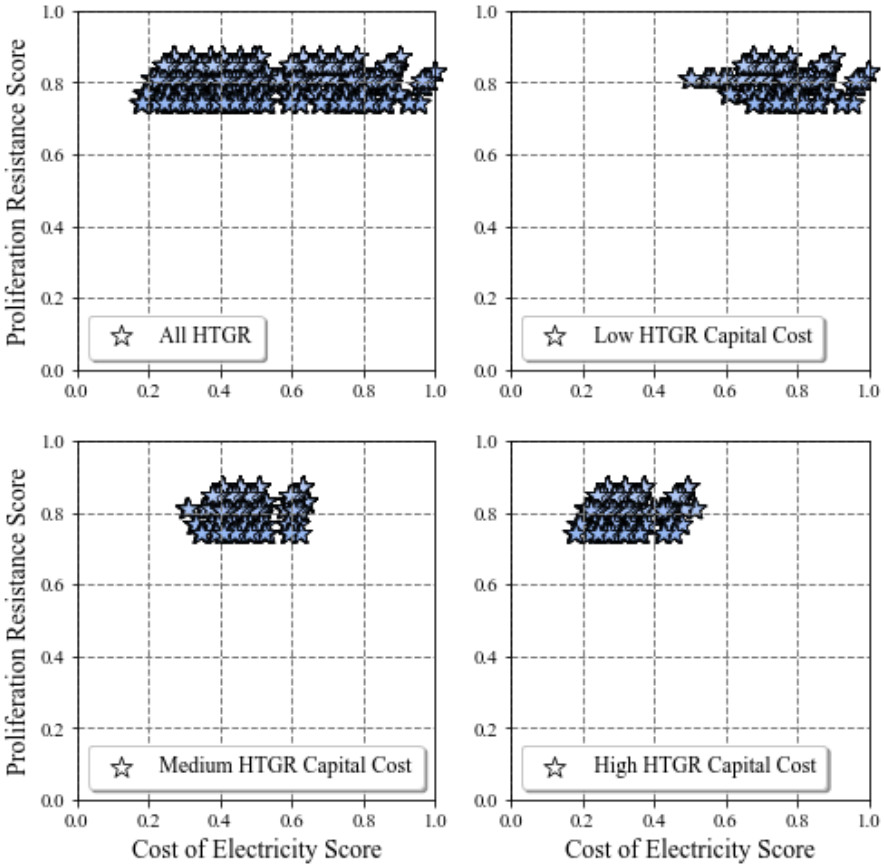

Figure 6.5: Uncertainty in Cost of Electricity score for HTGR paths due to uncertainty in SNF and HLW Disposal Costs.

Decay Heat and Proliferation Resistance scores are more readily interpreted using Fig. 6.6, where uncertainties in fuel cycle and reactor technology costs have been marginalized out. Decay Heat and Proliferation Resistance scores are seen to be strongly negatively-correlated. Recycling of used fuel avoids ultimate disposal and heat load to the waste repository, though at the cost of separated actinides and significant quantities of fissile materials flowing through the fuel cycle. Conversely, a mild improvement in the Decay Heat score heat load to the repository is lessened for paths $\vartheta^{U}_{d^1,d^2,HTGR}$ (in comparison

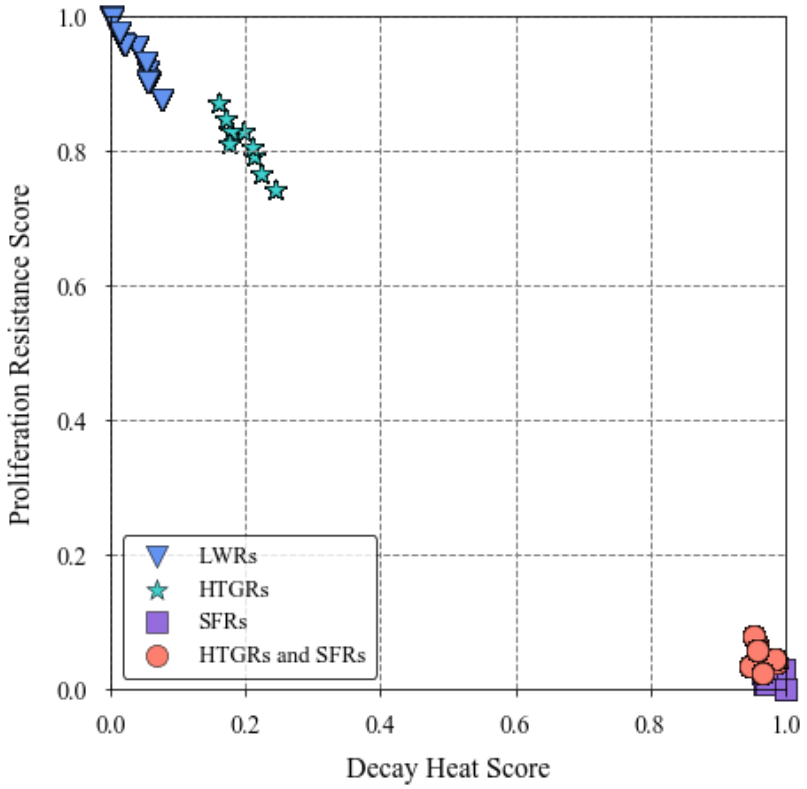

Figure. 6.6 Proliferation Resistance and Decay Heat scores with marginalized cost uncertainties

to the case where *U* chooses $\vartheta^{U}_{d^1,d^2 LWR}$), due to the higher fuel efficiency of HTGRs. Fuel requirements for the different fuel cycle technologies, and relevant reactor performance parameters for the calculation, are given in Table 6.1. The Proliferation Resistance score of paths $\vartheta^{U}_{d^1,d^2,HTGR}$ is greatly improved over ϑ^{U}_{SFR} and $\vartheta^{U}_{d^1,d^2,HTGR-SFR}$. The difference in the Proliferation Resistance scores for LWR and HTGR strategies arises from the ^{235}U enrichment in fresh fuel. Proliferation resistance and decay heat calculations were assumed to have no associated uncertainty. Variations due to ORIGEN inputs (cross sections, activities, etc.) are expected to be minor in comparison to the large associated uncertainties in fuel cycle and reactor technology costs. Further, in the absence of realistic uncertainties

in reactor technology performance, variations in decay heat and proliferation resistance could not be calculated as generic reactor types are modeled after those identified in the E&S Study.

Table 6.1: Reactor fuel requirement calculation parameters.

Reactor Type	LWR	HTGR	SFR	
Recirculating Power	0.02	0.02	0.02	$\frac{\text{MW}_\text{e} \text{ recycled to plant systems}}{\text{MW}_\text{e} \text{ produced}}$
Thermal Efficiency	0.33	0.50	0.40	MW(e)/MW(t)
Plant Size	1000	150	400	MW(e)
Discharge Burnup	50	120	73	MWd(t)/kgIHM
Mass Conversion	1,630	5,880	2,860	MWd(e)/tIHM
Capacity To Mass	0.020	0.006	0.001	tIHM/MW(e)
Fuel Requirement	20.1	0.84	4.59	tIHM/reactor

6.1.1 Absolute Paths

An *absolute path* is defined as that when *U* chooses the same strategy at each of his decision nodes (for instance, $\vartheta^{U}_{HTGR,HTGR,HTGR} \in \vartheta^{U}_{d^1,d^2,HTGR}$). By choosing an absolute path, the largest material- and technology-constrained penetration of advanced reactor technology may be achieved. Metric scores when *U* chooses an absolute path are examined here.

Fig. 6.7 shows the installed electricity generating capacity by each reactor type when each absolute path is followed. While transitions begin in 2035, advanced reactor technology deployment is limited to one unit per year for the first 10 years (HTGRs and SFRs with a capacity of 175 and 400 MW_e each, respectively). Relative to the generating capacity of the entire nuclear fleet, the installed HTGR and SFR capacity by 2045 is not visible in Fig. 6.7. Fig. 6.8 shows a magnified view of Fig. 6.7 during the initial prototype

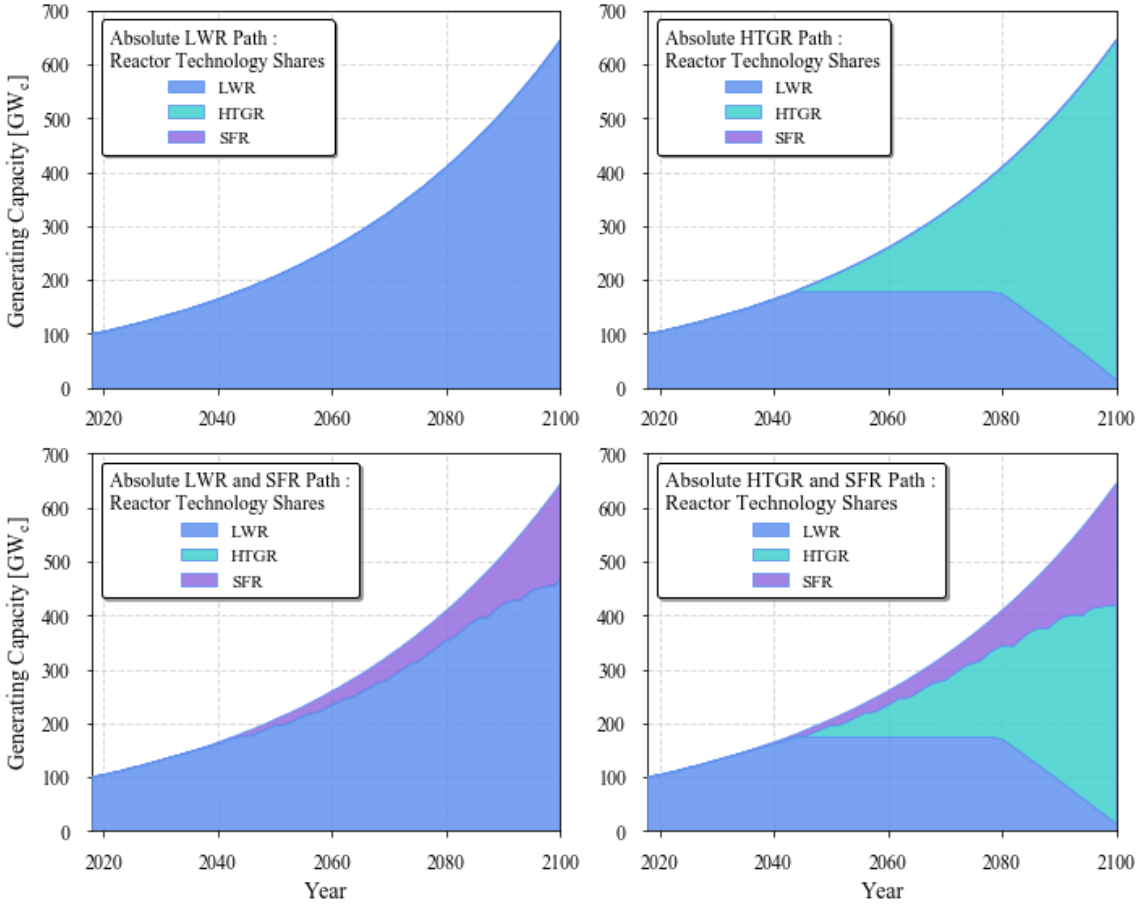

Figure 6.7: Constituent generating capacity [GW_e] for Player *U*'s absolute paths.

reactor deployment phase, depicting the linear ramp-up of generating capacity. Following 2045, when the deployment limit on prototype reactor technologies is lifted, penetration of the technologies is seen to increase dramatically. By the end of the simulation for both ϑ^{U}_{HTGR} and $\vartheta^{U}_{HTGR-SFR}$ that rely on HTGR instead of LWR technology for tier 0 generating capacity, the installed LWR capacity is below 15 GW_e. In the Transition Game, the initial

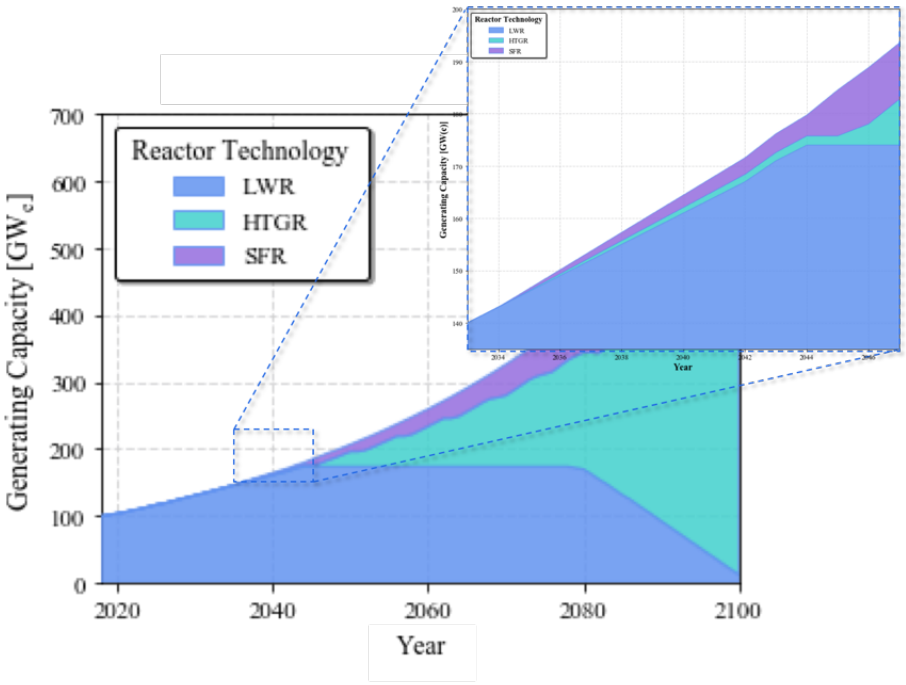

Figure 6.8: Annual electricity generating capacity by reactor type for Absolute *U HTGR-SFR* path (bottom-left) with magnified view of 2035 to 2045 learning-period with limited advanced reactor deployment.

100 GW_e LWR fleet is set to begin and finish retiring in 2018 and 2040, respectively. Then, the remaining LWR generating capacity by the end of the simulation is due to LWRs installed during 2035 and 2045 (to make up for electricity demand unfulfilled due to HTGR prototype deployment limits) completing their 60-year lifetime.

Net used fuel quantities for each of *U*'s absolute paths are shown in Fig. 6.9. Note that the net used fuel quantity is the amount of used fuel generated less the total amount of used fuel *eventually* reprocessed during the simulation. The largest amount of used fuel, nearly 500,000 tIHM, is accumulated when the absolute LWR path is taken. Due to their higher fuel burnup (fuel utilization) and improved electric-to-thermal efficiency, HTGRs require approximately one-third less fuel measured in tIHM than LWRs. Then, when *U*

chooses his absolute HTGR path, nearly 200,000 tIHM of this used fuel is avoided, though its decay heat content differs. Nearly the entire amount of used fuel is avoided when *U* chooses ϑ^{U}_{SFR} or $\vartheta^{U}_{HTGR-SFR}$.

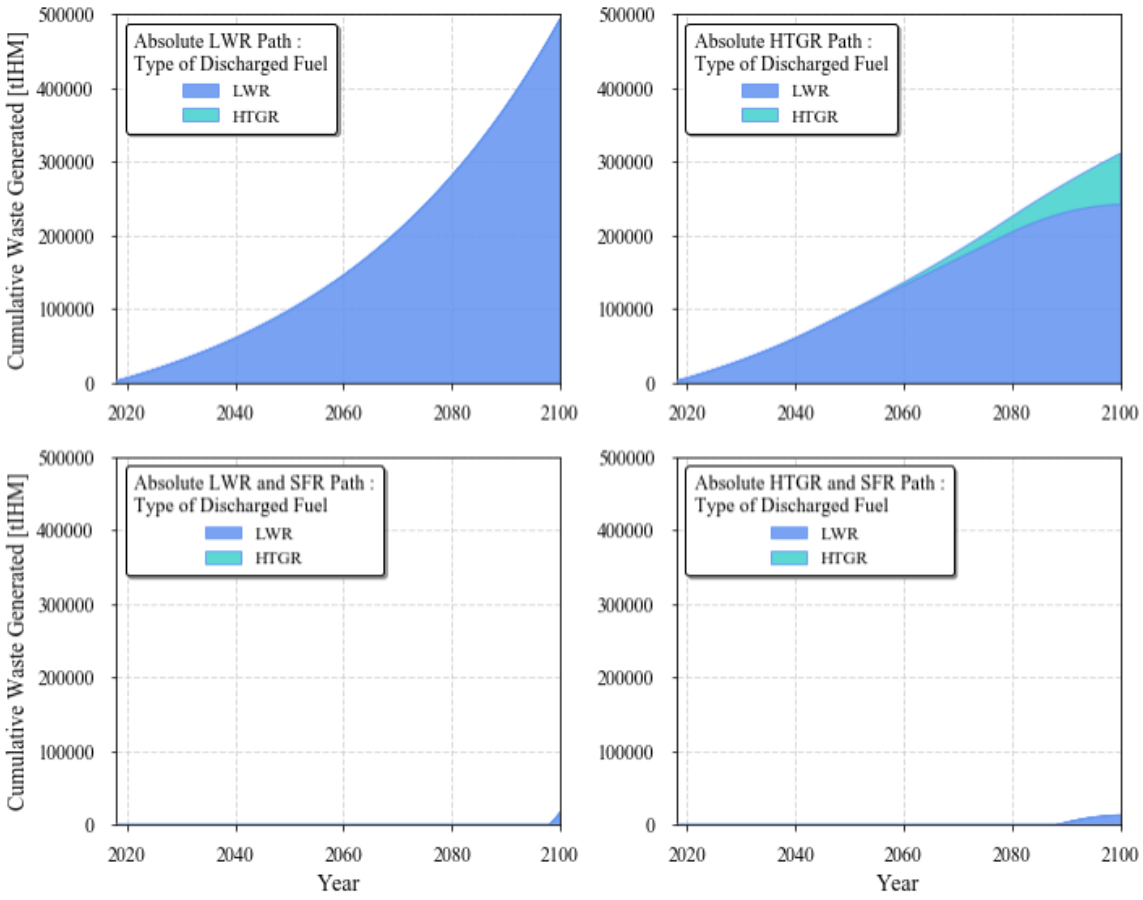

Figure 6.9: Used fuel quantities for each of Player *U*'s absolute paths.

Avoidance of excess used fuel quantities for *U*'s absolute SFR and HTGR-SFR paths is achieved by finding an optimal reprocessing capacity deployment schedule (Chapter 5, Section 1). Between 2035 and 2045 (the time period between *U*'s first and

second decisions) used fuel is reprocessed only on demand for prototype reactors built, which are limited to 1 per year during this period. Following the learning period, once another recycle strategy is chosen, the pilot reprocessing facility (with an annual capacity of 800 tIHM per yr) is run at full capacity and separated actinides are allowed to accumulate. For both *U*'s absolute recycle paths, the pilot facility provides sufficient capacity until around 2080, when 3 additional 1,600 tIHM per year reprocessing facilities are built to achieve the sub-20,000 tIHM cumulative used fuel allowance by the end of the simulation. The time-integrated reprocessing capacity is greater for *U*'s absolute HTGR-SFR path. As the HTGR:SFR support ratio is less than the LWR:SFR support ratio, HTGR fuel is assumed first in the reprocessing hierarchy. Consequently, the equivalent of 44 GW_e more SFRs are installed when *U* chooses his absolute HTGR-SFR path. More time-integrated reprocessing capacity is needed in this case to account for the larger installed SFR generating capacity. The optimal used fuel reprocessing capacity deployment and utilization for *U*'s absolute SFR and HTGR-SFR paths as well as the resulting installed SFR generating capacity in percentage quantities of the entire nuclear generating fleet is depicted in Fig. 6.10.

All metric scores for each of *U*'s absolute paths and each of *Nature*'s moves are shown in Fig. 6.11, with economic costs marginalized out in the bottom subplot. Coupling of the uncertainties in HTGR and SFR costs is seen to yield larger uncertainty in the eventual Cost of Electricity score when transitioning to SFRs supported by HTGRs, opposed to strategies that rely on only one of the advanced technologies. Again, a smaller spread in Cost of Electricity score is seen for the absolute SFR path due to the smaller penetration of SFR generating capacity. Interestingly, despite requiring larger amounts of

reprocessing, the absolute HTGR-SFR path performs better than the absolute SFR path in terms of proliferation resistance. Recycling of HTGR used fuel has two favorable properties: (1) its self-shielding factor due high radiation dose rates and (2) its higher concentration of even:odd Pu isotopes. These attributes are presented in Appendix A.

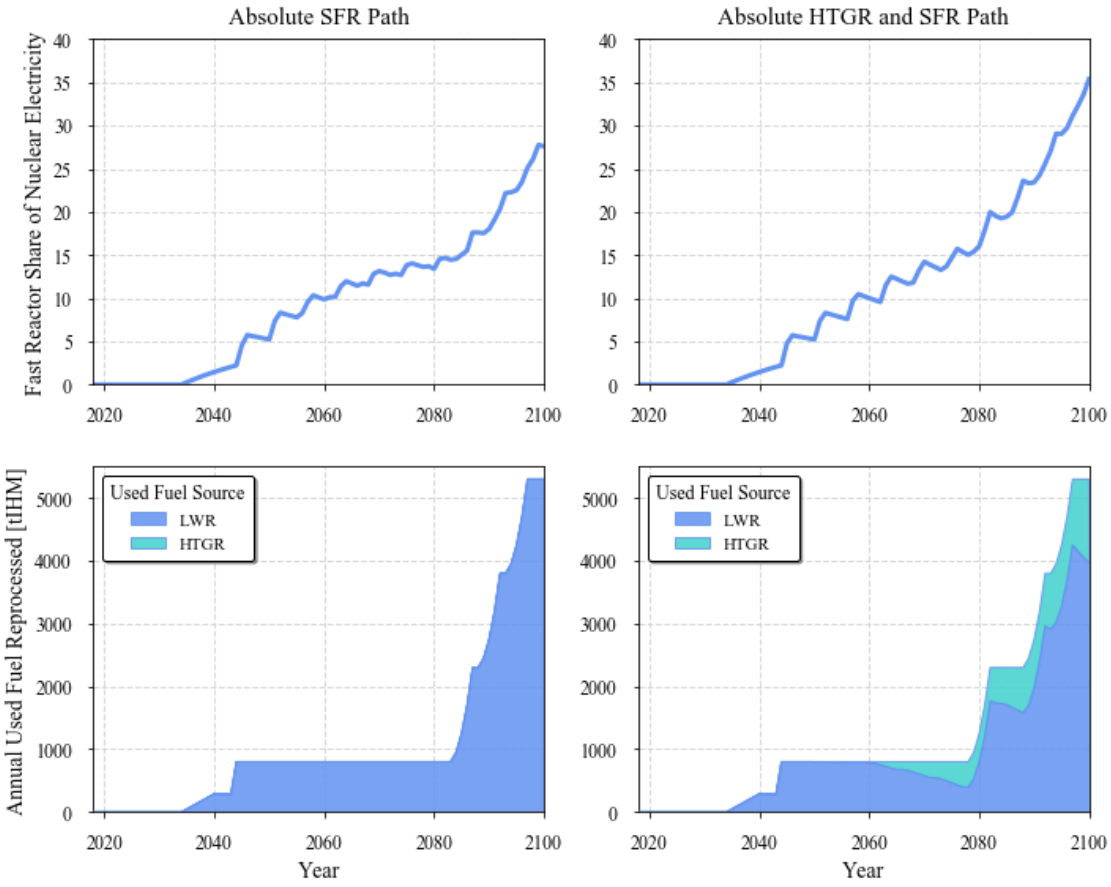

Figure 6.10: Fast reactor share of nuclear electricity generating (top) and associated annual used fuel reprocessed (bottom) for Player *U*'s recycle absolute paths.

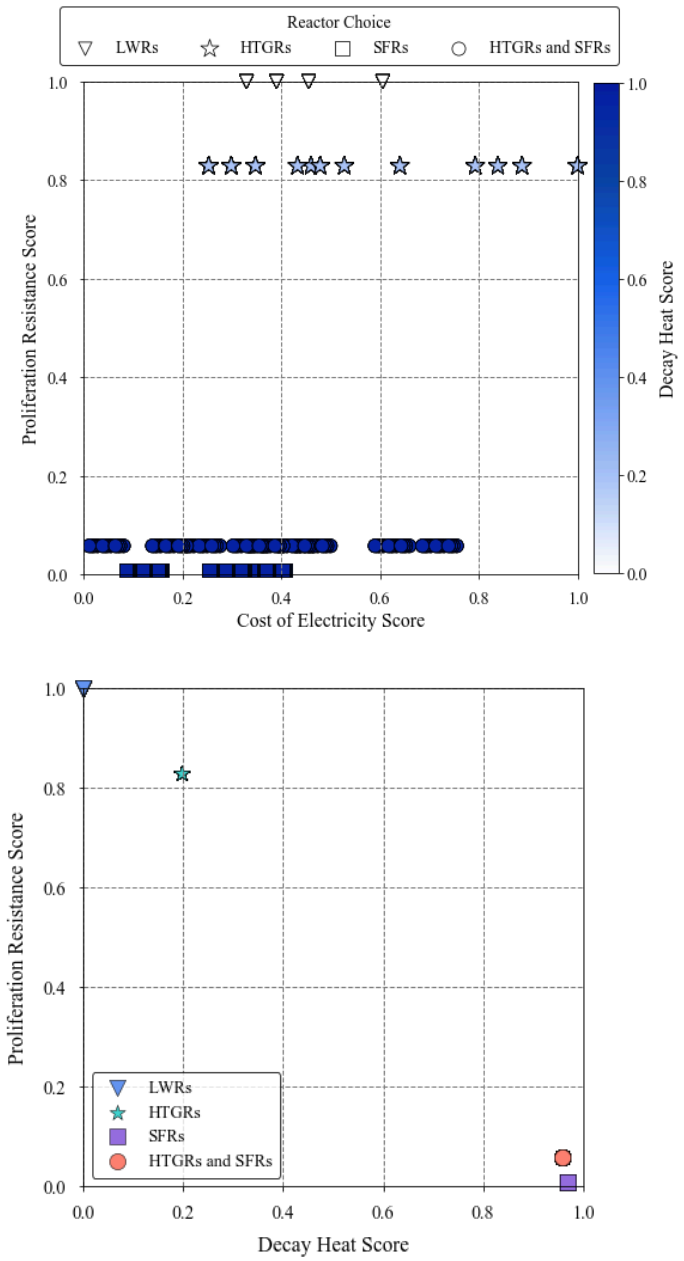

Figure 6.11: (Top) Decay Heat and Proliferation Resistance scores for each of Player *U*'s absolute paths. (Bottom) Decay Heat and Proliferation Resistance scores with Cost of Electricity score marginalized out.

6.2 Perfect Information and Optimal Hedging Strategies

The perfect information strategies represent those strategies that would be taken *if* the decision maker knew all of *Nature*'s moves in advance. Additionally, these strategies require that each player correctly anticipates the moves of the other player. Each player makes their decision based on a unique set of decision criteria, though the objective functions associated payoff calculation with these criteria are assumed the same (see Chapter 4). The baseline weighting of these criteria for Players *G* and *U* are given in Table 6.2. The sum of each player's criteria weighting must sum to unity.

Table 6.2: Player *G*'s and *U*'s baseline decision criteria weighing.

	Criterion Weighting	
Evaluation Criterion (*c*)	Player *G*	Player *U*
Cost of Electricity	$0.\overline{3}$	1.0
Decay Heat	$0.\overline{3}$	0.0
Proliferation Resistance	$0.\overline{3}$	0.0

Fig. 6.12 compares one path along the Transition Game decision tree, when *G* and *U* are hedging optimally (top) and when *G* and *U* act with perfect information (bottom). Both players choose their strategies with their baseline criteria weighting (see radar chart). When hedging, *G* and *U* consider all 36 possible states of the world (4 possible waste disposal costs, 3 possible HTGR capital costs and 3 possible SFR capital costs) and choose strategies that perform well on the average. For illustration, Fig. 6.12 takes *one* possible state of the world, where *Nature*'s moves are a (1) high waste disposal cost, (2) high HTGR capital cost, and (3) low SFR capital cost. In this particular state of the world, transition to a closed fuel cycle is favorable for both *G* and *U*.

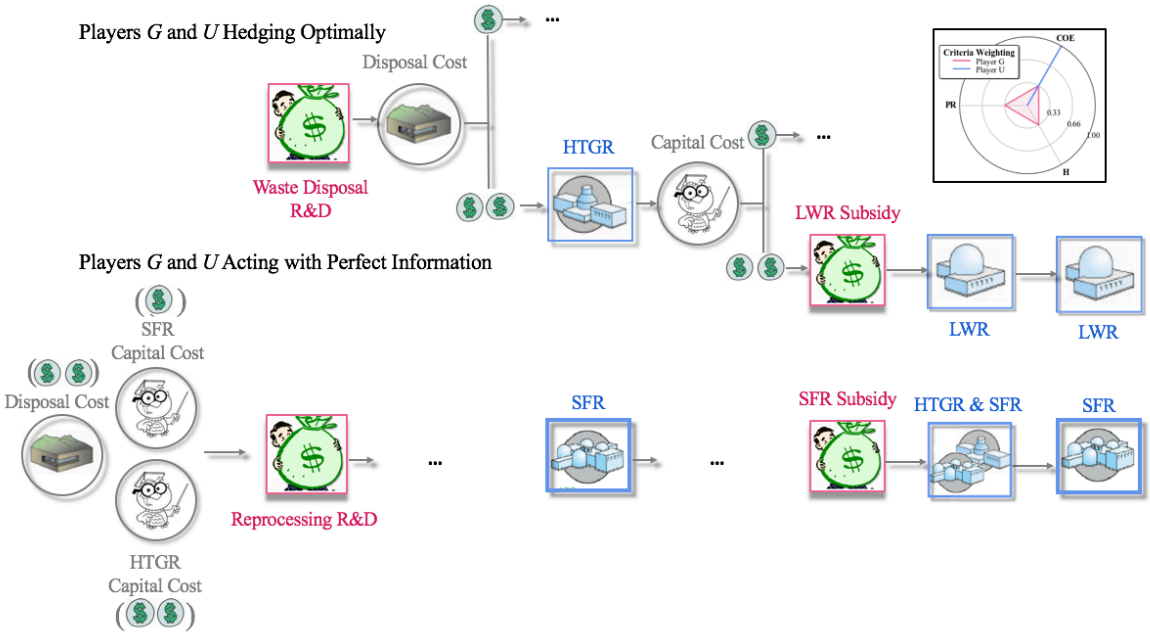

Figure 6.12: Player *G*'s and *U*'s decisions with perfect information (top) and when hedging optimally (bottom). *G*'s and *U*'s optimal hedging strategies shown in response to one specific example of the evolution of *Nature*'s moves (high disposal costs and high HTGR costs – *Nature* never moves to reveal SFR costs since *U* never chooses *SFR* strategy).

Examining the bottom path in Fig. 6.12, when *G* and *U* act with perfect information, both have determined that in this particular state of the world, transitioning to a closed fuel cycle is favorable. *G* then chooses her *Only Reprocessing R&D* strategy at her first decision node. By doing so, she drives the cost of reprocessing down, knowing that used fuel will be reprocessed instead of disposed. At his first decision node, *U* readily adopts SFR technology, though interestingly, chooses his *HTGR-SFR* strategy at his second decision node, despite high HTGR capital costs. When *U* follows partial path $\vartheta^{U}_{SFR,HTGR-SFR,SFR}$, less used fuel is eventually disposed during the simulation compared with ϑ^{U}_{SFR} though only by approximately 10,000 tIHM (see Fig. 6.13). Cost savings from avoiding disposal of

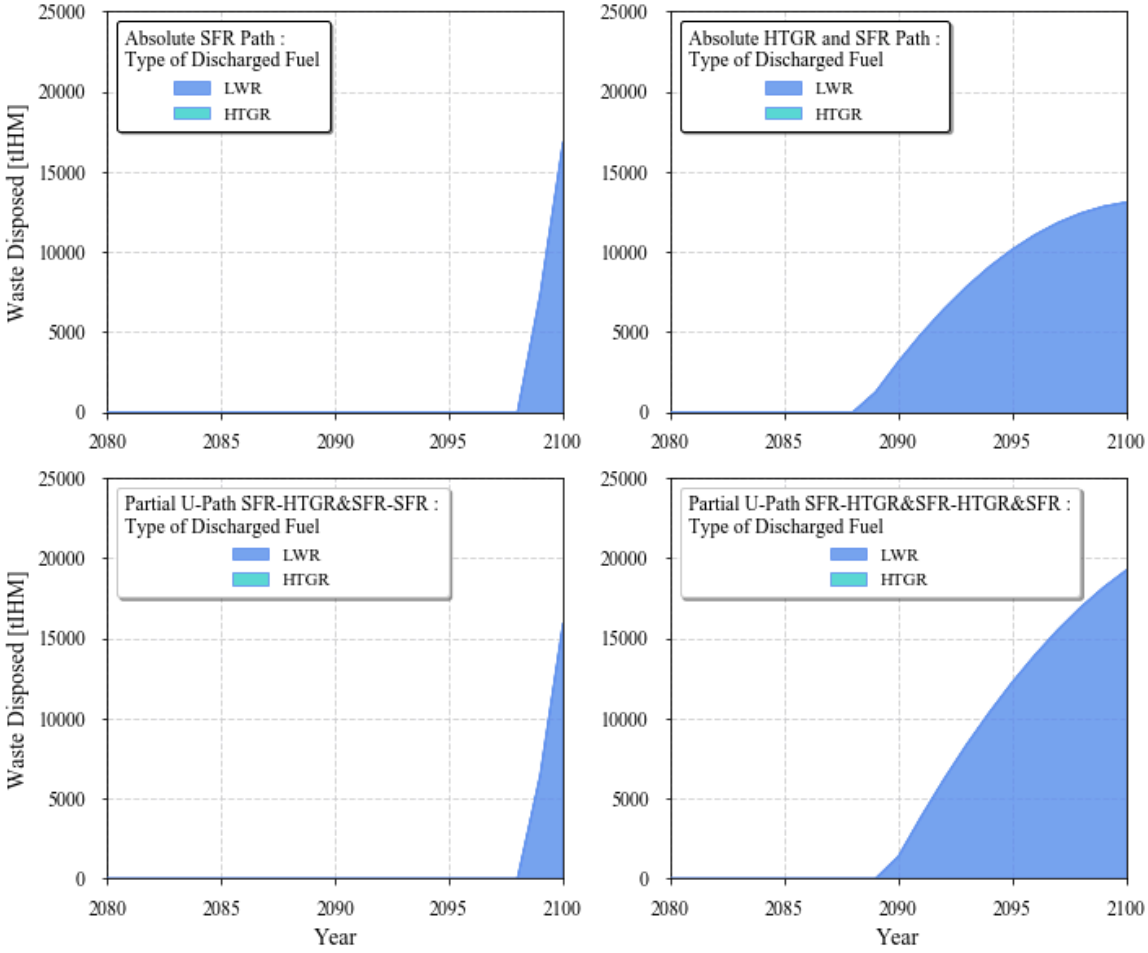

Figure 6.13: Amount of used fuel disposed for absolute U-paths (top-left) ϑ^{U}_{SFR} and (top-right) $\vartheta^{U}_{HTGR\&SFR}$, and partial U-paths (bottom-left) $\vartheta^{U}_{SFR-HTGR\&SFR-SFR}$ and (bottom-right) $\vartheta^{U}_{SFR,HTGR\&SFR,HTGR\&SFR}$.

used fuel are in U's favor. Further, by building only the first 10 HTGR facilities, U is able to deploy SFRs at a faster rate, allowing more cost savings to be realized (part of the reactor capital cost payment period is cutoff before the decision making time period is over). For a similar reason, G is seen to subsidize SFRs, despite U choosing his HTGR-SFR strategy. The capital subsidy is calculated such that if a reactor type is subsidized, the discount will

be equivalent over the lifetime of the reactor, and across the reactors built during the allotted time period. Because of this nature, a small deviation in the Cost of Electricity score is seen across *G*'s options to subsidize HTGRs, SFRs, or HTGRs and SFRs. While behavior is nonintuitive, the overall expected trends are consistent.

Fig. 6.14 shows metric scores for each path along the Transition Game decision tree when both players act with perfect information. While there are 36 possible states of the world, corresponding to paths along the tree representing every combination of *Nature*'s moves, some metric scores overlap and cannot be differentiated in Fig. 6.14. For instance, if *U*'s perfect information strategies result in his absolute LWR path, then *Nature*'s moves choosing HTGR and SFR capital costs have no effect on the metric scores. Of the 36 states of the world, only 3 yield conditions where SFR technology is chosen: (1) moderate disposal costs, high HTGR capital costs, and low SFR capital costs (2) high disposal costs, high HTGR capital costs, and low SFR capital costs and (3) high disposal costs, moderate HTGR capital costs and low SFR capital costs. (1) and (2) lead to *U*'s partial $\vartheta^{U}_{SFR,HTGR-SFR,SFR}$ path, while (3) leads to *U*'s absolute HTGR-SFR path. *G*'s capital subsidy selection is seen to follow the technology that *U* chooses. Because the expected state of the world is unfavorable to SFR technology, *U* hedges only with his HTGR strategy; for 60 percent of the 36 possible states of the world, *U* chooses his absolute HTGR strategy. The dominance of the HTGR hedging strategy is due to the possibility of achieving a significantly lesser capital cost (3000 \$/kW$_e$) than LWRs (4177 \$/kW$_e$), with even the most probable HTGR capital cost (4000 \$/kW$_e$) still less than LWR capital costs. This heavy dominance may be an indicator of an overly optimistic expectation on the performance of future HTGRs.

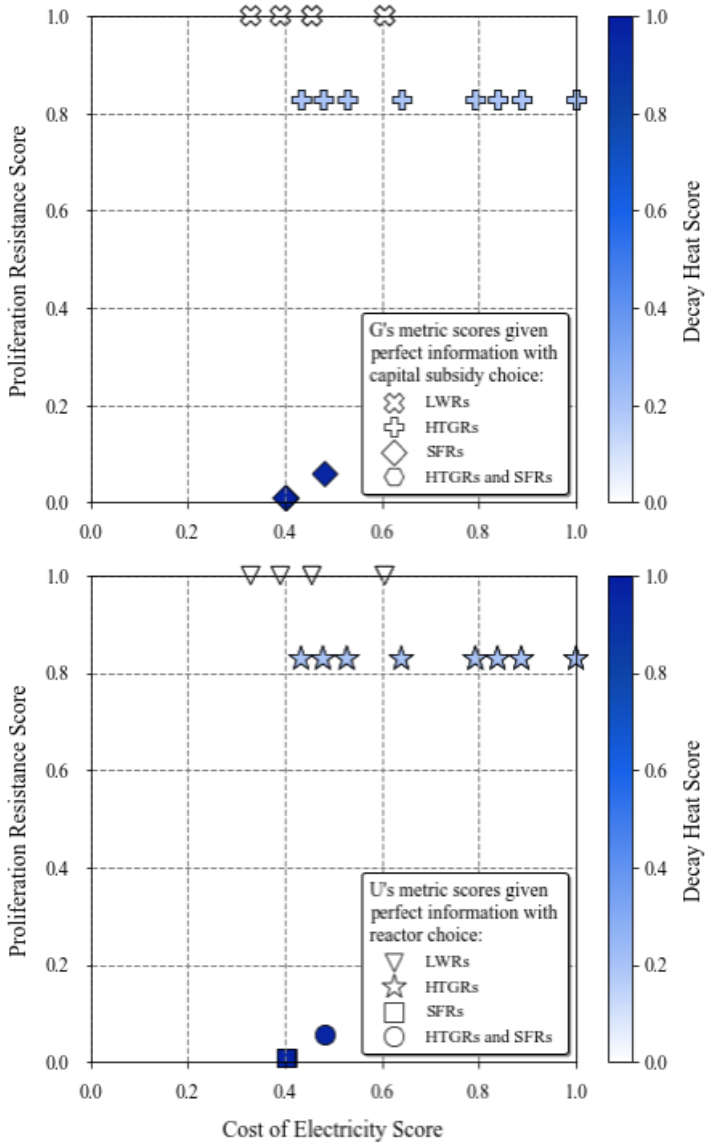

Figure 6.14: Metric scores for Player *G*'s and *U*'s perfect information strategies for all combinations of *Nature*'s moves.

When *G* and *U* are hedging optimally, their strategies are fairly different. The state of the world is expected to be unfavorable for closing the fuel cycle, so *G* instead chooses to invest all her R&D budget into waste disposal. *U* observes this decision, and is further

unwilling to risk building SFR technology, especially since the cost of reprocessing is high. Now, if *Nature* moves to reveal an expensive HTGR capital cost. All prospects of implementing advanced reactor technology are dissolved, and LWR technology is again instated.

Fig. 6.15 shows metric scores for each path along the Transition Game decision tree when both players are hedging optimally. *G*'s first hedging strategy is always (under the baseline criteria weighting) her *Only Waste Disposal R&D*. Then, regardless of the waste disposal cost *Nature* reveals, *U* hedges with his *HTGR* strategy. After *Nature* makes the HTGR capital cost known, *G* and *U* will revert to LWR technology if HTGRs are expensive or continue deploying HTGR technology if cheap. *G*'s Proliferation Resistance and Decay Heat scores will improve if *U* chooses his absolute HTGR path, however, *G*'s capital subsidy is insufficient to drive this transition, especially considering her payoff also considers the Cost of Electricity criterion. Then, *G* is seen to simply subsidize whichever reactor type *U* will choose at his next decision node.

6.3 Criteria Weighting Sensitivity

The strategies - both perfect information and hedging strategies – chosen by each player in the Transition Game are contingent on their decision criteria weightings. The exploration of these weightings allows for identification of robust hedging strategies when considering regime changes that may lead to policy makers or utilities taking on different character archetypes. The effect of these weightings is examined here.

The top-left quadrant of Fig. 6.16 depicts *G*'s decision matrix for selecting an optimal hedging strategy at her first decision node. The triangle-shaped decision matrix

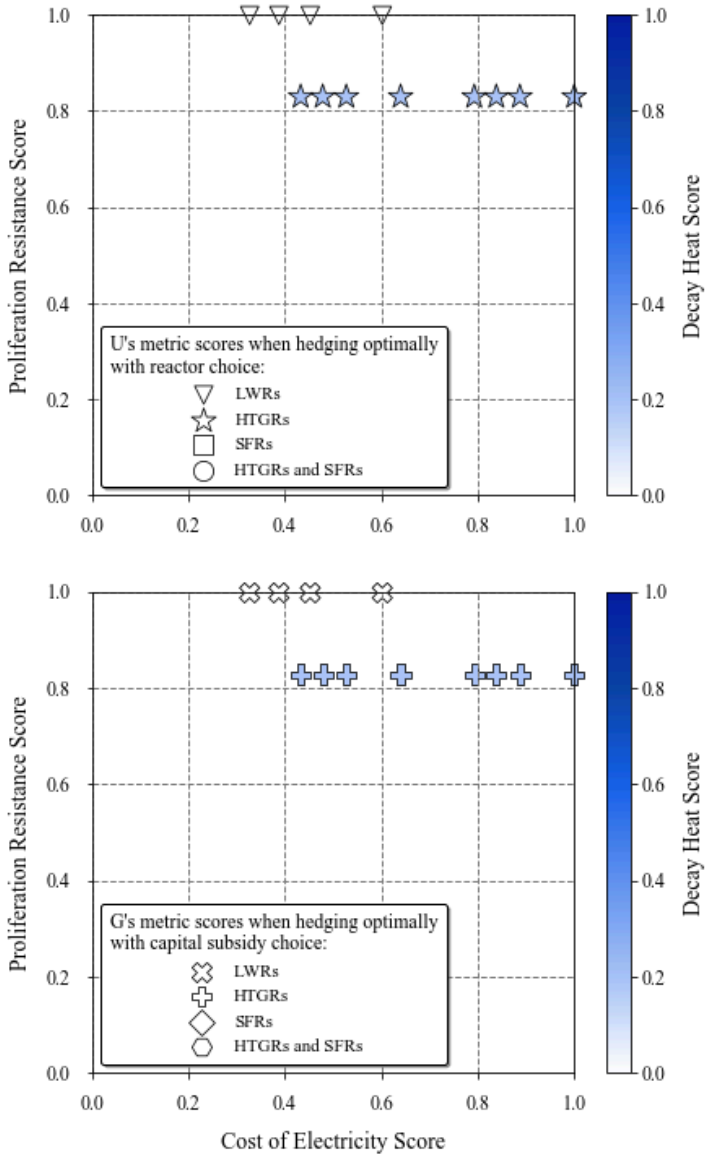

Figure 6.15 Metric scores for Player *G* and *U* optimally hedging for all combinations of *Nature*'s moves

represents the space of all possible criteria weighting, under the constraint that the sum of the weights equals unity. The bottom-right quantile is shaded yellow, which is interpreted as *G*'s optimal hedging strategy to be her *Only Reprocessing R&D* when she places all importance on the Decay Heat criterion (weights 0.0, 1.0 and 0.0 for the Cost of Electricity, Decay Heat and Proliferation Resistance criteria, respectively). Compare to the bottom-left quantile, which is shaded red as *G*'s optimal stage one hedging strategy is her *Only Waste Disposal R&D* when her Cost of Electricity criterion weight is 1.0. Fig. 6.16 depicts two decision matrices for *G*'s first hedging strategy, differentiated by the criteria weightings in their respective radar charts: (left) when *G*'s weights are varied and *U*'s weights are fixed at his baseline values, and (right) when *G*'s weights are fixed at her baseline value and *U*'s weights are varied. *G*'s stage one optimal hedge identified in Section 6.2, Fig. 6.12 is her *Only Waste Disposal R&D* strategy when *G* and *U* have their baseline criteria weights. Examining the decision matrices in Fig. 6.16, this hedging strategy is seen to dominate the decision space, proving to be a robust hedging strategy early in the Transition Game.

The bottom-left quadrant of Fig. 6.16 shows *G*'s expected metric scores for each of her available stage one strategies when both *G* and *U* have their baseline criteria weights. The *Only Reprocessing R&D* strategy has the lowest expected Cost of Electricity and Proliferation Resistance scores but the greatest expected Decay Heat score among *G*'s available stage one strategies. If *G* chooses her *Only Reprocessing R&D* strategy as her stage one hedge, more SFR generating capacity is expected since *G* influences the possible state of the world to be more favorable to SFRs. Though barely visible, the expected penetration of SFRs is reflected in the size of the marker in the bottom-left quadrant of Fig. 6.15. The size of the markers in Figs. 6.16, 6.17 and 6.19 are each normalized

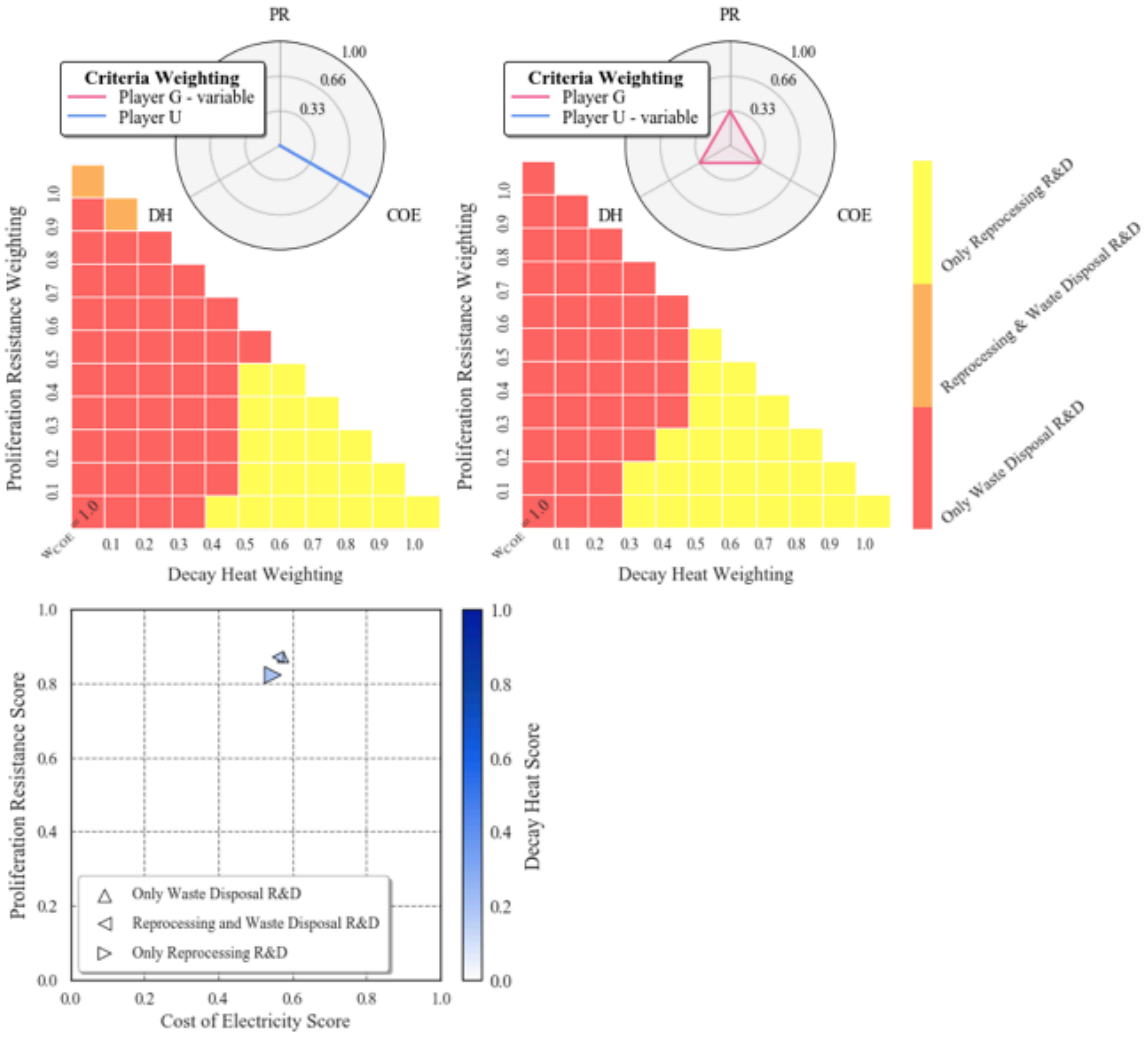

Figure 6.16: Player *G*'s weighted decision matrices (top-left when varying *G*'s criteria weighting and top-right when varying *U*'s criteria weighting) for her stage one hedging strategy and expected metric scores and SFR penetration (relative marker size) associated with *G*'s stage one hedging strategy with *G* and *U*'s baseline criteria weightings.

identically. Then, since the expected penetration of SFRs is merely 1.3 percent (Fig. 6.16, bottom-left, *Only Reprocessing R&D*), its larger size is barely visible over the 0 percent baseline size (Fig. 6.16, bottom-left, *Only Waste Disposal R&D* and *Reprocessing and*

Waste Disposal R&D). Both expected metric scores and expected SFR penetration are affected by *G*'s and *U*'s criteria weightings as that determines their strategy plays.

Fixing *G*'s stage one hedging strategy as her *Only Waste Disposal R&D* strategy (and in turn choosing an expensive reprocessing technology cost) and assuming that *Nature* moves to choose a high waste disposal cost, Fig. 6.17(left) shows *U*'s stage one hedging strategy as a response based on his criteria weighting. Consistent with Fig. 6.12, at *U*'s first decision node, his optimal hedging strategy is his *HTGR* strategy (found moving up 4 and right 4 quantiles from the bottom-left in *U*'s decision matrix). Considering the entire criteria-weighting space, *U*'s most frequently chosen hedging strategy at his second decision node is his *HTGR-SFR* strategy, with the tradeoff between the Decay Heat and Proliferation Resistance decision criteria evident. Fig. 6.17(right) gives *U*'s expected metric scores for each of his stage one hedging strategies, with the expected SFR penetration corresponding to the marker size. Fig. 6.17(right) data points are labeled as the (Cost of Electricity score, Proliferation Resistance score, Decay Heat score, expected SFR generating capacity penetration). The expected value of each metric score does not differ greatly across each of *U*'s available strategies, reflected in the tight range of each axis in Fig. 6.17(right). Fig. 6.18 shows the expected scores relative to the range of possible metric scores for each of *U*'s strategies when *U* chooses his strategies with his baseline criteria weighting. For all cases, the expected score does not correspond with any individual outcome. The expected score is a probability-weighted score based on the probability distribution of *Nature*'s moves and each players' downstream responses. If *U* chooses his *SFR* or *HTGR-SFR* strategy at his first decision node, *Nature* often reveals a state of the world that is unfavorable for recycle. Then, *U* typically chooses either his *LWR* or *HTGR*

strategy as a recourse decision when choosing his strategy with his baseline criteria weighting. The expected scores for *U*'s recycle strategies at his first decision node then reflect the probable downstream adjustment in his strategy.

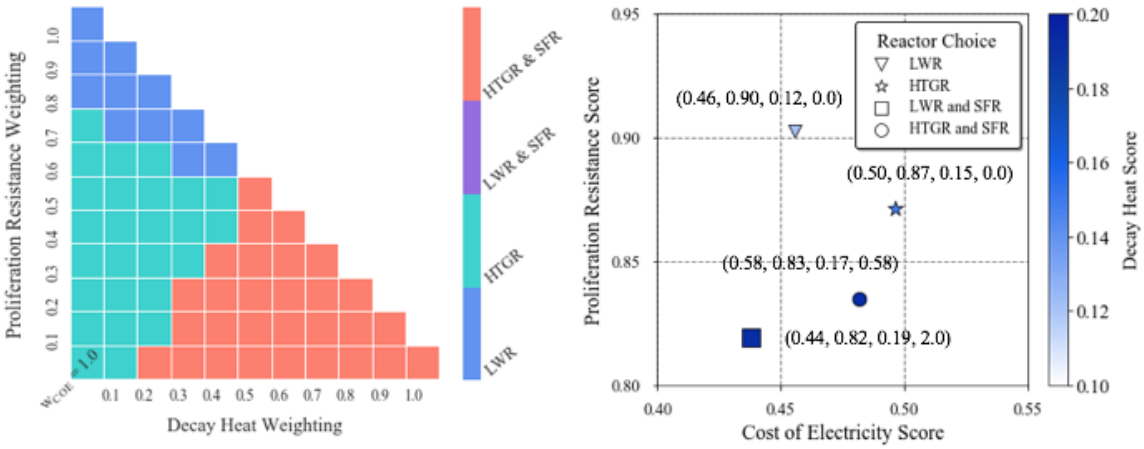

Figure 6.17: Player *U*'s weighted decision matrix when varying his criteria weighting for his stage one hedging strategy (left) and expected metric scores and SFR penetration (relative marker size) associated with *U*'s stage one hedging strategy with *G*'s and *U*'s baseline criteria weightings.

Fig. 6.19 shows the expected metric scores for each criterion in the bottom row, labeled according to *U*'s stage two decision. These expected scores are derived assuming that at *U*'s last decision node, he chooses a strategy with his baseline criteria weights. Findings depicted in Fig. 6.19 are dependent on the following: (1) *G* choosing her *Only Waste Disposal R&D* strategy at her first decision node and thereby choosing a high reprocessing cost, (2) *Nature* moving to choose a high waste disposal cost, and (3) *U* choosing his *HTGR* hedging strategy at his first decision node. From left to right, results in Fig. 6.19 are further dependent on *Nature* moving to choose a low, moderate and high

HTGR capital cost after *U*'s stage one decision. The resulting decision matrices for selecting *G*'s and *U*'s optimal hedging strategies at their second decision nodes are shown in the middle and bottom rows, respectively.

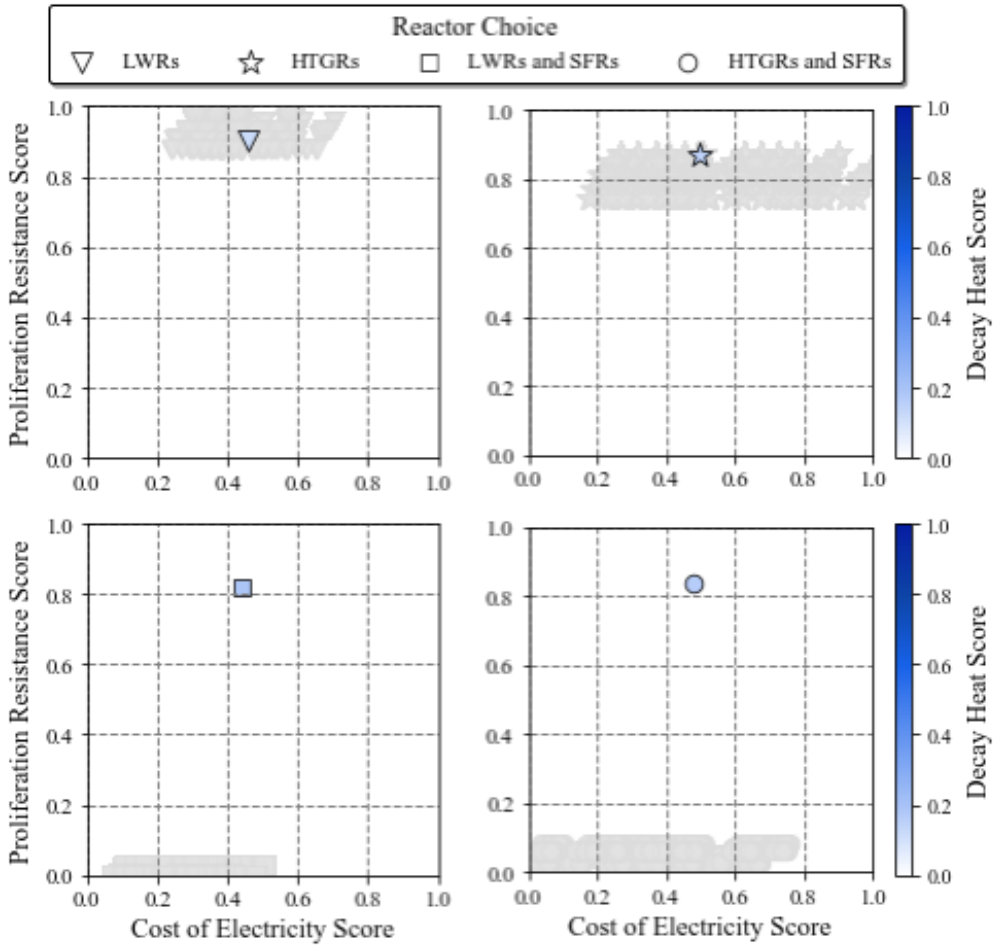

Figure 6.18: Player *U*'s stage one expected metric scores for each available hedging strategy (blue symbols) and possible metric scores following paths in the Transition Game decision tree (transparent grey symbols).

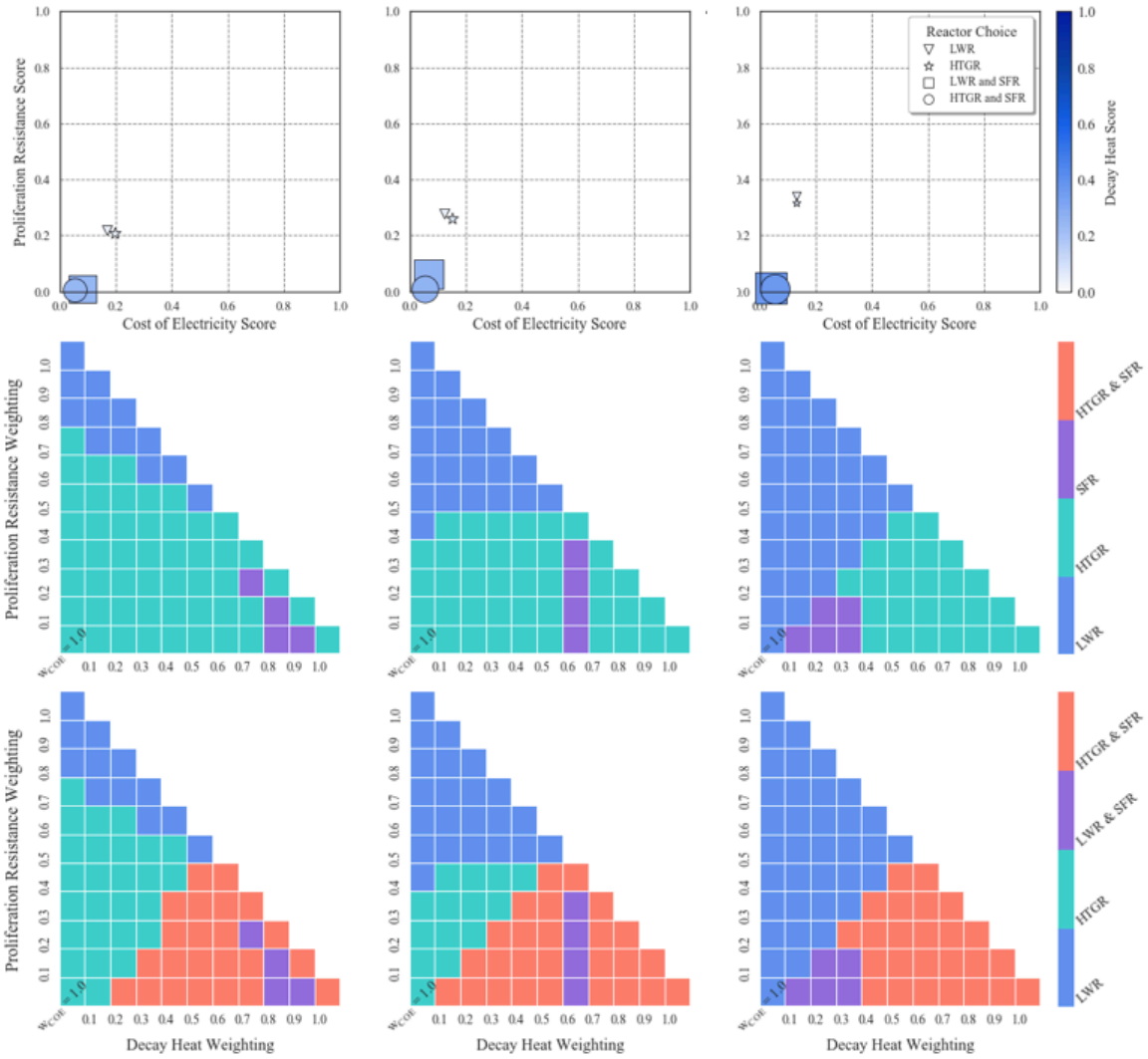

Figure 6.19: Metric scores for all available hedging strategies at *U*'s second decision node (top row) with assumed upstream conditions: *G*'s *Only Waste Disposal R&D* stage one hedge, *Nature* revealing high waste disposal cost and *U*'s HTGR stage one hedge. Marker size reflects expected penetration of SFR generating capacity. Columns from left to right correspond to *Nature* choosing a low, moderate and high HTGR capital cost. Players *G*'s (middle row) and *U*'s (bottom row) decision matrices for selecting optimal hedging strategies at their respective second decision nodes.

Fig. 6.19 demonstrates tradeoffs between the various decision criteria. As one moves from the bottom right to top left corners for any of *U*'s stage two decision matrices (bottom row), the optimal hedging strategy moves from recycling used fuel to direct disposal. In fact, following from bottom right to top left corner along each of the matrices' (top row for *G* and bottom row for *U*) hypotenuse yields the same determined optimal hedging strategies for *U* as the Cost of Electricity criterion weight is 0 (and Proliferation Resistance and Decay Heat scores are fixed for a *U*-path ϑ^U). Generally, as *U*'s criteria weights shifts towards Decay Heat, *U*'s optimal hedging strategy adopts SFR technology (choosing either his *SFR* or *HTGR-SFR* strategy), with the transition occurring more readily as HTGR costs increase. Moving along the y-axis of *U*'s decision matrix depicts the tradeoff between the Cost of Electricity and Proliferation Resistance scores. Moving along this axis, *U* is seen to abandon HTGR technology as the importance of proliferation resistance increases to him, with the abandonment occurring quicker as HTGR capital costs increase. Finally, traveling along the x-axis reveals the Decay Heat criterion weighting quickly encourages *U* to transition toward a closed fuel cycle. Expectedly, *G* subsidizes the technology that is built at *U*'s next decision node. In some cases, *G* is seen to subsidize HTGRs and then *U* chooses his *HTGR-SFR* strategy. Due to the implementation of the capital subsidy, where the total integrated discount is equivalent across reactor types, the effect of subsidizing HTGRs, SFRs or both is identical. Then, the strategy that is first in the selection order is returned as the strategy with the greatest expected payoff despite all three being equal.

6.3.1 DEMONSTRATION CASE

For illustration, examine the case where *G* and *U* have the decision criteria weighting given in Table 6.3. In this situation, *U* is influenced by his unanticipated commitment to onsite storage of used fuel with *G* failing to provide an acceptable waste repository. While *G* chose her *Only Waste Disposal R&D* strategy, delays in siting and construction ultimately drove waste disposal costs up (*Nature* moves to choose a high disposal cost) and accumulated waste quantities during delays suggest the need for an additional repository. The following narrative describes the particular path through the Transition Game decision tree depicted in Fig. 6.20. All of *G*'s and *U*'s strategies may be determined by examining the decision matrices in Figs. 6.16, 6.17 and 6.19, which are derived with the assumption that *Nature* moves to choose a high disposal cost.

Table 6.3: Player *G*'s and *U*'s alternate decision criteria weighing for Demonstration Case.

	Criterion Weighting	
Evaluation Criterion (*c*)	Player *G*	Player *U*
Cost of Electricity	$0.\overline{3}$	0.9
Decay Heat	$0.\overline{3}$	0.1
Proliferation Resistance	$0.\overline{3}$	0.0

The example illustrates the robustness of *G*'s *Only Waste Disposal R&D* hedging strategy. *G* chooses this strategy both when *U* hedges with his baseline weights and when *U* hedges with the alternative weights in Table 6.3. By examining *G*'s decision matrix in Fig. 6.16 when varying *U*'s weights (top-right), *G* can choose a hedging strategy that will perform well over a range of *U*'s weights. This proves valuable as *U*'s weights shift based on the *Nature*'s move following *G*'s first decision (where *U* is now concerned with the

Decay Heat criterion due to his onsite storage commitment). Given these upstream conditions, *U*'s optimal hedging strategy is found using the decision matrix in Fig. 6.17 and applying *U*'s weights. By doing so, *U* chooses his *HTGR* strategy.

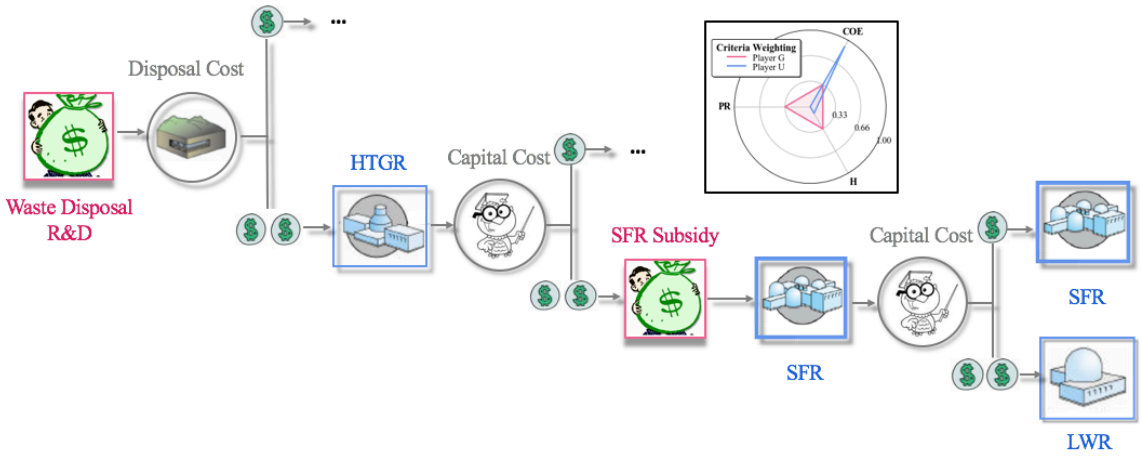

Figure 6.20: Optimal path through Transition Game decision tree for the Demonstration Case when Players *G* and *U* hedge optimally with alternate criteria weighting. Assumes *Nature* determines (1) high disposal costs and (2) high HTGR capital costs.

After *U* chooses his *HTGR* strategy, *Nature* moves to reveal the HTGR capital cost. Each of *G*'s optimal hedging strategies as a response to this move by *Nature* can be determined using the middle-row of Fig. 6.19, moving from left to right gives *G*'s strategy based on a low, moderate and high HTGR capital cost. Assuming that *Nature* determines a high HTGR capital cost, *G* subsidizes SFRs and *U* chooses his *SFR* strategy. If *Nature* then determines a high SFR capital cost, all advanced reactor technologies are abandoned, and *U* chooses his *LWR* strategy at his last decision node. However, if *Nature* determines a low or moderate SFR capital cost, *U* continues the SFR transition. Notice that the

conditions up until *G*'s capital subsidy play are identical to those portrayed in Fig. 6.12. Now however, *G* can influence *U* to adopt SFR technology by offering the appropriate subsidy given *U*'s new criteria weighting.

The decision matrices depicted in Figs. 6.16, 6.17 and 6.19 may be constructed for all combinations of *Nature*'s moves, and as well, one may be constructed for *U*'s final decision which he makes with complete information.

CHAPTER 7: CONCLUSIONS

This work presents a novel methodology for optimizing nuclear fuel cycle transitions that captures interactions between a policy maker and electric utility company. The methodology couples a nuclear fuel cycle simulator with multiple objective function calculators and a stochastic and game theoretic optimization solver and is demonstrated using a two-person general-sum sequential game with uncertainty (the Transition Game). Fuel cycle transition strategies are input to the VEGAS simulator to calculate a material- and technology-constrained material balance, which is input to multiple fuel cycle metric objective function calculators. Objective function values are then translated into payoffs for each player in the Transition Game using their unique set of decision criteria and weightings. The optimization solver explicitly handles uncertainties using a stochastic programming approach with chance nodes depicted as a *Nature* player who moves randomly. The input data and selected player strategies and decision criteria are by no means entirely comprehensive or exhaustive; the transition examined, and its resulting analysis are intended as a proof-of-concept game theoretic approach to nuclear fuel cycle transition analysis and optimization.

The Transition Game is informed by the VEGAS nuclear fuel cycle simulator. While not the focus of the work, many enhancements to the VEGAS code are documented in this dissertation. These changes allowed for further distinction between fuel transition strategies and add richness and realism to those strategies, furthering VEGAS's value and versatility as a preconditioner tool. Most notably, the reprocess used fuel at *full-capacity* feature, supplemental to the reprocess *on-demand* feature, and its allowed adjustments during a fuel cycle transition allow realism during an initial learning period when building

advanced reactor technology. The two reprocessing schemes affect the material balance calculation, which results in changes in the calculated fuel cycle metric objective function values. This feedback between decisions and objective function values is the root cause for the development of fuel cycle simulators.

The Transition Game features a policy maker that must choose R&D investments in competing used fuel reprocessing and waste disposal technologies and capital subsidies for available reactors in the transition scenario; and an electric utility company that chooses reactor technologies to deploy in order to fulfill a fixed demand for nuclear electricity. Two advanced reactor technologies are available, HTGR and SFR technologies, though are subject to uncertain capital costs. The game theoretic optimization solver finds near-term hedging strategies that balance the exchange between the risk of immediate action and delay and maintain flexibility to allow for intelligent recourse decisions once uncertainties are resolved. These hedging strategies are shown to react to changes in decision criteria weighting, though robust hedging strategies that appear for many combinations of decision criteria weighting are found.

Results from the Transition Game indicate that transition to a closed fuel cycle relying on recycling used fuel in SFRs is only favorable (under a baseline set of decision criteria weightings) if players have perfect information regarding *Nature*'s future moves. Then, under a limited set of conditions, transition to a closed fuel is observed. However, when players act with imperfect information and hedge against *Nature*, transition to a closed fuel cycle is never observed.

One of the more compelling results from the Transition Game is the identification of a robust near-term hedging strategy being adoption of HTGR technology over

approximately 80 percent of the utility generating company's space of possible decision criteria weightings. A subset of this time (an estimated 44 percent) suggest HTGR technology be adopted concurrently with SFR technology. After a learning period, either technology may be abandoned if capital costs are unfavorable. When only HTGR technology is chosen and later abandoned, transition to used fuel recycling in SFRs may be spurred by capital subsidies under certain criteria weightings. This change in fuel cycle strategies as a response to information gained during the transition illustrates autonomous decision making within the fuel cycle simulator.

FUTURE WORK

Many components of the analysis presented in this dissertation may be expanded. Briefly, these expansions may be:

- Inclusion of additional policy incentives, such as an adjustment of the Nuclear Waste Fund fee
- Inclusion of additional decision criteria, such as safety or resource utilization and additional fuel cycle metrics within these criteria
- Inclusion of more decisions or refinement on those decisions, such as the rate at which to build SFRs
- Inclusion of simultaneous decisions, where multiple utility companies compete to fulfill a fixed demand for nuclear electricity
- Inclusion of the selection of reprocessing capacity deployment schedule and utilization methods as a player decision
- Better parameterization of the effects of R&D on technology cost estimates
- Different scalarization methods for multi-objective optimization

A large criticism of this area of research is its heavy reliance on accurate input data. In this work, most cost estimates are dated, and in some cases rely on the private judgements of only a handful of fuel cycle experts. The latest cost estimates are taken from private industry reports that may be overly optimistic, and in fact results show a tendency towards these technologies. Better informed cost estimates would greatly increase the value of the analysis presented here. Further, the assumption used in this dissertation is that the preferences of a decision maker respond linearly and are therefore risk neutral. Alternatively, a decision maker may choose to examine temporal effects where, for instance, they are averse to the cost of electricity surpassing some threshold value during a portion of the simulation.

Most importantly, while this dissertation addresses several short-comings of past fuel cycle analysis studies, many of its own short-comings arise from the limitations of the fuel cycle simulator chosen. Some potential capabilities of more detailed fuel cycle simulators include the ability to model discrete facilities and materials, allowing for determination of fresh fuel isotopic requirements and disruption analysis through tracking the operations status of individual facilities. The potential coupling of VEGAS as a preconditioner tool to a higher-fidelity simulator (for simplicity, H-SIMULATOR) is depicted in Fig. 7.1. H-SIMULATOR initializes the fuel cycle transition scenario given a set of user-input parameters. At each chosen time-step when a decision of interest must be made, H-simulator invokes VEGAS, inputting the current state of the fuel cycle. VEGAS uses input from H-SIMULATOR and the defined player strategies, decision criteria and uncertainties to optimize a fuel cycle transition over a user-defined "forecast" period. The optimized transition strategy is then returned to H-SIMULATOR, which marches the outer optimized

transition forward in time. When another decision of interest must be made, the process is repeated. The VEGAS preconditioner subroutine procedure is iteratively called until H-SIMULATOR reaches its designated end time.

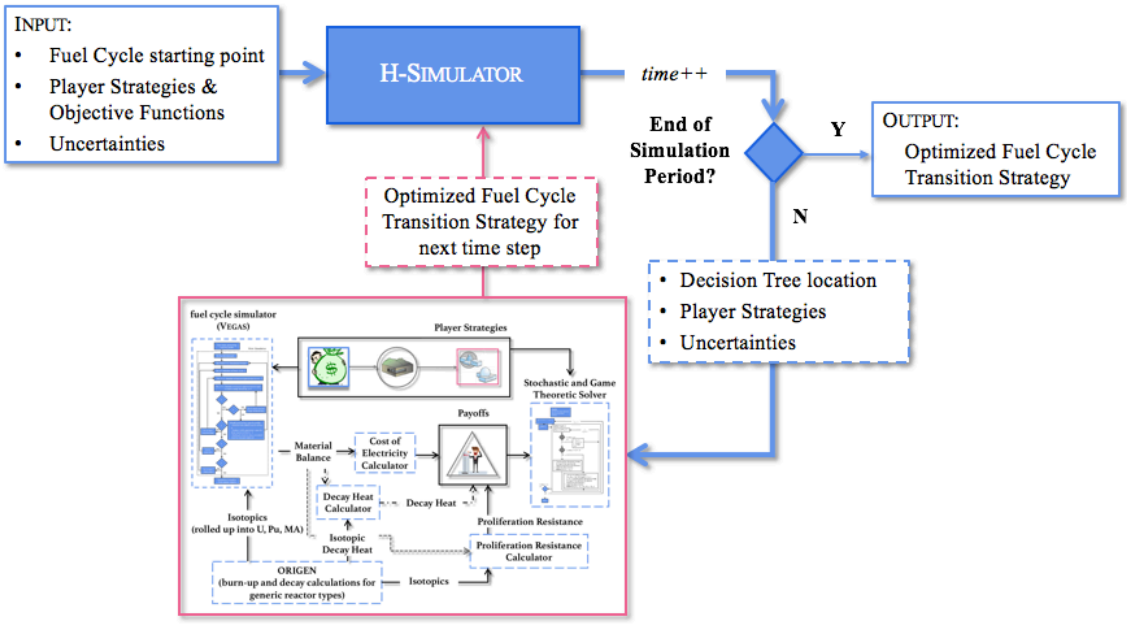

Figure 7.1: Potential coupling of VEGAS as a preconditioner tool for scoping promising fuel cycle transition strategies for higher-fidelity simulators.

Outside the realm of fuel cycle transition analysis, the work presented here has further applications in nuclear safeguards and security, where a fuel cycle simulator may be used to identify vulnerabilities in the fuel cycle. The novel coupling of a fuel cycle simulator to an adversarial game offers the ability to more realistically calculate objectives such as the time requirement for significant diversion of special nuclear material, idle capacity, or quantities of stockpiled separated actinides. A temporal cross section in a fuel cycle simulation may give initial conditions for a breakout scenario where an aggressive

strategy to produce or divert large quantities of high-value special nuclear material is pursued, or at worst, a regime change where a civilian nuclear power program is abandoned in favor of a nuclear weapons-production program.

APPENDIX A: PROLIFERATION RESISTANCE CALCULATION

Charlton et al. (2017) derived the *nuclear security measure* metric for evaluating the proliferation resistance of a nuclear fuel cycle. Novel to the methodology is focus on the temporal evolution of the proliferation resistance as material moves through the fuel cycle, which allows for a dynamic assessment of proliferation resistance with material constantly in a state of change. The methodology relies on a dynamic material balance (provided either through process flow sheets or a fuel cycle simulator) and a series of attributes (for instance, material attractiveness level and radiation dose rates), and their associated weights and utility functions that relate the change in the value of the attribute to its effect on the proliferation resistance value.

ATTRIBUTES

The attributes included in this work are only those capable of being evaluated through measurement of intrinsic barriers to proliferation resistance. These intrinsic barriers are resultant from inherent properties of the materials themselves. For instance, the material handling requirements become more complex as the (measurable) heat rate from Pu increases. Table A.1 lists the attributes identified by Charlton et al., with those included in this work indicated. More information on the exclusion of certain attributes is given in Section 4.2.

Table A.1: Nuclear security attributes and weighting factors from Charlton et al. (2017). Weighting (Left w_j column) in Charlton et al. (2017) and (Right w_j column) re-normalized weighting used due to omitted attributes.

j	Attribute	w_j		Included
A. Material Attractiveness Level				
1	DOE attractiveness level (IB through IVE)	0.10		✓
2	Heating rate from Pu in material (W)	0.05		✓
3	Weight fraction of even Pu isotopes	0.06		✓
B. Concentration				
4	Concentration (SQs per tonne)	0.10		✓
F. Handling Requirements				
5	Radiation dose rates (rem per hr at distance of 1 m)	0.08		✓
6	Size/weight	0.06	×	×
G. Type of Accounting System				
7	Frequency of measurement	0.09	×	×
8	Measurement uncertainty (SQs/yr)	0.10	×	×
9	Separability	0.03		✓
10	Percentage of processing steps that use item accounting	0.05	×	×
H. Accessibility				
11	Probability of unidentified movement	0.07	×	×
12	Physical barriers	0.10	×	×
13	Inventory (SQs)	0.05	×	×
14	Fuel load type (batch or continuous reload)	0.06	×	×

Utility functions for each attribute as given by Charlton et al. (2017), each requiring user input, are given below. The output composition of the material at each fuel cycle process is the evaluated material to obtain a given utility function for the next downstream process. For example, the utility function value of the U conversion process is evaluated for solid NU as U_3O_8.

Attribute 1: DOE Attractiveness Level

Categories of material with their description and category corresponding to form and quantity of material from DOE M474.1-1 (DOE, 2000) are given in Table A.2. Materials with lower qualities rank higher on the proliferation resistance scale and are less likely to be stolen and diverted by a proliferation. DOE attractiveness level IA is not included, as it was assumed that category IA, material as assembled weapons and test devices, would never be present in a civilian fuel cycle. The DOE attractiveness level determined for each fuel cycle process is given in Table A.3, along with its utility function value.

Attribute 2: Heating Rate from Pu

Materials with a high heat source require careful management, resulting in increased difficulty of designing an explosive device (NRC, 1995). The utility function of this metric is given by Eq. A.1.

$$u(x) = 1 - exp\left[-3\left(\frac{x}{x_{max}}\right)^{0.8}\right] \tag{A.1}$$

where x = heating rate from Pu in watts per kg

x_{max} = maximum heat rate (heat rate of pure ^{238}Pu, 570 watts per kg)

If the quantity of Pu in the material is zero, the utility function value is set to unity. The utility function values for this attribute for each reactor type and fuel cycle process are given below. Heat rate of Pu was altered based on private correspondence for normalization purposes (*William Charlton, 2018).* The calculated heat rate from Pu for each fuel cycle process is given in Table A.4 with corresponding utility function value given in Table A.5.

Table A.2: DOE special nuclear material categories and attractiveness levels with corresponding utility function values (A) and definitions (B).

A. Utility Function for DOE Attractiveness Level						
			Category			
			I	II	III	IV
	Attractiveness	B	0.00	0.05	0.10	0.15
		C	0.15	0.25	0.34	0.45
		D	NA	0.40	0.65	0.90
		E	NA	NA	NA	1.00
B. DOE Safeguarded Terms from DOE M474.1-1						
			Pu/^{233}U Category [^{235}U Category] (kg)			
Weapons: Assembled weapons and test devices	Attractiveness	A	All [All]	NA [NA]	NA [NA]	NA [NA]
Pure products: Pits, major components, button ingots, recastable metal, directly convertible materials		B	≥2 [≥5]	≥0.4<2 [≥1<5]	≥0.2<0.4 [≥0.4<1]	<0.2 [<0.4]
High-grade materials: Carbides, oxides, solutions (≥25 g/ℓ) nitrates, etc., fuel elements and assemblies, alloys and mixtures, UF_4 and UF_6 (≥50% enriched)		C	≥6 [≥20]	≥2<6 [≥6<20]	≥4<2 [≥2<6]	<0.4 [<2]
Low-grade materials: Solutions (1 to 25 g/ℓ), process residues requiring extensive reprocessing, moderately irradiated material, ^{238}Pu (except waste), UF_4 and UF_6 (≥20%<50% enriched)		D	NA [NA]	≥16 [≥50]	≥3<16 [≥8<50]	<3 [<8]
All other materials: Highly irradiated forms, solutions (<1 g/ℓ), uranium containing <20% ^{235}U (any form, any quantity)		E	NA [NA]	NA [NA]	NA [NA]	All [All]

Table A.3: Determined DOE Attractiveness Level and Material Category for each fuel cycle process and corresponding utility function values.

	DOE Attractiveness Level | Utility Function Value					
Fuel Cycle Process	LWR		HTGR		SFR	
U Mining and Milling	IVE	1.00	IVE	1.00	IVE	1.00
Conversion	IVE	1.00	IVE	1.00	IVE	1.00
Enrichment	IVE	1.00	IVE	1.00	NA	NA
Fuel Fabrication	IVE	1.00	IVE	1.00	IIID	0.65
Fuel Fabrication (SFR)	NA	NA	NA	NA	IC	0.15
SNF Storage	IVE	1.00	IVE	1.00	IVE	1.00
SNF Disposal	IVE	1.00	IVE	1.00	IVE	1.00
Reprocessing	IC	0.15	IC	0.15	IC	0.15
HLW Disposal	IVE	1.00	IVE	1.00	IVE	1.00

Table A.4: Calculated heat rate of Pu and corresponding utility function values.

	Heat Rate from Pu (watts per tIHM) | Utility Function Value					
Fuel Cycle Process	LWR		HTGR		SFR	
U Mining and Milling	0.00	1.00	0.00	1.00	0.00	1.00
Conversion	0.00	1.00	0.00	1.00	0.00	1.00
Enrichment	0.00	1.00	0.00	1.00	NA	NA
Fuel Fabrication	0.00	1.00	0.00	1.00	269.92	0.32
Fuel Fabrication (SFR)	NA	NA	NA	NA	4150.99	0.92
SNF Storage	261.49	0.25	568.08	0.41	3533.41	0.90
SNF Disposal	246.11	0.24	539.61	0.40	3821.47	0.91
Reprocessing	0.62	0.24	539.61	0.40	4150.99	0.92
HLW Disposal	0.00	1.00	0.00	1.00	0.00	1.00

Attribute 3: Weight Fraction of Even Pu Isotopes

Construction of a nuclear explosive is complicated by the concentration of even Pu isotopes (NRC, 1995). In particular, ^{240}Pu has a high rate of spontaneous fission and can increase the probability of a preinitiation in a nuclear explosive device. The weight fraction of Pu isotopes is the utility function value and is calculated using Eq. A.2. If the quantity of Pu in the material is zero, the utility function value is set to unity.

$$x = \frac{\text{sum of even Pu isotopes (g)}}{\text{sum of all Pu isotopes (g)}} \tag{A.2}$$

The calculated attribute and corresponding utility function value, for each reactor type and fuel cycle process, are given in Table A.5.

Table A.5: Calculated weight fraction of even Pu isotopes and corresponding utility function values.

	Weight Fraction of Even Pu Isotopes Utility Function Value					
Fuel Cycle Process	LWR		HTGR		SFR	
U Mining and Milling	0.00	1.00	0.00	1.00	0.00	1.00
Conversion	0.00	1.00	0.00	1.00	0.00	1.00
Enrichment	0.00	1.00	0.00	1.00	NA	NA
Fuel Fabrication	0.00	1.00	0.00	1.00	0.36	0.43
Fuel Fabrication (SFR)	NA	NA	NA	NA	0.36	0.43
SNF Storage	0.34	0.40	0.44	0.56	0.35	0.41
SNF Disposal	0.36	0.43	0.45	0.56	0.36	0.43
Reprocessing	0.36	0.43	0.46	0.58	0.36	0.43
HLW Disposal	0.00	1.00	0.00	1.00	0.00	1.00

Attribute 4: Concentration

A higher concentration of fissile materials is considered more attractive, as a lower mass (or volume) of material must be diverted or stolen in order to acquire a useable mass of SNM or alternate nuclear material (ANM; defined as separated ^{237}Np or Am). The computed significant quantities of SNM or ANM for each reactor type and fuel cycle process and its corresponding utility function values (Eq. A.3) for this attribute are given in Table A.6.

$$u(x) = \begin{cases} 1 & \text{if } x < 0.01 \\ \exp\left[-3\left(\frac{x}{x_{max}}\right)^{0.8}\right] & \text{if } x \geq 0.01 \end{cases} \quad \text{(A.3)}$$

where x = concentration of the material in SQs per tonne

x_{max} = maximum possible concentration (125 SQs per tonne of pure Pu metal)

Table A.6: Calculated concentration of special nuclear material of each fuel cycle process and corresponding utility function values.

	Concentration of Special Nuclear Material (SQs per tIHM) | Utility Function Value					
Fuel Cycle Process	LWR		HTGR		SFR	
U Mining and Milling[a]	0.095	0.998	0.095	0.998	0.095	0.998
Conversion[a]	0.095	0.998	0.095	0.998	0.095	0.998
Enrichment[b]	0.768	0.985	2.186	0.957	NA	NA
Fuel Fabrication	0.560	0.989	2.067	0.960	33.072	0.516
Fuel Fabrication (SFR)	NA	NA	NA	NA	20.850	0.659
SNF Storage	0.560	0.989	2.067	0.960	20.850	0.659
SNF Disposal	0.560	0.989	2.067	0.960	20.850	0.659
Reprocessing	0.560	0.989	2.067	0.960	20.850	0.659
HLW Disposal	0.000	1.000	0.000	1.000	0.000	1.000

[a] SQ per tU as U_3O_8

[b] SQ per tSWU (SWU required for enrichment to 4.21 and 15.5 percent ^{235}U is calculated)

Attribute 5: Radiation Dose Rates

The utility function for the radiation dose rate attribute was developed based on acute biological effects of whole-body radiation dose to the potential proliferator. High-dose rates are more hazardous, a danger to the physical well-being of the proliferator and may require the use of expensive and unique equipment for remote handling. Above a threshold of 200 mrem per hr per SQ, the proliferation resistance includes a small credit for the costs of specialized equipment and a larger effect on proliferation resistance for high dose rates which would quickly incapacitate a proliferator. Above a threshold of 600 rem per hr per SQ, there is no continued increase in proliferation resistance since death is certain in all cases. The utility function for radiation dose rate is given by Eq. A.4. The methodology for obtaining radiation dose rates is given in Section 4.1. The calculated attribute values for each reactor type and fuel cycle process and corresponding utility function values are given in Table A.7.

$$u(x) = \begin{cases} 0 & \text{if } x \leq 0.2 \\ 0.0520833x - 0.010416 & \text{if } 0.2 < x \leq 5 \\ 0.0035714x + 0.232143 & \text{if } 5 < x \leq 75 \\ 0.00095238x + 0.428571 & \text{if } 75 < x \leq 600 \\ 1 & \text{if } x > 600 \end{cases} \quad \text{(A.4)}$$

where x = dose rate concentration in rem per hr per SQ for the unshielded material

ORIGEN's depletion and decay calculations output gamma-ray emission rates, in gamma-rays released per second, for specified energy windows in MeV, from a point source. Emission rates are translated into particles released per second per cm^2 assuming a distance of 10 m. Dose intensity values (mrem per hr per MeV) were obtained from the

ICRP 21, data from which are used in MCNP 6.2, part of ORNL's SCALE 6.2 package. The radiation dose rate is then given by Eq. A.5.

$$D = \sum_{e=E_0}^{E} \phi_{\gamma,e} \cdot d_{\gamma,e} \qquad \text{(A.5)}$$

where $d_{\gamma,e}$ = dose in mrem per hr from gamma-ray emission rates [particles/cm^2·s] for energy window e

$\phi_{\gamma,e}$ = gamma-ray emission rates [particles/cm^2·s] for energy window e

Table A.7: Calculated gamma-ray dose rate in rem per hr per SQ at 1m for each fuel cycle process and corresponding utility function values.

	Dose Rate (rem/hr/SQ) at 1 m Utility Function Value					
Fuel Cycle Process	LWR		HTGR		SFR	
U Mining and Milling	1.16E-01	0.000	1.16E-01	0.000	1.16E-01	0.000
Conversion	1.16E-01	0.000	1.16E-01	0.000	1.16E-01	0.000
Enrichment	4.43E-02	0.000	3.36E-04	0.000	NA	NA
Fuel Fabrication	4.43E-02	0.000	3.36E-04	0.000	2.31E+05	1.000
Fuel Fabrication	NA	NA	NA	NA	6.27E+03	1.000
SNF Storage	1.01E+04	1.000	5.53E+05	1.000	2.26E+05	1.000
SNF Disposal	2.50E+04	1.000	3.00E+04	1.000	6.27E+03	1.000
Reprocessing	2.50E+04	1.000	3.00E+04	1.000	6.27E+03	1.000
HLW Disposal	4.82E+13	1.000	3.09E+13	1.000	2.97E+13	1.000

Attribute 6: Separability

Table A.8 gives the utility function values for special nuclear material in various fuel forms, and Table A.9 gives the determined fuel form for each fuel cycle process and its utility function value. As material is separated further into its constituents, it is more

Table A.8: Utility function values for special nuclear material in various fuel forms as defined by Charlton et al. (2017).

Fuel Form (x)	Utility Function Value
Pu/HEU metal solid (a)	0.00
Separated Pu/HEU solution (b)	0.20
Mixed Pu solution (contains minor actinides, U, and/or fission products) or LEU solution (c)	0.50
Solid fuel without structural materials (d)	0.75
Solid fuel with structural materials (e)	1.00

conducive for production of weapons, and the proliferation resistance value decreases. The utility function values for this attribute, for each reactor type and fuel cycle process, are given below. Both LWRs and HTGRs, while requiring vastly different ^{235}U enrichment, perform the same on this attribute. Fuel is proceeds in the same form from cradle to grave. However, SFRs (are assumed to) require some form of aqueous fuel, though still containing minor actinides, that allows for continuous recycle and separation during operation.

Table A.9: Determined fuel form of materials at each fuel cycle process and corresponding utility function values.

	Separability | Utility Function Value					
Fuel Cycle Process	LWR		HTGR		SFR	
U Mining and Milling	d	0.75	d	0.75	d	0.75
Conversion	d	0.75	d	0.75	d	0.75
Enrichment	d	0.75	d	0.75	NA	NA
Fuel Fabrication	e	1.00	e	1.00	c	0.50
Fuel Fabrication (SFR)	NA	NA	NA	NA	c	0.50
SNF Storage	e	1.00	e	1.00	e	1.00
SNF Disposal	e	1.00	e	1.00	e	1.00
Reprocessing	c	0.50	c	0.50	c	0.50
HLW Disposal	e	1.00	e	1.00	e	1.00

REFERENCES

[Avenhaus, 2013] Avenhaus, R. (2013). *Safeguards Systems Analysis: With Applications to Nuclear Material Safeguards and Other Inspection Problems*. Springer Science & Business Media.

[Balachandra and Friar, 1997] Balachandra, R., & Friar, J. H. (1997). Factors for success in R&D projects and new product innovation: a contextual framework. *IEEE Transactions on Engineering management*, *44*(3), 276-287.

[Binsbergen and Marx, 2007] Van Binsbergen, J. H., & Marx, L. M. (2007). Exploring relations between decision analysis and game theory. *Decision Analysis*, *4*(1), 32-40.

[Bistline, 2013] Bistline, J. E. (2013). *Essays on Uncertainty Analysis in Energy Modeling: Capacity Planning, R & D Portfolio Management, and Fat-tailed Uncertainty* (Doctoral dissertation, Stanford University).

[Bowman and Gauld, 2010] Bowman, S. M. & Gauld, I. C. (2010). *OrigenArp Primer: How to Perform Isotopic Depletion and Decay Calculations with SCALE/ORIGEN* (ORNL/TM-2010/43). Oak Ridge National Laboratory.

[Bergelson et al., 2005] Bergelson, B., Gerasimov, A., & Tikhomirov, G. (2005). Influence of high burnup on the decay heat power of spent fuel at long-term storage

[Braathen, 2004] Braathen, N. A. (2004). Addressing the Economics of Waste. *Addressing the Economics of Waste*, 7-21.

[Butler et al., 2013] Butler, J. C., Cronin, P. M., Dyer, J. S., Edmunds, T. A., & Ward, R. M. (2013). *Decision Analysis Methods For the Analysis of Nuclear Terrorism Threats with Imperfect Information* (No. LLNL-TR-635767). Lawrence Livermore National Laboratory.

[Carlsen, 2016] Carlsen, R. W. (2016). *Advanced Nuclear Fuel Cycle Transitions: Optimization, Modeling Choices, and Disruptions* (Doctoral dissertation, The University of Wisconsin-Madison).

[Cetnar, 2006] Cetnar, J. (2006). General solution of Bateman equations for nuclear transmutations. *Annals of Nuclear Energy*, *33*(7), 640-645.

[Charlton et al., 2017] Charlton, W. S., LeBouf, R. F., Gariazzo, C., Ford, D. G., Beard, C., Landsberger, S., & Whitaker, M. Proliferation Resistance Assessment Methodology for Nuclear Fuel Cycles. *Nuclear Technology, 157,* 143-156.

[DeHart and Bowman, 2017] DeHart, M. D., & Bowman, S. M. (2011). Reactor physics methods and analysis capabilities in SCALE. *Nuclear Technology*, *174*(2), 196-213.

[Deutch et al., 2003] Deutch, J., Moniz, E., Ansolabehere, S., Driscoll, M., Gray, P., Holdren, J., ... & Todreas, N. (2003). *The future of nuclear power*. *An MIT Interdisciplinary Study,* Massachusetts Institute of Technology.

[Deutch et al., 2009] Deutch, J. M., Forsberg, C. W., Kadak, A. C., Kazimi, M. S., Moniz, E. J., & Parsons, J. E. (2009). *Update of the MIT 2003 future of nuclear power*. Massachusetts Institute of Technology.

[Dixon et al., 2009] Dixon, B., Kim, S., Shropshire, D., Piet, S., Matthern, G., & Halsey, B. (2008). *Dynamic systems analysis report for nuclear fuel recycle* (No. INL/EXT-08-15201). Idaho National Laboratory (INL).

[Djokic et al., 2015] Djokic, D., Scopatz, A., Greenberg, H. R., Huff, K. D., Nibbleink, R. P., & Fratoni, M. (2015). *The application of CYCLUS to fuel cycle transition analysis* (No. LLNL-CONF-669315). Lawrence Livermore National Lab.(LLNL), Livermore, CA (United States).

[DOE, 2000] U.S. Department of Energy. (2000). *Manual for Control and Accountability of Nuclear Material.* (DOE M (2000): 474-1).

[DOE, 2004] U.S. Department of Energy. (2004) *Nuclear Waste Policy Act (Amended with appropriations acts appended)*. Office of Civilian Radioactive Waste Management.

[Driscoll et al., 2015] Driscoll, M., Baglietto, E., Buongiorno, J., Lester, R., Brady, P., & Arnold, B. W. (2015). *Optimization of Deep Borehole Systems for HLW Disposal* (No. 12--3298). Sandia National Laboratory.

[EMWG, 2007] [EMWG, 2007] Economic Modeling Working Group. (2007). *Cost estimating guidelines for Generation IV nuclear energy systems*. (GIF/EMWG/2007/004). Generation IV International Forum.

[Feng et al., 2016] Feng, B., Dixon, B., Sunny, E., Cuadra, A., Jacobson, J., Brown, N. R., ... & Gregg, R. (2016). Standardized verification of fuel cycle modeling. *Annals of Nuclear Energy*, *94*, 300-312.

[Ferguson, 2014] Ferguson, T. S. (2014). Game Theory (2nd edition). *Mathematics Department, UCLA*, *2014*.

[Flicker et al., 2014] Flicker, M., Schneider, E. A., & Campbell, P. Evaluation criteria for analyses of nuclear fuel cycles. *Transactions of the American Nuclear Society*, *111*, 233-236.

[Forsberg, 2015] Forsberg, C. (2015). Implications of Plutonium isotopic separation on closed fuel cycles and repository design. *Nuclear Technology*, *189*(1), 63-70.

[Gabbert et al., 2010] Gabbert, S., Van Ittersum, M., Kroeze, C., Stalpers, S., Ewert, F., & Olsson, J. A. (2010). Uncertainty analysis in integrated assessment: the users' perspective. *Regional Environmental Change*, *10*(2), 131-143.

[Gauld et al., 2011] Gauld, I. C., Radulescu, G., Ilas, G., Murphy, B. D., Williams, M. L., & Wiarda, D. (2011). Isotopic depletion and decay methods and analysis capabilities in SCALE. *Nuclear Technology*, *174*(2), 169-195.

[Golub et al., 2014] Golub, A., Narita, D., & Schmidt, M. G. (2014). Uncertainty in integrated assessment models of climate change: Alternative analytical approaches. *Environmental Modeling & Assessment*, *19*(2), 99-109.

[Hardin et al., 2011] Hardin, E., Blink, J., Greenberg, H., Sutton, M., Fratoni, M., Carter, J., ... & Howard, R. (2011*). Generic repository design concepts and thermal analysis*. (SAND2011-6202). Sandia National Laboratory.

[DOE, 2013] U.S. Department of Energy. (2013). *Strategy for the management and disposal of used nuclear fuel and high-level radioactive waste.*

[Hubbard, 1991] Hubbard, H. M. (1991). The real cost of energy. *Scientific American*, *264*(4), 36-43.

[Huff and Dixon, 2010] Huff, K. & Dixon, B. (2010). Next generation fuel cycle simulator functions and requirements document (*draft*). Idaho National Laboratory, FCRD-SYSA-2010-000110

[Huff et al., 2016] Huff, K. D., Gidden, M. J., Carlsen, R. W., Flanagan, R. R., McGarry, M. B., Opotowsky, A. C., ... & Wilson, P. P. (2016). Fundamental concepts in the Cyclus nuclear fuel cycle simulation framework. *Advances in Engineering Software*, *94*, 46-59.

[IAEA, 2001] International Atomic Energy Agency. (2001). *Safeguards Glossary: 2001 Edition*. International Nuclear Verification Series, *3*, 23.

[Jacobson et al., 2010] Jacobson, J. J., Yacout, A. M., Matthern, G. E., Piet, S. J., Shropshire, D. E., Jeffers, R. F., & Schweitzer, T. (2010). Verifiable fuel cycle simulation model (VISION): a tool for analyzing nuclear fuel cycle futures. *Nuclear Technology*, *172*(2), 157-178.

[Juchau et al., 2010] Juchau, C. A., Dunzik-Gougar, M. L., & Jacobson, J. J. (2010). Modeling the nuclear fuel cycle. *Nuclear technology*, *171*(2), 136-141.

[Kann and Weyant, 2000] Kann, A., & Weyant, J. P. (2000). Approaches for performing uncertainty analysis in large-scale energy/economic policy models. *Environmental Modeling & Assessment*, *5*(1), 29-46.

[Leibowicz, 2018] Leibowicz, B. D. (2018). The cost of policy uncertainty in electric sector capacity planning: Implications for instrument choice. *The Electricity Journal*, *31*(1), 33-41.

[Marler and Aurora, 2004] Marler, R. T., & Arora, J. S. (2004). Survey of multi-objective optimization methods for engineering. *Structural and multidisciplinary optimization*, *26*(6), 369-395.

[Milnor, 1951] Milnor, J. (1951). *Games against nature* (No. RAND-RM-679). Rand Project Air Force Santa Monica, CA.

[NEI, 2018] Nuclear Energy Institute. (2018) https://www.nei.org/advocacy/make-regulations-smarter/used-nuclear-fuel. Accessed July 2018.

[NRC, 1995] National Research Council. (1995). *Management and Disposition of Excess Weapons Plutonium: Reactor-Related Options*. National Academies Press.

[OECD, 2018] Organisation for Economic Co-operation and Development, Nuclear Energy Agency. (2018). The Full Costs of Electricity Provision. *Available: oecd-nea.org*.

[Rearden and Jessee, 2016] Rearden, B. T. & Jessee, M. A. (2016). *SCALE Code System* (ORNL/TM-2005/39, Version 6.2). Oak Ridge National Laboratory.

[Phathanapirom and Schneider, 2016] Phathanapirom, U. B., & Schneider, E. A. (2016). Nuclear fuel cycle transition analysis under uncertainty. *Nuclear Science and Engineering*, *182*(4), 502-522.

[Pierpoint, 2011] Pierpoint, L. M. (2011). *A decision analysis framework for the U.S. nuclear fuel cycle* (Doctoral dissertation, Massachusetts Institute of Technology).

[Pierpoint, 2017] Pierpoint, L. M. (2017). Illuminating Fuel Cycle Decision Drivers Using a Decision Analysis Framework. *Nuclear Science and Engineering*, *186*(1), 66-82.

[Piet et al., 2009] Piet, S. J., Dixon, B. W., Jacobson, J. J., Matthern, G. E., & Shropshire, D. E. (2009). *Lessons learned from dynamic simulations of advanced fuel cycles* (No. INL/CON-08-15052). Idaho National Laboratory (INL).

[Sathaye et al., 2011] Sathaye, J., Lucon, O., Rahman, A., Christensen, J., Denton, F., Fujino, J., ... & Shmakin, A. (2011). *Renewable energy in the context of sustainable development.* Physics Faculty Publications. Potsdam Institute for Climate Impact Research. Cambridge University.

[Schneider et al., 2005] Schneider, E. A., Bathke, C. G., & James, M. R. (2005). NFCSIM: a dynamic fuel burnup and fuel cycle simulation tool. Nuclear Technology, 151(1), 35-50.

[Schneider and Phathanapirom, 2016] Schneider, E. A., & Phathanapirom, U. B. (2016). VEGAS: A Fuel Cycle Simulation and Preconditioner Tool with Restricted Material Balances. *Nuclear Technology*, *193*(3), 416-429.

[Shropshire et al., 2009] Shropshire, D. E., Williams, K. A., Boore, W. B., Smith, J. D., Dixon, B. W., Dunzik-Gougar, M., ... & Schneider, E. (2009). *Advanced fuel cycle cost basis*. (INL/EXT-07-12107) Idaho National Laboratory.

[UTEI, 2018] University of Texas at Austin Energy Institute. (2018). The Full Cost of Electricity (FCe-): A series of white papers. Available: energy.utexas.edu.

[Walker et al., 2003] Walker, W. E., Harremoës, P., Rotmans, J., van der Sluijs, J. P., van Asselt, M. B., Janssen, P., & Krayer von Krauss, M. P. (2003). Defining uncertainty: a conceptual basis for uncertainty management in model-based decision support. *Integrated assessment*, *4*(1), 5-17.

[Ward and Schneider, 2016] Ward, Rebecca M., and Erich A. Schneider. "A game theoretic approach to nuclear safeguards selection and optimization." *Science & Global Security* 24.1 (2016): 3-21.

[Wian, 2013] Tian, W. (2013). A review of sensitivity analysis methods in building energy analysis. *Renewable and Sustainable Energy Reviews*, *20*, 411-419.

[Wigeland et al., 2006] Wigeland, R. A., Bauer, T. H., Fanning, T. H., & Morris, E. E. (2006). Separations and transmutation criteria to improve utilization of a geologic repository. *Nuclear Technology*, *154*(1), 95-106

[Wigeland et al., 2014] Wigeland, R., Taiwo, T., Ludewig, H., Todosow, M., Halsey, W., Gehin, J., Jubin, R., Buelt, J., Stockinger, S., Jenni, K., & Oakley, B. (2014). Nuclear fuel cycle evaluation and screening – final report. Idaho National Laboratory, INL/EXT-14-31465, FCRD-FCO-2014-000106

[Wright, 1936] Wright, T. P. (1936). Factors affecting the cost of airplanes. *Journal of aeronautical sciences*, *3*(4), 122-128.

[WNA, 2017a] World Nuclear Association. (2017). *Nuclear Power Economics and Project Structuring*. (No. 2017/001).

[WNA, 2017b] World Nuclear Association. (2017). *Generation IV Nuclear Reactors.* Available: world-nuclear.org

[Yacout et al., 2004] Yacout, A., Van Den Durpel, L., Wade, D., & Finck, P. (2004). Scenarios for the Expanded use of nuclear energy. In *2004 International Congress on Advances in Nuclear Power Plant (ICAPP'04), Pittsburgh, PA USA*.

[Yacout et al., 2005] Yacout, A. M., Jacobson, J. J., Matthern, G. E., Piet, S. J., & Moisseytsev, A. (2005, July). Modeling the nuclear fuel cycle. In *The 23rd International Conference of the System Dynamics Society," Boston*.

[WNA, 2017b] Yacout, A. M., Jacobson, J. J., Matthern, G. E., Piet, S. J., & Moisseytsev, A. (2005). Modeling the nuclear fuel cycle. In *The 23rd International Conference of the System Dynamics Society," Boston*.

VITA

Birdy was born and raised in Texas, and her research has taken her for extended stays in Las Vegas, NV; Idaho Falls, ID; and Vienna, Austria. Her research focuses on incorporating decision-theoretic approaches to nuclear fuel cycle transition analysis through the use and development of modeling and simulation tools and optimization solvers. She completed her B.S. in physics in 2012 and M.S. in nuclear and radiation engineering in 2014 from the University of Texas at Austin. Birdy has accepted a position as a postdoctoral research associate in the Reactor and Nuclear Systems division at the Oak Ridge National Laboratory. Birdy is a world explorer and adventure seeker. She lives in Knoxville, TN with her faithful companion, Mrs. Butterscotch.

Permanent email: bphathanapirom@utexas.edu
This dissertation was typed by the author.